The Dissertation Committee for Erica Jacqueline Di Pierro Certifies that this is the approved version of the following dissertation:

Unexpected Biochemistry Determines Endotoxin Structure in Two Enteric Gram-Negatives

Committee:

Michael Stephen Trent, Supervisor

Bryan Davies

Lauren Ehrlich

Jennifer Maynard

Shelley Payne

Unexpected Biochemistry Determines Endotoxin Structure in Two Enteric Gram-Negatives

by

Erica Jacqueline Di Pierro, B.S.Bio.

Dissertation

Presented to the Faculty of the Graduate School of

The University of Texas at Austin

in Partial Fulfillment

of the Requirements

for the Degree of

Doctor of Philosophy

The University of Texas at Austin

May 2015

Dedication

To my husband, Michele, for helping me zoom out and enjoy the big picture, but also appreciate the small moments that ultimately fill and make a life

Acknowledgements

I am deeply indebted to my mentor, Dr. M. Stephen Trent for helping me to develop and hone a broad range of both science and life skills. Dr. Trent has provided me with a wealth of important opportunities that have allowed me to be very successful in my graduate career. I am sincerely grateful for the time and effort he has invested in my future and feel extremely fortunate to have spent time under his guidance. I would also like to recognize my committee for their direction and patience: Dr. Bryan Davies, Dr. Lauren Ehrlich, Dr. Jennifer Maynard, and Dr. Shelley Payne. Further, I must extend a huge thank you to current and past members of the Trent lab, who have provided advice, suggestions, troubleshooting ideas, consolation, great conversation, and lots of laughs. It would have been difficult to get through without you all.

Thanks to the best mom and dad I could hope for: for celebrating all the victories with me, big and small, and giving me the strength to keep on keeping on during the tough stretches. And finally to my husband, Dr. Michele, who went through it with me and for himself at the same time: thanks for supporting me every day.

Unexpected Biochemistry Determines Endotoxin Structure in Two Enteric Gram-Negatives

Erica Jacqueline Di Pierro, Ph.D.

The University of Texas at Austin, 2015

Supervisor: Michael Stephen Trent

Most gram-negative organisms require lipopolysaccharide and its membrane anchor, lipid A, for growth and survival. Also known as endotoxin, lipid A is synthesized via a nine-step enzymatic process, culminating in a conserved hexa-acylated, *bis*-phosphorylated disaccharide of glucosamine. This framework is often altered by condition- or species-specific lipid A modifications, which change the biochemical properties of the molecule in response to and to defend against environmental stress signals. Here, we expound on two stories in different gram-negative organisms, both involving novel or unanticipated biochemistry that impacts lipid A structure. First, the missing acyltransferase in the Epsilonproteobacterium *Helicobacter pylori* lipid A biosynthesis pathway is identified. This enzyme transfers a secondary acyl chain to the 3'-linked primary acyl chain of lipid A like *E. coli* LpxM, but shares almost no sequence similarity with the *E. coli* acyltransferase. It is reannotated as LpxJ and demonstrated to possess an unprecedented ability to act before the 2'-secondary acyltransferase, LpxL, as well as the 3-deoxy-D-*manno*-octulosonic acid transferase, KdtA. LpxJ is one member of a large class of acyltransferases found in a diverse range of organisms that lack an *E. coli* LpxM homolog, suggesting that LpxJ participates in lipid A biosynthesis in place of an LpxM homolog. The second story focuses on regulation of modifications to endotoxin structure that occur after the conserved biosynthesis pathway. *E. coli pmrD* is shown to be required for PmrAB-dependent lipid A modifications in conditions that exclusively activate PhoPQ; this result proves that PmrD connects PhoPQ and PmrAB despite previous reports that it is an inactive connector in this organism. Further, RNA sequencing and

polymyxin B survival assays solidify the role of *E. coli pmrD* in influencing expression of *pmrA* and its target genes and promoting survival during exposure to cationic antimicrobial peptides. Notably, the presence of an unknown factor or system capable of activating *pmrD* to promote lipid A modification in the absence of the PhoPQ system is also revealed. In all, the findings presented here expand our understanding of alternative approaches to lipid A biosynthesis and the complex systems that regulate modifications of this dynamic molecule.

Table of Contents

List of Tables xi

List of Figures xii

Chapter 1: Introduction 1

1.1 Lipopolysaccharide and Lipid A Biosynthesis 1

1.1.1 The Gram-negative cell envelope 1

1.1.2 The Raetz pathway 4

1.2 Modification of Lipid A 7

1.2.1 Constitutive modification of *Helicobacter pylori* lipid A 7

1.2.2 Conditional lipid A modifications 11

1.2.2.1 Temperature changes acylation state of Yersinia pestis lipid A 12

1.2.2.2 A novel two-component system regulates a novel lipid A modification in Vibrio cholerae 13

1.2.2.3 Regulation of lipid A modifications by two-component systems in Salmonella enterica and Escherichia coli 15

Chapter 2: Identification of a broad family of lipid A late acyltransferases with non-canonical substrate specificity 19

2.1 Introduction 19

2.2 Results 23

2.2.1 *H. pylori* encodes an enzyme functionally comparable to *E. coli* LpxM 23

2.2.2 $LpxJ_{Hp}$ complements a penta-acylated *E. coli lpxM* mutant, restoring a hexa-acylated phenotype 26

2.2.3 Homologs of $LpxJ_{Hp}$ are found in other Epsilonproteobacteria 28

2.2.4 DUF374 proteins are found in a diverse range of organisms 30

2.2.5 $LpxJ_{Hp}$ acts on tetra- or penta-acylated lipid A, with or without Kdo sugars 32

2.2.6 *Campylobacter* and *Wolinella* LpxJ only use tetra-acylated lipid A as substrate 35

2.2.7 LpxJ activity can precede LpxL activity 39
2.3 Discussion 41

Chapter 3: PmrD is required for modifications to *Escherichia coli* endotoxin that promote antimicrobial resistance 46
3.1 Introduction 46
3.2 Results 52
3.2.1 pEtN and L-Ara4N lipid A modifications are induced in wild-type *E. coli* grown in low Mg^{2+} and are *pmrD*-dependent 52
3.2.2 pEtN/L-Ara4N lipid A modifications are PmrA-dependent, but only partially PhoPQ-dependent 58
3.2.3 *pmrD* is transcriptionally active in a *phoPQ* mutant and its expression is not influenced by PmrAB 61
3.2.4 PmrD plays a role in expression of *pmrA*, thereby indirectly affecting expression of downstream *pmrA*-dependent genes 63
3.2.5 Polymyxin B resistance in *E. coli* is *pmrD*-dependent in low Mg^{2+} but not in mildly acidic pH 65
3.3 Discussion 68

Chapter 4: Conclusion 72
4.1 Future Directions and Concluding Themes 72
4.2 The Next Steps for Lipid A: Antibiotics and Therapeutics 75

Chapter 5: Experimental Procedures 82
5.1 Materials and Methods 82
5.1.1 Bacterial strains and growth conditions 82
5.1.2 Isolation and analysis of lipid A species from $^{32}P_i$-labeled cells 82
5.1.3 Mass spectrometry of lipid A species 83
5.1.4 Construction of genetic mutant and chromosomal complementation of *H. pylori* J99 jhp0255 ($lpxJ_{Hp}$). 83
5.1.5 Generation of low-copy plasmids for expression of late acyl transferases from Epsilonproteobacteria and the *E. coli pmrD* gene 85
5.1.6 Preparation of radiolabeled lipid substrates for *in vitro* enzymatic assays 86

5.1.7 *In vitro* assay of $LpxJ_{Hp}$, $LpxJ_{Cj}$, and $LpxJ_{Ws}$ activities. 87
5.1.8 Preparation of cell-free extracts, double-spun cytosol, and washed membranes 87
5.1.9 Generation of *E. coli* mutants 88
5.1.10 Total RNA Isolation and Quantitative RT-PCR 88
5.1.11 Construction of Illumina libraries, RNA sequencing, and data analysis.....89
5.1.12 Polymyxin B survival assays 89
5.2 Bacterial strains and oligonucleotides 91
References.....99

List of Tables

Table 2.1: Genetic relationships between *E. coli* LpxM and relevant proteins. .24

Table 2.2: LpxJ homologs in Pfam DUF374 31

Table 2.3: Homologs of $LpxJ_{Hp}$ found in DUF374.....32

Table 3.1: Densitometry analysis values for Figure 3.5 60

Table 3.2: Select RNAseq data comparing gene expression in wild-type and *pmrD*$^-$ *E. coli* strains grown in low versus high magnesium minimal medium 64

Table 5.1: Bacterial strains and plasmids used in Chapter 2 91

Table 5.2: Oligonucleotides used in Chapter 2 93

Table 5.3: Bacterial strains and plasmids used in Chapter 3 95

Table 5.4: Oligonucleotides used in Chapter 3 97

List of Figures

Figure 1.1: Gram-negative bacterial cell envelope.....3

Figure 1.2: The *E. coli* Raetz pathway of lipid A biosynthesis.....5

Figure 1.3: Modification of *H. pylori* lipid A generates its unique structure.....9

Figure 1.4: Conditional lipid A modifications in *Y. pestis* and *V. cholerae*.....14

Figure 1.5: Lipid A modifications in *S. enterica* and *E. coli* alter the physiological properties of the molecule.....17

Figure 2.1 Final steps of the Raetz pathway in *E. coli* and the missing late acyltransferase of *H. pylori*.....22

Figure 2.2 $lpxJ_{Hp}$ is an essential gene that can only be knocked-out after prior complementation.....25

Figure 2.3 $LpxJ_{Hp}$ and homologs in two other Epsilonproteobacteria complement a hexa-acylated lipid A phenotype in a penta-acylated *E. coli* LpxM mutant.....27

Figure 2.4 MALDI-TOF mass spectrometry of *E. coli* LpxM mutant, BN2 expressing acyltransferase genes from three Epsilonproteobacteria.....29

Figure 2.5 MALDI-TOF mass spectrometry of hexa-acylated control strain BN1.....30

Figure 2.6 Enzymatic characteristics of $LpxJ_{Hp}$.....33

Figure 2.7 Enzymatic characteristics of $LpxJ_{Cj}$ and $LpxJ_{Ws}$.....36

Figure 2.8 UVPD mass spectra of doubly deprotonated lipid A species and corresponding fragmentation maps.....38

Figure 2.9 Multiple routes are possible at the end of the Raetz pathway in *H. pylori* and *C. jejuni* 40

Figure 3.1 *E. coli* and *S. enterica* modify lipid A in response to environmental signals, altering the integrity of the outer membrane 51

Figure 3.2 *pmrD* is required for addition of pEtN and L-Ara4N to lipid A in low Mg^{2+} conditions 53

Figure 3.3 MALDI-TOF mass spectrometry of lipid A from *E. coli* W3110 wild-type, *pmrD*$^{-}$, and complemented *pmrD* mutant in high and low Mg^{2+} 55

Figure 3.4 MALDI-TOF mass spectrometry of negative control strain W3110 *pmrA*$^{-}$ 57

Figure 3.5 pEtN/L-Ara4N lipid A modifications are PmrA-dependent, but only partially PhoPQ-dependent 59

Figure 3.6 *pmrD* expression in a *phoPQ* mutant is not influenced by PmrAB ..62

Figure 3.7 *pmrD* impacts transcription of *pmrA* and its downstream genes.....65

Figure 3.8 *pmrD* plays a role in polymyxin B resistance 67

Figure 4.1: *Acinetobacter baumannii* can survive without LOS in the laboratory and the clinic.....76

Figure 4.2: Molecular engineering applications in lipid A studies 79

Chapter 1: Introduction

1.1 Lipopolysaccharide and Lipid A Biosynthesis

1.1.1 The Gram-negative cell envelope

In gram-negative bacteria, the cell envelope is distinguished by the presence of an outer membrane, a complex structure that acts as a dynamic canvas for response to, interaction with, and protection against a rapidly changing environment. The outer membrane is made of an inner leaflet of phospholipids and an outer leaflet populated by the bioactive macromolecule lipopolysaccharide (LPS) (Fig 1.1) (1). LPS is anchored to the membrane via its lipid A domain, an acylated disaccharide of glucosamine also referred to as endotoxin. Attached to the lipid A is a set of core sugars, which typically includes two 3-deoxy-D-*manno*-octulosonic acid (Kdo) residues, heptose, and various hexose sugars. Beyond the core, many gram-negatives also have a long chain of repeating oligosaccharides known as the O-antigen, which shows extensive variation in sugar composition and residue number across this class of bacteria (2).

The prototypical lipid A structure is that produced by the well-studied enteric bacterium *Escherichia coli*. Consisting of a β(1,6)-linked disaccharide of glucosamine that is *bis*-phosphorylated and hexa-acylated, this specific structure is the strongest known agonist for the Toll-like receptor 4/myeloid differentiation factor-2 (TLR4/MD2) complex present on circulating immune cells (2–4). During infection, LPS is extracted from the outer bacterial membrane or picked up in aggregates by LPS-binding protein and delivered to cluster of differentiation 14 (CD14) and TLR4/MD2 at the host cell

surface (5, 6). LPS establishes a highly specific interaction with TLR4/MD2 via its lipid A domain, which nestles five of its acyl chains into a large hydrophobic pocket within the MD2 co-receptor and dangles the sixth outside to interact with TLR4 (7). LPS binding induces dimerization of TLR4-MD2 complexes, which initiates intracellular signaling cascades that lead to production of pro-inflammatory cytokines necessary for clearance of infection. However, excessive activation of these pathways leads to vascular instability, multiple organ failure, and potential death for an infected host (8, 9). As such, lipid A is regarded as a major virulence factor for many gram-negative organisms. The lipid A domain can also be modified by enzymes that add and/or remove various chemical groups, which can affect the TLR4 response. Some organisms have evolved complex regulated modification cascades that create a mildly- or non-stimulatory final lipid A structure, allowing for evasion of immune recognition and survival within the host. Several such examples will be discussed in a later section.

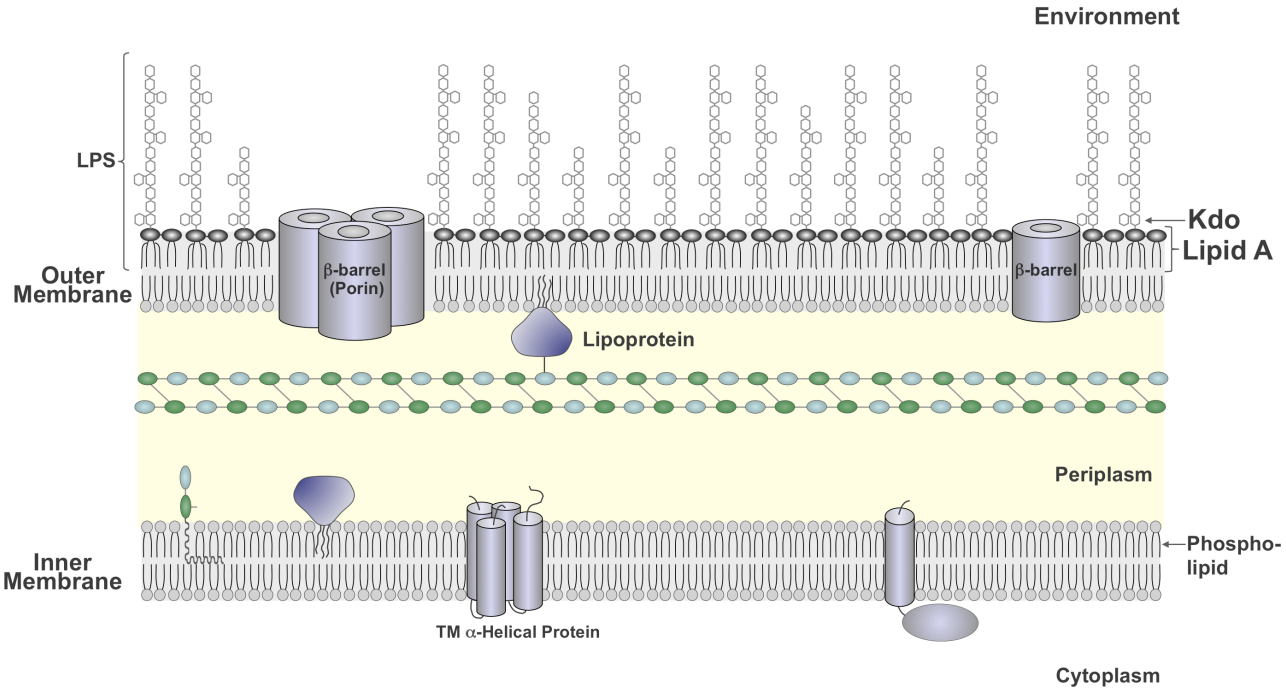

Figure 1.1: Gram-negative bacterial cell envelope

Gram-negative bacteria possess inner and outer lipid bilayer membranes separated by a periplasmic space containing a thin layer of peptidoglycan. The outer membrane is composed half of phospholipids (inner leaflet) and half of lipopolysaccharide (outer leaflet), while the inner membrane is predominantly phospholipids. β-barrel proteins punctuate the outer membrane while α-helical proteins are found at the inner membrane.

1.1.2 The Raetz pathway

The vast majority of gram-negative organisms require lipid A for growth and survival. This crucial membrane component is built at the cytosolic leaflet of the inner membrane by the successive activities of nine well-conserved Lpx enzymes of the Raetz pathway, first described in *E. coli* (Fig 1.2) (2). Briefly, the process begins with the activity of LpxA, which adds an acyl chain to the activated nucleotide sugar donor, uridine diphosphate N-acetylglucosamine (10). In the following early steps of the pathway, this substructure is deacetylated by metalloamidase LpxC, further acylated by LpxD, and cleaved at the pyrophosphate bond by LpxH or LpxI to form the lipid X species (11–14). Next, the defining β(1,6)-glycosidic linkage of lipid A is formed by glycosyltransferase LpxB, generating disaccharide 1-phosphate, which is then 4′-phosphorylated by LpxK to form lipid IV_A (15, 16). The late steps include transfer of two Kdo sugars to the distal glucosamine by WaaA (KdtA), and finally addition of 2′- and 3′-secondary acyl chains by LpxL and LpxM, respectively (17–19). The Raetz pathway culminates in formation of hexa-acylated Kdo_2-lipid A, which is then united with core and O-antigen sugars and transported across membrane compartments for display at the outer leaflet.

While many gram-negatives encode homologs to the *E. coli* Lpx enzymes for completion of their respective Raetz pathways, some organisms use enzymes with unique sequence and/or substrate specificity to build lipid A. These differences can be as subtle as hydrocarbon ruler length preference in the enzyme active site, or as significant as a total lack of sequence identity with the corresponding *E. coli* Lpx enzyme.

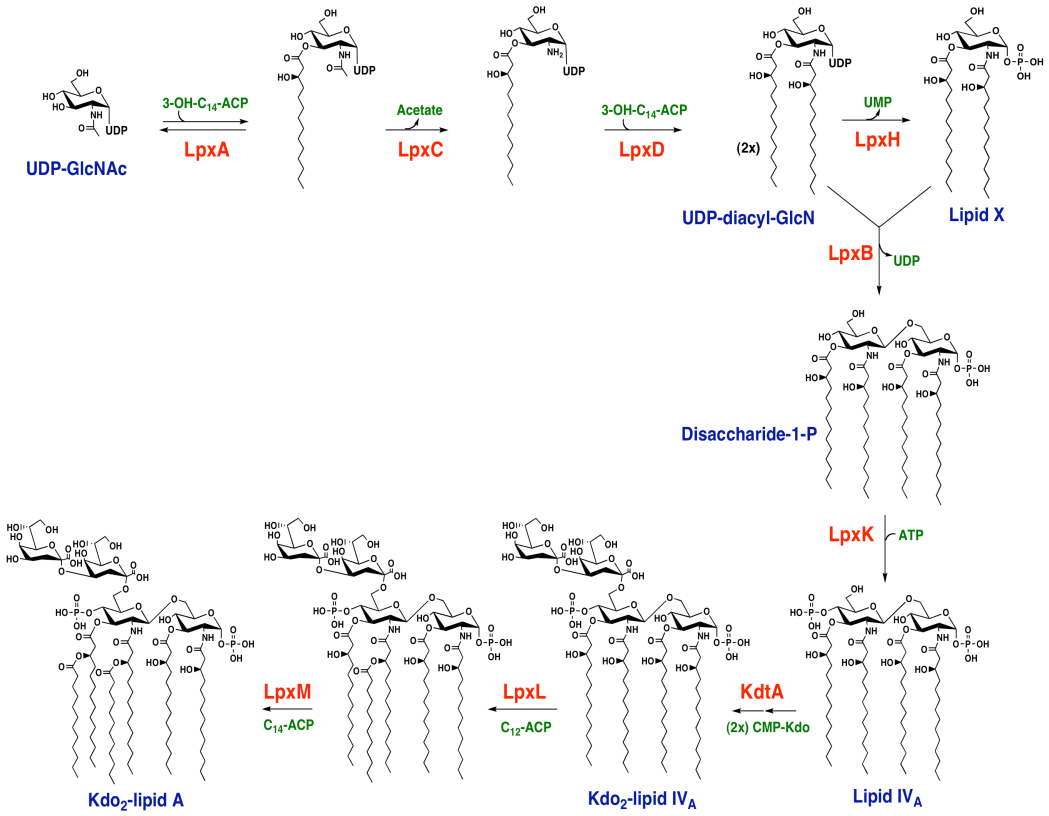

Figure 1.2: The *E. coli* Raetz pathway of lipid A biosynthesis

Lipid A is constructed in a nine-step conserved enzymatic pathway by the Lpx enzymes, shown in red. The final product of the Raetz pathway in *E. coli* is a β(1,6)-linked disaccharide of glucosamine that is *bis*-phosphorylated and hexa-acylated.

For example, while *Pseudomonas aeruginosa* and *Helicobacter pylori* both encode homologs of *E. coli* LpxA, each has a hydrocarbon ruler with different acyl chain length demands: *E. coli* LpxA requires a 14-carbon chain, *P. aeruginosa* a 10-carbon chain, and *H. pylori* a 16-carbon chain (20–22). These enzymatic preferences are reflected directly in the lipid A frameworks produced by each organism.

Further, *E. coli* and many other gram-negatives use LpxH to generate lipid X from UDP-diacyl glucosamine. Other organisms including members of the α-proteobacteria, however, encode LpxI, a protein unrelated by sequence to and employing a unique catalytic mechanism from LpxH (13). Specifically, LpxH orchestrates attack of the α-phosphate of UDP-diacyl glucosamine while LpxI instead targets the β-phosphate (12, 13).

E. coli can also depart from the conserved Raetz pathway in certain conditions. When growth temperature is shifted to 12°C, incorporation of palmitoleate (C16:1) into the lipid A increases due to the activity of cold-shock acyltransferase LpxP (23). A homolog of late acyltransferase LpxL, LpxP uses Kdo_2-lipid IV_A as substrate, transferring a palmitoleate to the same position on the lipid A molecule as LpxL, the hydroxyl group of the 3′-primary acyl (23). At this sub-normal growth temperature, LpxP is transcriptionally upregulated and the enzyme performs acyltransfer to this position in place of LpxL. This divergence from the typical late Raetz pathway is an adaptation thought to maintain membrane fluidity at a lower temperature, as well as increasing barrier function against antibiotics (23, 24)

In this work, another Raetz pathway enzymatic anomaly is identified and characterized, this time in *H. pylori* and other ε-proteobacteria. This enzyme, from hereon referred to as LpxJ, transfers the secondary acyl chain to the 3′-linked primary acyl chain of *H. pylori* lipid A, similarly to LpxM in *E. coli*. However, LpxJ exhibits flexibility in substrate specificity not observed with LpxM, performing acyltransfer regardless of the presence of Kdo sugars and the ability to do so before the *H. pylori* LpxL homolog (22, 25). This enzyme, discussed in detail in Chapter 2, represents an extensive previously uncharacterized family of lipid A late acyltransferases that may allow for multiple routes at the end of the lipid A biosynthesis pathway.

1.2 Modification of Lipid A

A sampling of outer leaflets across multiple gram-negatives reveals considerable diversity in terms of the precise chemical composition of surface-presented lipid A. Variability in lipid A structure occurs due to the activity of enzymes that add or remove assorted chemical groups, sometimes resulting in a final structure that only vaguely resembles the unmodified Raetz pathway output product. Such modifications occur constitutively in some organisms or may be strictly regulated to promote survival in certain conditions.

1.2.1 Constitutive modification of *Helicobacter pylori* lipid A

A classic example of an organism with extensively modified lipid A is *H. pylori*. This adapted gastric pathogen colonizes half the world's population and can cause life-long infection in the form of peptic ulcers and gastric cancer (26). During transport to the

outer membrane, its lipid A becomes the substrate for five constitutive modification enzymes that dramatically alter its structure and biochemical properties (Fig 1.3). First, the 1-phosphate group is removed by LpxE and a phosphoethanolamine (pEtN) is added in its place by EptA (27). Next, the terminal Kdo sugar added by WaaA is removed by the two-protein Kdo-hydrolase complex, Kdo H1/H2, leaving a single Kdo at the inner core (28). The 4′-phosphate group is then removed by LpxF, just before the lipid A molecule is joined with the core sugars and O-antigen to form a mature LPS molecule (29). After transport to the outer leaflet of the outer membrane, the lipid A moiety undergoes a final modification: removal of the 3′-linked acyl chains by LpxR, producing the final tetra-acylated lipid A structure characteristic of the *H. pylori* outer membrane (Fig 1.3, inset)(22).

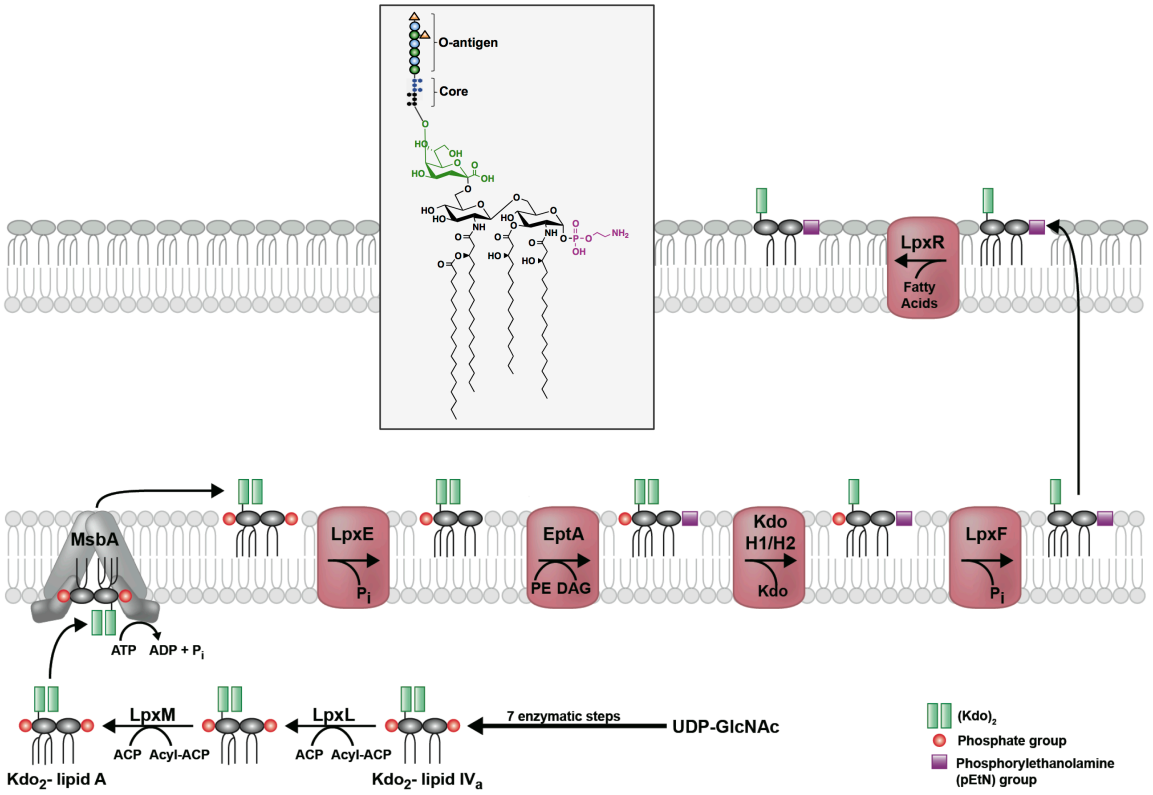

Figure 1.3: Modification of *H. pylori* lipid A generates its unique structure

Kdo_2-lipid A is flipped to the periplasmic leaflet of the inner membrane by the conserved ABC-transporter MsbA. The 1-phosphate group is removed by LpxE, and a phosphorylethanolamine (pEtN) group is added in its place by EptA. The latter activity generates diacylglycerol (DAG), as phosphatidylethanolamine (PE) is likely the donor molecule for the pEtN group. Next, a two-protein Kdo-hydrolase complex, Kdo H1/H2, removes the terminal Kdo group. The last modification to occur before transport across the periplasm is the removal of the 4′-phosphate group by LpxF. Finally, the outer-membrane β-barrel LpxR catalyzes removal of the 3′-linked acyl chains, generating the final lipid A structure in the outer membrane of *H. pylori* (inset). The core oligosaccharide and O-antigen chain with fucose additions are only shown in the inset for simplicity.

While drastically altering the physical construction of lipid A, these successive modifications also impact its interaction with the environment. For example, both the addition of EptA and removal of the 1- and 4′-phosphate groups reduce the net negative charge of each lipid A molecule and the outer membrane as a whole, thereby promoting resistance to cationic antimicrobial peptides (CAMPs) like polymyxin B, which will be discussed in further detail in a later section (30). Importantly, alterations in acyl chain number and length, phosphate groups, and presence of polar functional groups can all impact the strength of the TLR4 response (8). The most iconic example of this concept is exhibited by the fact that hexa-acylated lipid A is the most potent known TLR4 agonist, while penta-acylated lipid A is 100-fold less active and tetra-acylated lipid A is actually antagonistic (7, 31). It is thought that under-acylation alters TLR4-reactivity because the acyl chains of lipid A have more space in which to move freely within the hydrophobic pocket of MD2, which could disrupt TLR4/MD2 dimerization (7). In the case of *H. pylori*, removal of the two 3′-acyl chains by LpxR is a major determinant in limiting the TLR4 response elicited by this organism's lipid A. The two phosphate groups also contribute to the ligand-receptor interaction, as they contact positively charged residues within the TLR4/MD2 multimer (7). As such, deletion of one or both phosphate groups, as occurs with *H. pylori* lipid A, has been shown to greatly diminish endotoxic activity (32). Indeed, *H. pylori* surface-presented lipid A is up to 1000-times less immunostimulatory than that of *E. coli* as a result of this stringently adapted modification cascade (33–35). Ultimately, its lipid A structure helps this rugged enteric pathogen to

become a long-term resident of the human gut epithelium, striking a balance between causing disease and staying below the radar of the host immune system.

1.2.2 Conditional lipid A modifications

H. pylori is expertly adapted to life in the human gut epithelium, its only known reservoir. Its lipid A has evolved an optimal structure to flourish in this niche and the enzymes that modify it are constitutively expressed. This is not the case, however, in gram-negatives with complex life cycles or that experience rapidly changing environments. Common challenges that bacteria may encounter in the host or other surrounding environment include CAMPs, temperature fluctuations, changes in pH, and depletion of divalent cations.

CAMPs, as the name would suggest, are short cationic amphipathic peptides with the ability to associate with and penetrate the negatively charged Gram-negative outer membrane. Produced by organisms from bacteria and fungi to animals, their modes of action include membrane permeabilization and targeting key processes like DNA, protein, and cell wall synthesis (36, 37). Modification of anionic outer membrane structures like lipid A can reduce the net negative charge of the membrane, minimizing interaction with CAMPs. This is crucial to promote survival in the human host where CAMPs are produced by cells at practically every point of bacterial entry and niche of infection: for example, skin keratinocytes, epithelial glands of the respiratory and genitourinary tract, epithelial cells in the crypts of the small intestine, and phagocytic cells of the innate immune system (38).

Survival in limited concentrations of divalent cations such as Mg^{2+} and Ca^{2+} is also problematic for gram-negative organisms. These metals create ionic bridges between neighboring negative lipid A molecules, which contribute significantly to outer membrane stability (39). When environmental divalent cations are low, the membrane becomes vulnerable in the absence of this crucial reinforcement, and the bacterium must respond in a manner that fortifies the membrane (40). Such responses can include various lipid A modifications that increase hydrophobicity and/or decrease negative charge of the molecule to stabilize lipid A within the LPS leaflet (39). Below are several examples of organisms that modify their lipid A to promote survival in difficult or changing conditions.

1.2.2.1 Temperature changes acylation state of **Yersinia pestis** *lipid A*

Yersinia pestis causes multiple forms of plague, which decimated the European population in the mid-1300s (41). In the environment, this pathogen typically passes between rodents and fleas, and can be transmitted to humans via both of these reservoirs (42). While proliferating in the flea gut, *Yersinia* experiences temperatures 10-15 degrees, lower (21-27°) than in a human host (37°C). It has been found that this host temperature switch induces a change in this organism's lipid A; *Y. pestis* produces TLR4-stimulatory hexa-acylated lipid A inside the flea but antagonistic tetra-acylated lipid A in humans (Fig 1.4A)(43, 44). The immuno-evasive tetra-acylated structure is reminiscent of *H. pylori* lipid A, and is thought to allow undetected proliferation of *Y. pestis* in the human bloodstream during early infection (44, 45). This lipid A phenotypic adaptation appears

to be critical in pathogenesis, as a mutant strain that can only produce hexa-acylated lipid A is avirulent in mice (44).

1.2.2.2 A novel two-component system regulates a novel lipid A modification in **Vibrio cholerae**

Certain lipid A modifications have been shown to be regulated by two-component system (TCS) protein networks that act as sentinels for detection and integration of various signals in the form of targeted transcriptional regulation. A typical TCS consists of a sensor histidine kinase that detects specific environmental queues and a cognate response regulator, which carries out changes in expression of a subset of genes known as its regulon. Upon recognition of a given signal, the sensor first autophosphorylates and then phosphorylates the response regulator, causing it to activate or repress gene expression within the regulon. When the signal is no longer present or detectable, the sensor deactivates the response regulator by dephosphorylation, thereby terminating transcriptional control of affected genes (46–48). Some bacteria like *E. coli* possess an extensive network of well-characterized TCSs, while others may encode only one or two known systems.

The aquatic pathogen *Vibrio cholerae* has caused millions of infections in repeated global pandemics since the early 1800s, producing intense diarrheal disease that can quickly lead to death. In a recent major shift for *V. cholerae* epidemiology, the classical biotype responsible for the first six pandemics has been superseded by the El Tor biotype, the cause of the current seventh pandemic (49). The El Tor biotype is

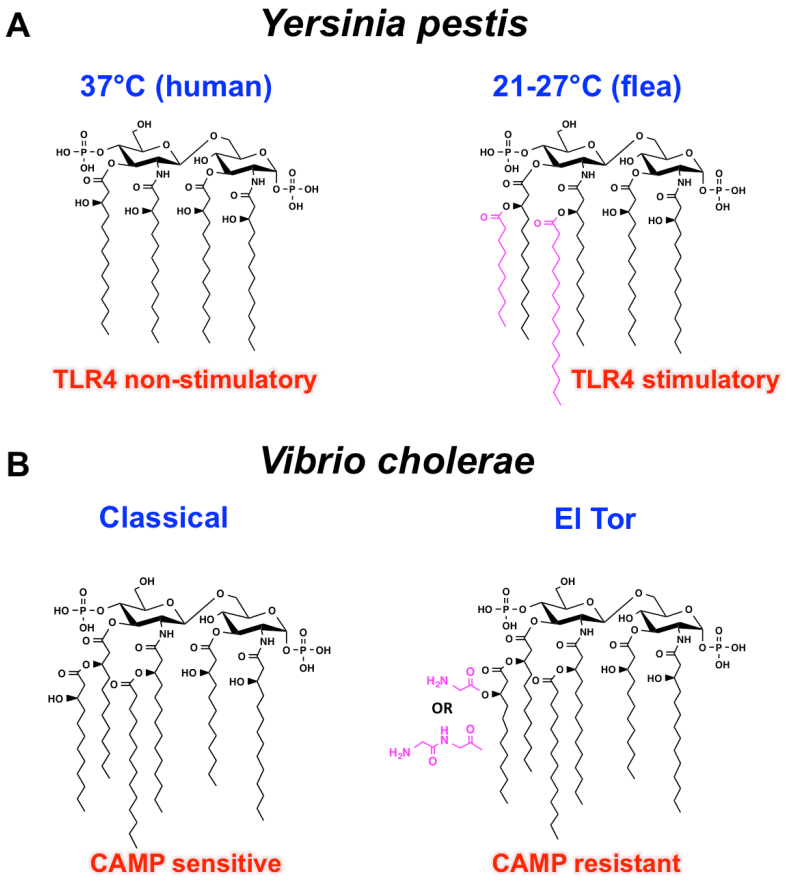

Figure 1.4: Conditional lipid A modifications in *Y. pestis* and *V. cholerae*

(A) *Y. pestis* produces endotoxic hexa-acylated lipid A while in the flea host. When it enters the human host, it encounters a shift in temperature, which induces synthesis of tetra-acylated TLR4-antagonistic lipid A. **(B)** *V. cholerae* classical strains produce hexa-acylated lipid A that is sensitive to CAMPs like polymyxin B. El Tor strains evolved machinery to add a glycine or diglycine (pink) to the distal acyl chain, which drastically increases CAMP resistance.

resistant to the CAMP polymyxin B, while classical strains are not. This phenotypic difference has been attributed to the fact that El Tor strains modify their lipid A with glycine or diglycine residues, which increase the net positive charge of the outer membrane and promote resistance to CAMPs (Fig 1.4B)(50). Addition of this amino acid is orchestrated by proteins encoded by the *almEFG* operon, recently shown to be under the transcriptional control of novel TCS, VprAB (50, 51). While the *V. cholerae* genome contains a number of TCSs, VprAB is the first to be identified as playing a role in regulation of lipid A structure. Sensor VprB responds to environmental queues present in the intestinal lumen including bile and mildly acidic pH, and response regulator VprA controls expression of the *alm* operon upon activation by VprB. Mutants of VprAB do not modify their lipid A with glycine, and thus are sensitive to CAMPs. These mutants also show colonization defects in a suckling mouse model, establishing VprAB-dependent glycine modification as important for *V. cholerae* pathogenesis (52).

1.2.2.3 Regulation of lipid A modifications by two-component systems in Salmonella enterica *and* Escherichia coli

Salmonella enterica serovar *typhimurium* is another enteric pathogen known to encode several TCSs that regulate lipid A modification under different growth and life cycle conditions. The lipid A produced by this organism is structurally identical to that of *E. coli* when unmodified. Both organisms have evolved complex circuitry at the transcriptional and post-translational level to regulate lipid A modifications in different environmental conditions. Two major TCSs, PhoPQ and PmrAB, are known to control expression of a number of modification enzymes in these enteric organisms; conditions

such as low pH and presence of CAMPs can activate both systems, while low levels of divalent cations are sensed only by PhoQ and high levels of Fe^{3+} are sensed only by PmrB (40, 53–55). Alterations to the lipid A structure induced by a given external signal often change the immunogenicity or charge of the molecule in a manner that helps the bacterium survive. For example, *S. enterica* alters its lipid A structure to better survive in the intestinal lumen and within host macrophages, its primary niches during infection (56, 57).

The PhoPQ regulon of *Salmonella* spp. includes two genes involved in lipid A modification: *pagP,* encoding an outer membrane palmitoyl transferase, and *pagL,* encoding an outer membrane deacylase (Fig 1.5)(58, 59). The structural changes that these enzymes bring to the lipid A molecule are thought to limit TLR4 stimulation, reinforce the barrier function of the outer membrane, and protect against attack by CAMPs (60, 61). EptA, a phosphoethanolamine (pEtN) transferase, and ArnT, a 4-amino-4-deoxy-L-arabinose (L-Ara4N) transferase, are upregulated under PmrB-activating conditions (62–65). These groups mask the anionic charge of the phosphate groups, yielding an outer membrane that is not as attractive to destructive CAMPs (Fig 1.5)(63, 64).

While there exists some overlap in which signals are sensed by these two systems, they are also linked at a post-translational level by small protein, PmrD (66). *pmrD* is expressed under PhoPQ-activating conditions and as a protein, it maintains PmrA in an active transcriptional regulator state (67–69). As a result, CAMP-protective PmrAB-

dependent lipid A modifications by EptA and ArnT also occur when environmental conditions exclusively activate PhoPQ in *Salmonella* spp. (66). Chapter 3 of this work explores the same PhoPQ-PmrAB cross-talk network in *E. coli,* which was previously thought not to be capable of connecting these systems (70).

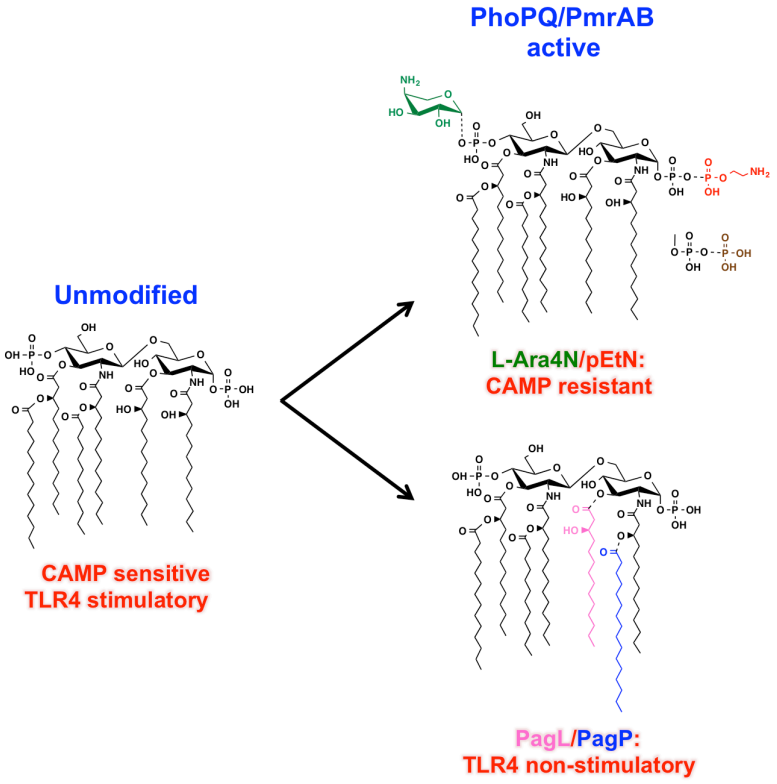

Figure 1.5: Lipid A modifications in *S. enterica* and *E. coli* alter the physiological properties of the molecule

Salmonella and *E. coli* modify their lipid A with multiple chemical groups in various conditions. Addition of L-Ara4N (green) and pEtN (red) promotes CAMP resistance, while removal of the 3-linked acyl chain by PagL and addition of a secondary palmitate at the 2-linked primary acyl chain decreases TLR4 stimulation.

The following body of research explores two stories in gram-negative organisms that occupy vastly different ecological niches, united by the common thread of lipid A structure and function. In *H. pylori,* a Raetz pathway late acyltransferase with the same activity as *E. coli* LpxM but unique substrate preferences is discovered and characterized (25). Its activity is essential for downstream modification of *H. pylori* lipid A and survival of this hardy organism. In *E. coli,* the PmrD protein is found to be an active connector of PhoPQ and PmrAB, promoting modification of the lipid A with amine-containing groups that protect against CAMPs (70). This finding has overturned a previous long-held belief in this field that *E. coli* PmrD is an inactive connector of these TCSs.

Chapter 2: Identification of a broad family of lipid A late acyltransferases with non-canonical substrate specificity[1]

2.1 INTRODUCTION

The outer membrane of most gram-negative bacteria is an asymmetric bilayer, with the inner leaflet composed of phospholipids and the outer leaflet consisting of lipopolysaccharide (LPS) (1). LPS is anchored to the outer bacterial membrane by the lipid A domain. Lipid A, also known as endotoxin, is a bioactive molecule that triggers the host innate immune response when it binds the Toll-like receptor 4/myeloid differentiation factor 2 (TLR4/MD2) complex (71). High LPS concentrations experienced during infection can activate signaling cascades that lead to endotoxic shock, which can prove fatal for the host (3, 4). In this way, lipid A is a major virulence factor for most gram-negative organisms.

Interestingly, some organisms produce lipid A that does not elicit a strong immune response. For example, *Helicobacter pylori* lipid A is up to 1000-times less immunostimulatory than the typical lipid A of *Escherichia coli* (33–35). The discrepancy in toxicity between *E. coli* and *H. pylori* lipid A can be attributed to important structural differences in the two biomolecules (Fig 2.1). *E. coli* generates a *β*-(1',6)-linked disaccharide of glucosamine that is *bis*-phosphorylated, hexa-acylated, and attached to

[1]Large portions of this chapter have been previously published (copyright by John Wiley and Sons, re-used with permission). Rubin EJ, O'Brien JP, Ivanov PL, Brodbelt JS, Trent MS. 2014. Identification of a broad family of lipid A late acyltransferases with non-canonical substrate specificity. Mol Microbiol 91:887–899. (E.J.R. designed and performed experiments and wrote the manuscript under the supervision of M.S.T.; J.P.O designed and performed the ESI and UVPD-MS experiments under the supervision of J.S.B.; P.L.I. assisted in cloning experiments).

two Kdo sugars (Fig 2.1A) (71). Conversely, the final *H. pylori* lipid A structure displays alterations in acyl chain length and number, phosphate group and Kdo sugar number, as well as addition of a polar functional group, phosphoethanolamine (pEtN) (Fig 2.1B, right) (22, 27–29, 72). Importantly, such structural changes have been shown to alter the TLR4 response and therefore the innate immune reaction in the host (8, 73). Indeed, *H. pylori* lipid A is a poor stimulator of the TLR4/MD2 complex, which allows it to evade the host immune response and establish a long-term infection in the gastric epithelium (29, 34, 74, 75).

As in other gram-negative organisms, *H. pylori* lipid A is synthesized via the Raetz pathway, which builds the lipid A starting from an activated nucleotide sugar donor (76). This process occurs in the bacterial cytoplasm and produces a structure very similar to that of *E. coli* lipid A (Fig 2.1B, left). This hexa-acylated species is then heavily modified by a 5-enzyme cascade during transport across the inner and outer membranes, yielding the final surface-presented structure (Fig 2.1B, right) (22, 27, 29, 72, 77).

In *E. coli* lipid A biosynthesis, the Kdo sugars must be present in order for 2′- and 3′-secondary acylation of lipid IV_A, catalyzed by late acyltransferases LpxL and LpxM, respectively (Fig 2.1A) (78). Further, the substrate preferences of the late acyltransferases establish their enzymatic order; LpxL acts before LpxM (18, 19). Here, we characterize a lipid A acyltransferase in *H. pylori* that is functionally similar to but lacks complete or significant sequence homology to *E. coli* LpxM (Table 2.1). This enzyme, from hereon referred to as LpxJ, transfers the secondary acyl chain to the 3′-linked primary acyl chain

of *H. pylori* lipid A, similarly to LpxM in *E. coli*. However, LpxJ can perform acyltransfer regardless of the presence of Kdo sugars and can do so before the *H. pylori* LpxL homolog, Jhp0265 (22). The enzymatic flexibility of LpxJ allows for the unprecedented option of multiple routes at the end of the lipid A biosynthesis pathway, a possibility not observed in *E. coli* (Fig 2.9). Ultimately, the altered order of 3′-secondary acylation could reflect the importance of this chain in downstream processes, such as transport and presentation of *H. pylori* lipid A. We examine LpxJ homologs in two closely related organisms and demonstrate that these enzymes are also capable of non-ordered 3′-secondary acylation activity. Together, the enzymes studied here represent a previously uncharacterized family of lipid A late acyltransferases with homologs in a wide range of bacterial species. While functionally related to *E. coli* LpxM, these proteins are different at the primary sequence level, resulting in unique enzymatic characteristics and a less stringently ordered lipid A biosynthesis pathway.

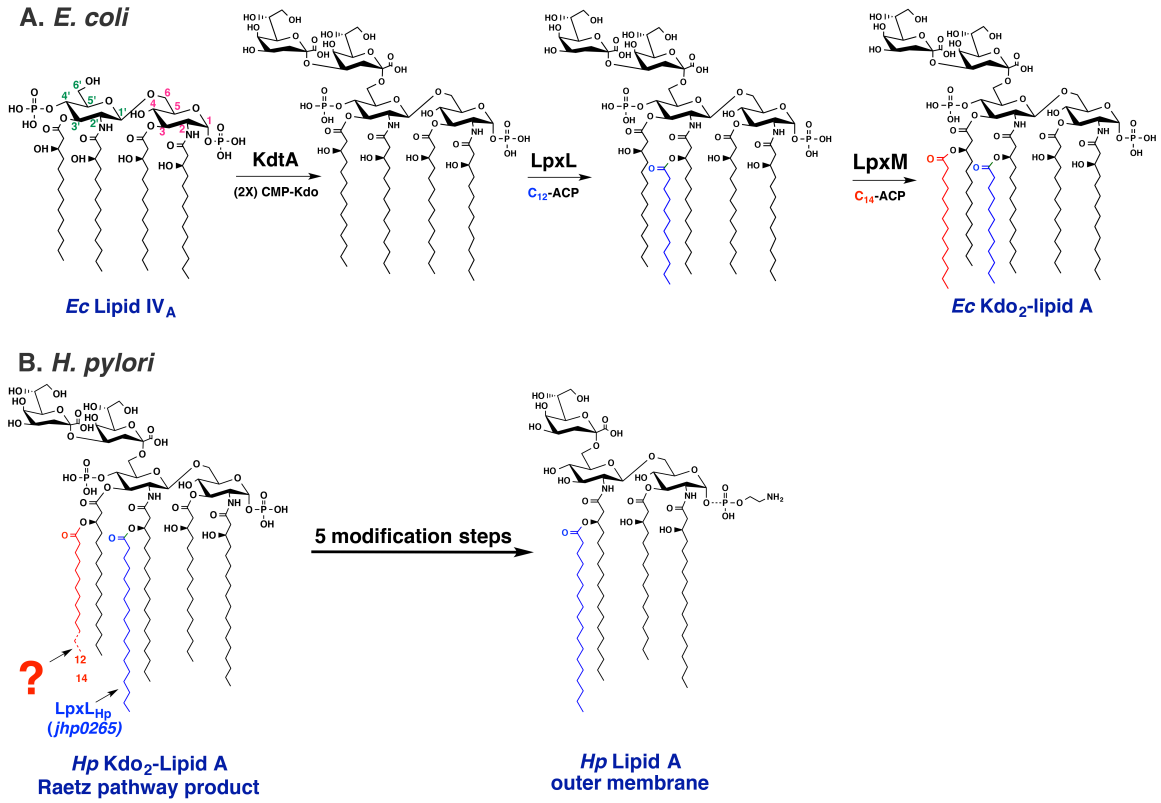

Figure 2.1 Final steps of the Raetz pathway in *E. coli* and the missing late acyltransferase of *H. pylori*

(A) In *E. coli* once lipid IV_A is synthesized, KdtA then transfers 2-Kdo sugars to the hydroxyl group at the 6′ position. Only then are secondary acyl chains transferred to the 2′- and 3′-primary acyl chains by LpxL and LpxM, respectively, generating first penta-acylated lauroyl-Kdo_2-lipid IV_A and finally Kdo_2-lipid A. Carbon numbers are shown for reference in the left-most structure. **(B)** *H. pylori* produces a hexa-acylated lipid A product via the Raetz pathway (left), which is then modified by a series of enzymes to create the structure presented in the outer membrane (right). Previously unknown was the identity of the acyltransferase that transfers the secondary acyl chain to the 3′-primary acyl chain during Raetz pathway biosynthesis (red question mark). We have identified this enzyme as $LpxJ_{Hp}$, encoded by gene *jhp0255* in *H. pylori* strain J99.

2.2 RESULTS

2.2.1 *H. pylori* encodes an enzyme functionally comparable to *E. coli* LpxM

Previously, we characterized *H. pylori* $LpxL_{Hp}$ (*jhp0265*), a homolog of *E. coli* LpxL that transfers a C18:0 secondary acyl chain to the 2′-linked acyl chain of *H. pylori* lipid IV_A (22). Because *H. pylori* has been shown to produce a hexa-acylated lipid A precursor (Fig. 2.1B, left) that is further processed by the modification pathway, it follows that an unidentified acyltransferase functionally similar to *E. coli* LpxM is required (30, 72, 79). Stead et al. observed a putative LpxM-like activity by demonstrating that purified *H. pylori* membranes are capable of adding a secondary acyl chain to the 3′-linked primary chain of penta-acylated lipid A substrate *in vitro* (22). However, a PSI-BLAST search using LpxM as the query sequence revealed only $LpxL_{Hp}$, suggesting that *H. pylori* encodes a functional equivalent of *E. coli* LpxM that is not identifiable based on sequence homology.

We identified *jhp0255* as a strong candidate to encode the "missing" late acyltransferase by consulting the Pfam database, an online tool that groups proteins by predicted functional domains (80). Specifically, we looked within the acyltransferase clan (CL0228), which contains proteins with a putative acyl acceptor pocket domain, suggesting a functional role in acyl transfer reactions. This clan has four families: a lipid A acyltransferase family, of which LpxM and $LpxL_{Hp}$ are members, the diacylglycerol acyltransferase family, glycerolipid acyltransferase family, and the domain of unknown function family (DUF374). The DUF374 protein for *H. pylori* is Jhp0255, which is previously uncharacterized and located close on the chromosome to other previously

studied LPS biosynthesis genes including $lpxL_{Hp}$ (81). Because both Jhp0255 and *E. coli* LpxM are grouped into separate families within the same Pfam clan, they likely share a distant common ancestor that diverged through evolution. At the primary sequence level, however, the *H. pylori* enzyme differs significantly from LpxM (Table 2.1) and the acyl acceptor domain appears to be the only common sequence thread between the two proteins. Accordingly, we have reannotated Jhp0255 as LpxJ, as it was discovered in *H. pylori* strain J99.

Table 2.1: Genetic relationships between *E. coli* LpxM and relevant proteins.

Organism	Protein	Homology (gaps)[a]	Approximate E values
Helicobacter pylori	LpxJ (Jhp0255)	25, 41, 147 (33)	0.028
Campyobacter jejuni	LpxJ (Cjj81176_0482)	6, 6, 10 (0); 5, 8, 13 (0)	0.63, 1.4
Wolinella succinogenes	LpxJ (Ws1775)	9, 21, 48 (1)	0.37
Salmonella enterica subsp. enterica	MsbB	300, 314, 323 (0)	0.0
Klebsiella pneumonia	MsbB	270, 291, 323 (0)	0.0
Haemophilus influenzae	MsbB	136, 196, 301 (2)	3e-96

[a]Homology is given as the number of identities, number of positives, number of residues (including gaps) in the related segment(s) when compared with *E. coli* LpxM, a protein of 323 amino acid residues.

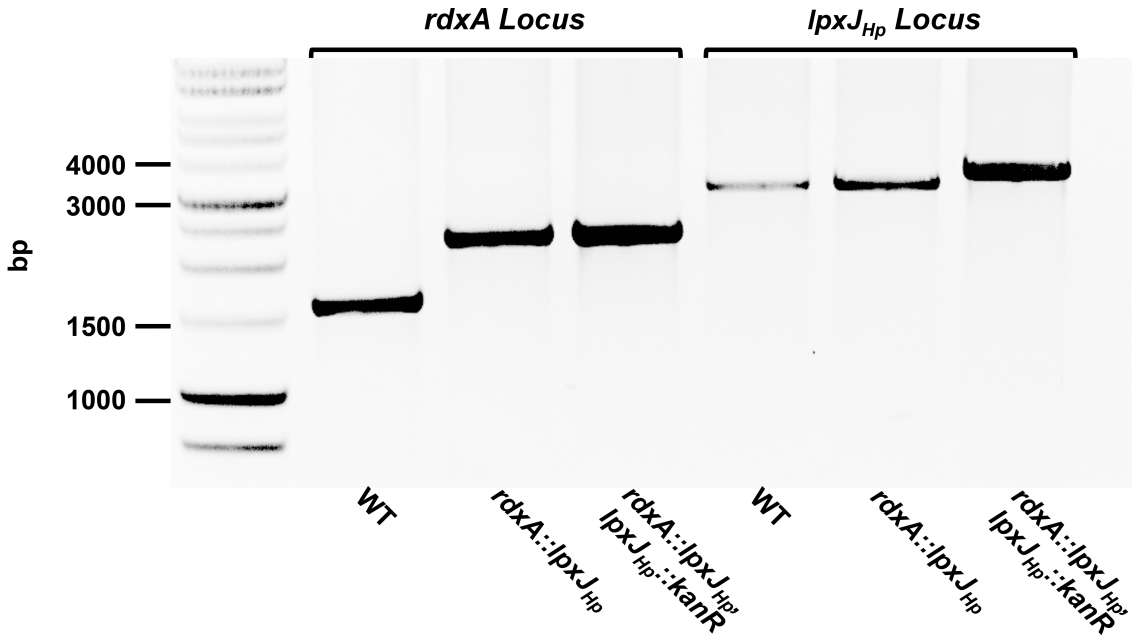

Figure 2.2 *lpxJ*$_{Hp}$ is an essential gene that can only be knocked-out after prior complementation

PCR analysis of genomic DNA isolated from *H. pylori* strain J99 wild type (WT), J99 with an additional copy of *lpxJ*$_{Hp}$ inserted into the *rdxA* locus (*rdxA::lpxJ*$_{Hp}$), and J99 with a copy of *lpxJ*$_{Hp}$ inserted into the *rdxA* locus and finally the endogenous copy of *lpxJ*$_{Hp}$ replaced with a kanamycin resistance cassette (*rdxA::lpxJ*$_{Hp}$*, lpxJ*$_{Hp}$*::kanR)*. Lanes 1-3 show that insertion of *lpxJ*$_{Hp}$ into the *rdxA* locus produces a chromosomal fragment ~650bp larger than the wild type fragment. Lanes 4-6 show that insertion of the kanamycin resistance cassette at the endogenous *lpxJ*$_{Hp}$ locus produces a fragment ~150bp larger. Insertion of the kanamycin cassette at the *lpxJ*$_{Hp}$ locus can only occur in a strain that already has a second copy of *lpxJ*$_{Hp}$ elsewhere on the chromosome (in this case, at *rdxA*). Attempts to chromosomally knock-out *lpxJ*$_{Hp}$ without prior complementation failed due to the essential nature of the gene.

2.2.2 $LpxJ_{Hp}$ complements a penta-acylated *E. coli lpxM* mutant, restoring a hexa-acylated phenotype

To investigate the role of $LpxJ_{Hp}$ in *H. pylori* lipid A biosynthesis, we attempted to generate a mutant strain by replacing its coding sequence in the genome with a kanamycin antibiotic resistance cassette. However, multiple efforts to obtain this mutant were unsuccessful in several *H. pylori* strains, suggesting that the gene product is essential for viability. Indeed, insertional deletion of $lpxJ_{Hp}$ was only successful after providing the bacterium with a second copy of the gene by chromosomal complementation at the *rdxA* locus (Fig 2.2). Inactivation of the *H. pylori rdxA* locus leads to metronidazole resistance, which can be used to select for colonies containing the complemented gene of interest at this locus.

In the absence of a viable deletion mutant, we expressed $LpxJ_{Hp}$ in the *E. coli lpxM* mutant strain BN2 (Table 5.1), which produces a penta-acylated lipid A, to determine if $LpxJ_{Hp}$ could generate hexa-acylated lipid A species *in vivo*. Indeed, chromatographic separation of radiolabeled lipid A isolated from BN2 expressing $LpxJ_{Hp}$ revealed a migration pattern consistent with the presence of hexa-acylated lipid A (Fig 2.3, lane 3). Hexa-acylated lipid A isolated and analyzed from strain BN1 served as a positive control (Table 5.1)(Fig 2.3, lane 1). Strain BN2 containing empty vector produced only penta-acylated lipid A (Fig 2.3, lane 2), suggesting that $LpxJ_{Hp}$ catalyzes transfer of the secondary acyl chain to the 3′-linked primary acyl chain of lipid A. These findings were confirmed by MALDI-TOF mass spectrometry; $LpxJ_{Hp}$ transfers a C12:0 or C14:0 chain (Fig 2.4B), to generate major molecular ions at *m/z* 1768.3 and 1796.3.

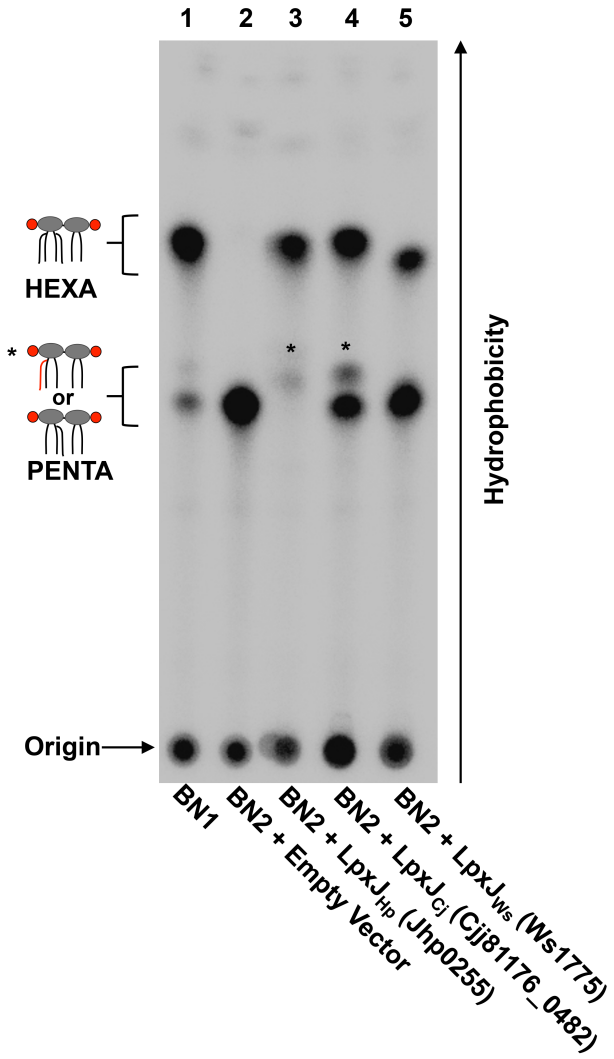

Figure 2.3 $LpxJ_{Hp}$ and homologs in two other Epsilonproteobacteria complement a hexa-acylated lipid A phenotype in a penta-acylated *E. coli* LpxM mutant

Radiolabeled lipid A from various *E. coli* strains was isolated and separated by TLC. Expression of $LpxJ_{Hp}$ (lane 3), $LpxJ_{Cj}$ (lane 4), and $LpxJ_{Ws}$ (lane 5) in strain BN2, which normally produces penta-acylated lipid A (lane 2), complements this penta-acylated strain to a hexa-acylated phenotype (as shown for positive control strain BN1, lane 1). Asterisks (*) in lanes 3 and 4 correspond to lipid A species formed by alternative acylation order (see cartoon at left). The presence of residual penta-acylated product in the $LpxJ_{Cj}$ and $LpxJ_{Ws}$ strains (dark spots migrating at the same level as BN2 vector control, lane 2) suggests these enzymes may not be as efficient as $LpxJ_{Hp}$ in this system.

The lipid A species that results from transfer of a C14:0 chain by $LpxJ_{Hp}$ is almost identical in molecular mass to the lipid A of hexa-acylated control strain BN1 (*m/z* 1796.0)(Fig 2.5). Taken together, these results strongly suggest that $LpxJ_{Hp}$ transfers a C12:0 or C14:0 secondary acyl chain to the 3′-linked primary acyl chain of *H. pylori* lipid A.

2.2.3 Homologs of $LpxJ_{Hp}$ are found in other Epsilonproteobacteria

Due to the unexpected sequence difference between $LpxJ_{Hp}$ and *E. coli* LpxM, we hypothesized that other bacteria may encode homologs of LpxJ instead of LpxM. In two closely related Epsilonproteobacteria, we identified *Campylobacter jejuni* protein Cjj81176_0482 ($LpxJ_{Cj}$) and *Wolinella succinogenes* protein Ws1775 ($LpxJ_{Ws}$) as homologs of $LpxJ_{Hp}$ and members of the DUF374 family. The *C. jejuni* and *W. succinogenes* proteins were expressed individually in strain BN2 and radiolabeled lipid A was isolated from each strain. Both proteins complemented the penta-acylated mutant, leading to formation of a hexa-acylated lipid A species (Fig 2.3, lanes 4, 5). TLC results for *C. jejuni* and *W. succinogenes* proteins were confirmed with MALDI-TOF mass spectrometry to show that $LpxJ_{Cj}$ transfers a C16:0 acyl chain and $LpxJ_{Ws}$ transfers a C12:0 chain to the penta-acylated lipid A framework (Fig 2.4C, D).

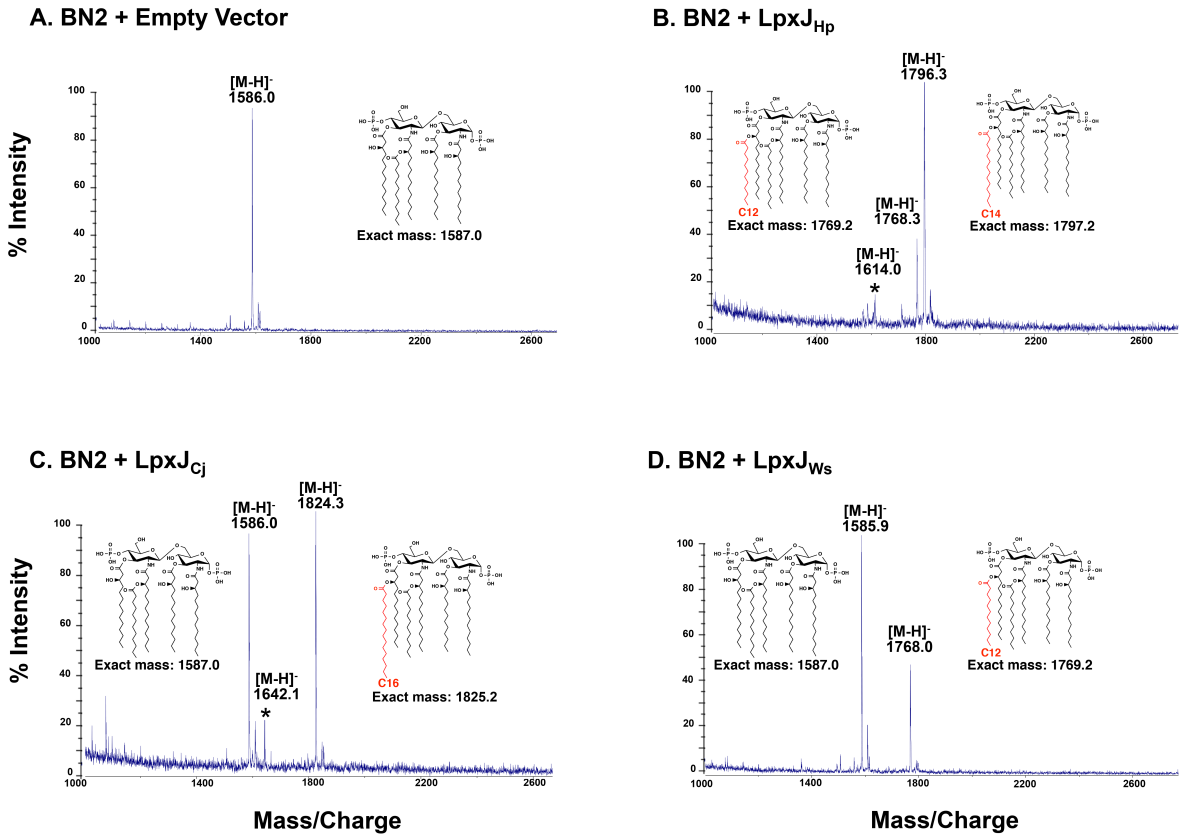

Figure 2.4 MALDI-TOF mass spectrometry of *E. coli* LpxM mutant, BN2 expressing acyltransferase genes from three Epsilonproteobacteria

(A) Strain BN2 produces a major molecular ion peak at *m/z* 1586.0, corresponding to penta-acylated lipid A. **(B)** Expression of $LpxJ_{Hp}$ in the BN2 background produces two main peaks at *m/z* 1768.3 and *m/z* 1796.3. The former peak corresponds to addition of a C12:0 group and the latter corresponds to addition of a C14:0 group to the 3′-linked acyl chain of lipid A. The asterisk (*), which indicates the peak at *m/z* 1614.0, represents penta-acylated lipid IV_A with the fifth chain on the 3′-primary acyl chain, which can form before 2′ secondary acylation occurs. This species is the same as the (*)-designated species in Fig. 2, lane 3. **(C)** Expression of $LpxJ_{Cj}$ in the BN2 background produces a major peak at *m/z* 1824.3, corresponding to C16:0 addition to the lipid A. The peak at *m/z* 1586.0 represents residual penta-acylated lipid A. The asterisk (*), which indicates the peak at *m/z* 1642.1, represents penta-acylated lipid IV_A with the fifth chain on the 3′-primary acyl chain, which can form before 2′ secondary acylation occurs. This species is the same as the (*)-designated species in Fig. 2, lane 4. **(D)** Expression of $LpxJ_{Ws}$ in the BN2 background produces hexa-acylated lipid A with a peak at 1768.0, corresponding to C12:0 addition to the lipid A.

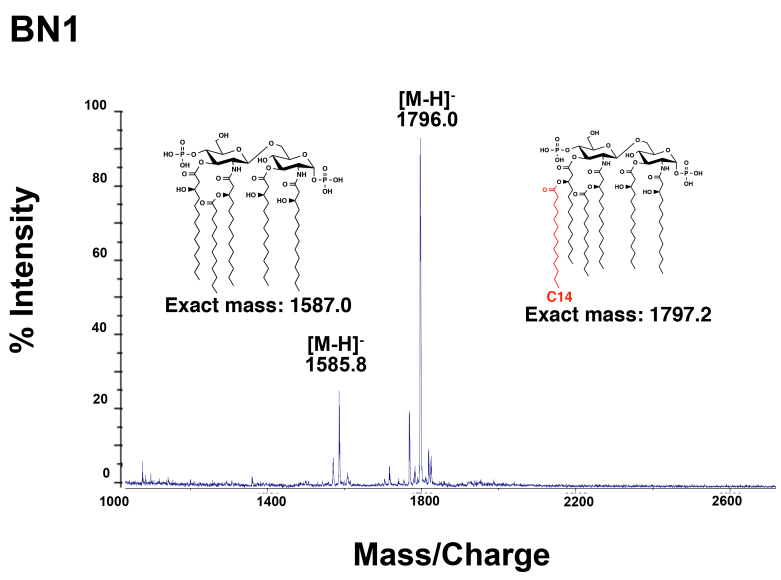

Figure 2.5 MALDI-TOF mass spectrometry of hexa-acylated control strain BN1

BN1 (Table 5.1) produces a hexa-acylated lipid A with major peak at *m/z* 1796.0. This strain also produces a residual penta-acylated species, represented by the peak at *m/z* 1585.8.

2.2.4 DUF374 proteins are found in a diverse range of organisms

Further investigation into Pfam family DUF374 revealed that over 500 species encode at least one protein that can be classified into this predicted acyltransferase family. $LpxJ_{Hp}$ has putative homologs in a surprisingly large number of organisms ranging from other bacterial classes including Alpha, Delta, and Zetaproteobacteria, to other phyla including Fusobacteria, Chlamydiae, Acidobacteria, and Spirochaetes (Table 2.2). Relevant BLAST scores demonstrating homology between $LpxJ_{Hp}$ and a number of other DUF374 proteins are provided in Table 2.3. Of note, the organisms that encode a homolog of $LpxJ_{Hp}$ possess a homolog to *E. coli* LpxL, but not LpxM (Table 2.2).

Table 2.2: LpxJ homologs in Pfam DUF374

Organism	Strain	Class	*E. coli* LpxL homolog	*E. coli* LpxM homolog	LpxJ homolog
Helicobacter pylori	J99	Epsilonproteobacteria	Yes/Jhp0265	No/--	Yes/$LpxJ_{Hp}$
Helicobacter hepaticus	ATCC 51449	Epsilonproteobacteria	Yes/HH0982	No/--	Yes/HH1275
Campylobacter jejuni	81-176	Epsilonproteobacteria	Yes/Cjj81176_1151	No/--	Yes/$LpxJ_{Cj}$
Campylobacter fetus subsp. fetus	82-40	Epsilonproteobacteria	Yes/CFF8240_1400	No/--	Yes/CFF8240_1376
Wolinella succinogenes	DSM1740	Epsilonproteobacteria	Yes/Ws1908	No/--	Yes/$LpxJ_{Ws}$
Bartonella bacilliformis	KC583	Alphaproteobacteria	Yes/BARBAKC583_0617	No/--	Yes/BARBAKC583_1205
Brucella melitensis	ATCC 23457	Alphaproteobacteria	Yes/BMEA_A0889	No/--	Yes/BMEA_A0457
Rickettsia rickettsia	Hlp #2	Alphaproteobacteria	Yes/RPK06045	No/--	Yes/RPK00655
Desulfovibrio vulgaris	Miyazaki F	Deltaproteobacteria	Yes/DvMF_0365	No/--	Yes/DvMF_0366
Fusobacterium nucleatum	CC53	Fusobacteriales	Yes/H848_01687	No/--	Yes/H848_04757
Escherichia coli	MG1655	Gammaproteobacteria	Yes/LpxL	Yes/LpxM	No/--
Salmonella enterica serovar Typhimurium	LT2	Gammaproteobacteria	Yes/LpxL	Yes/LpxM	No/--

Although enzymatic activity has not been confirmed for all members of DUF374, our results strongly suggest that this previously unstudied protein family contains acyltransferases that participate in lipid A biosynthesis in place of LpxM.

Table 2.3: Homologs of $LpxJ_{Hp}$ found in DUF374

Organism	Protein	I,P,G (%)[a]	E value[a]
Helicobacter pylori	Jhp0255 ($LpxJ_{Hp}$)	100, 100, 0	0.0
Helicobacter hepaticus	HH1275	41, 61, 1	4e-55
Campylobacter jejuni	Cjj81176_0482 ($LpxJ_{Cj}$)	33, 52, 1	6e-41
Campylobacter fetus subsp. fetus	CFF8240_1376	41, 60, 1	3e-35
Wolinella succinogenes	Ws1775 ($LpxJ_{Ws}$)	44, 66, 1	9e-52
Bartonella bacilliformis	BARBAKC583_1205	31, 42, 7	3e-10
Brucella melitensis	BMEA_A0457	26, 44, 7	1e-08
Rickettsia rickettsia	RPK00655	26, 46, 7	4e-17
Desulfovibrio desulfuricans	DvMF_0366	32, 48, 10	2e-25
Fusobacterium nucleatum	H848_04757	34, 54, 1	3e-23

[a]Alignments scores (I, identities; P, positives; G, gaps) and E values for each protein compared with H. pylori Jhp0255 using NCBI BLASTP2.2.27.

2.2.5 $LpxJ_{Hp}$ acts on tetra- or penta-acylated lipid A, with or without Kdo sugars

In *E. coli*, LpxL and LpxM can only acylate the lipid A structure after the two 6′-Kdo sugar residues are added to the tetra-acylated lipid IV_A donor (Fig 2.1A)(19). The same is true for $LpxL_{Hp}$, which also requires Kdo addition for activity (22). Surprisingly, enzymatic assays using radiolabeled lipid IV_A substrate showed that $LpxJ_{Hp}$ does not

require the presence of Kdo sugars to acylate lipid A (Fig 2.6A). This is particularly interesting given the fact that it is expected to catalyze the final step in the pathway as LpxM does in *E. coli*. Beyond this, the enzyme also displays flexibility in terms of substrate acyl chain number, adding to both Kdo_2-lipid IV_A (tetra) and lauroyl-Kdo_2-lipid IV_A (penta) (Fig 2.6A).

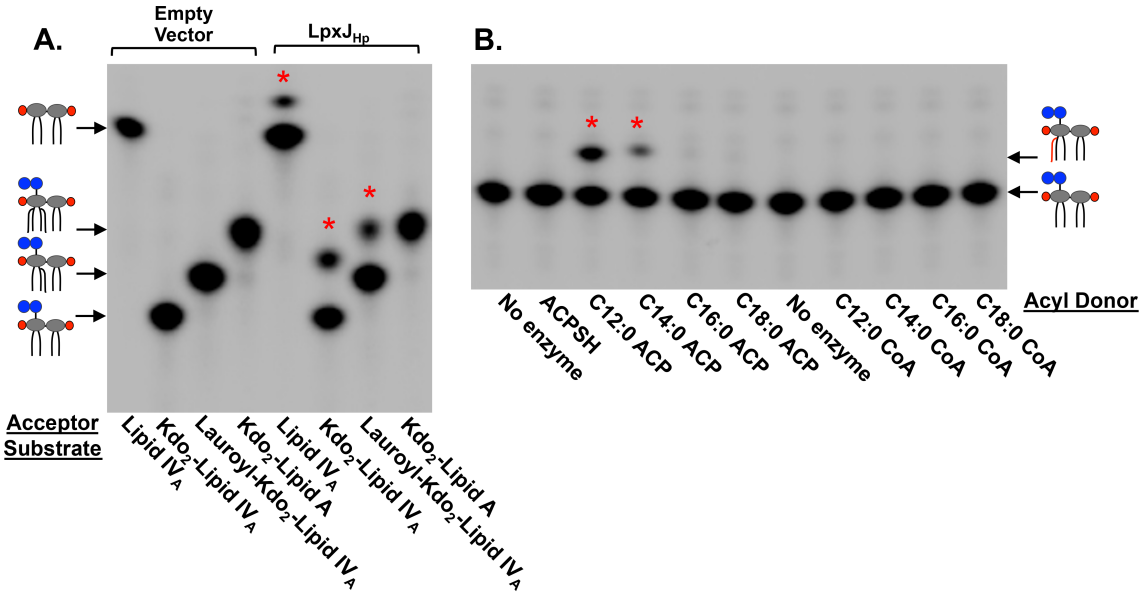

Figure 2.6 Enzymatic characteristics of $LpxJ_{Hp}$

(A) Membranes from strain BN2 containing empty vector or pWSK29*jhp0255* (*$lpxJ_{Hp}$*) were assayed with various [4′-^{32}P]-labeled lipid substrates and 5μM C12:0 acyl-ACP. Membranes from the empty vector strain showed no activity from endogenous *E. coli* proteins, while membranes expressing $LpxJ_{Hp}$ acylated all substrates except Kdo_2-[4′-^{32}P] lipid A. Acylated reaction products are indicated with red asterisks (*). **(B)** BN2 membranes expressing $LpxJ_{Hp}$ were tested with Kdo_2-[4′-^{32}P] lipid IV_A and 5μM acyl-ACPs/acyl-CoAs as labeled. $LpxJ_{Hp}$ uses C12:0 and C14:0 acyl-ACPs as donor molecules. Acylated reaction products are indicated with red asterisks (*).

The ability of $LpxJ_{Hp}$ to add to both a tetra- and penta-acylated substrate suggests that its activity can precede $LpxL_{Hp}$ activity, such that secondary acylation at the 3′-primary chain precedes secondary acylation at the 2′-primary chain. This order is reverse of the strict LpxL-then-LpxM order found in *E. coli* and many other Gram-negative organisms (18, 19).

$LpxJ_{Hp}$ does not, however, transfer an acyl chain to hexa-acylated substrate Kdo_2-lipid A, which already has secondary acyl chains attached to the 2′- and 3′-primary chains (Fig 2.6A). With this substrate, any further acylation by $LpxJ_{Hp}$ would have to occur at the hydroxyl groups of the primary acyl chains attached to the proximal glucosamine of the lipid A molecule. These results demonstrate that $LpxJ_{Hp}$ only transfers an acyl chain to the distal glucosamine (2′- or 3′-primary chain) and not the proximal (2- or 3-primary chain) side of the lipid A molecule. To confirm this result, we expressed $LpxJ_{Hp}$ in a tetra-acylated *E. coli* strain (MKV15b, Table 5.1) to allow the enzyme access to all possible secondary acylation positions, then subjected isolated lipid A to ultraviolet photo-dissociation (UVPD) mass spectrometry. UVPD of isolated lipid A allowed identification of a fragment ion (*m/z* 738.4, cleavage 12) that represents the unmodified proximal glucosamine of lipid A, which does not change between vector control and the strain expressing $LpxJ_{Hp}$ (Fig 2.8A,B). This confirms that the acylation pattern of the proximal sugar does not change upon expression of the *Helicobacter* acyltransferase, and therefore acylation by this enzyme must occur on the distal glucosamine.

With regard to acyl chain donor, $LpxJ_{Hp}$ is analogous to *E. coli* LpxM in that it can only utilize acyl-ACPs rather than acyl coenzyme A (acyl-CoA), preferring C12:0-ACP and C14:0-ACP (Fig 2.6B)(19). Importantly, isolated *H. pylori* lipid A has either a C12:0 or C14:0 secondary acyl chain at the 3′-primary acyl chain (29), suggesting that our *in vitro* system closely mimics an *in vivo* environment for this acyltransferase. These results combined with the ability of this enzyme to promote formation of hexa-acylated lipid A in a penta-acylated mutant allow us to definitively conclude that it adds a secondary acyl chain to the 3′-linked primary acyl chain of the lipid A molecule.

2.2.6 *Campylobacter* and *Wolinella* LpxJ only use tetra-acylated lipid A as substrate

Enzymatic activities of $LpxJ_{Cj}$ and $LpxJ_{Ws}$ were assayed with the same *in vitro* system and radiolabeled lipid substrates used for $LpxJ_{Hp}$. Both enzymes were unable to acylate a penta-acylated lipid A substrate and could only act on a tetra-acylated lipid A substrate, independent of Kdosylation state (Fig 2.7A). These results were initially confounding, given that both enzymes were capable of rescuing a penta-acylated mutant to a hexa-acylated phenotype *in vivo*. Taken together, this evidence indicates that $LpxJ_{Cj}$ and $LpxJ_{Ws}$ can only function before their respective 2′-secondary acyltransferase LpxL enzymes, requiring exclusively tetra-acylated substrate for activity (Fig 2.9). Similarly to $LpxJ_{Hp}$, neither $LpxJ_{Cj}$ nor $LpxJ_{Ws}$ utilized hexa-acylated Kdo_2-lipid A (Fig 2.7A). These results were also confirmed by UVPD mass spectrometry of lipid A isolated from strains individually expressing $LpxJ_{Cj}$ and $LpxJ_{Ws}$. The fragment ion representing the unmodified proximal side of the lipid A molecule was observed in lipid A from both strains

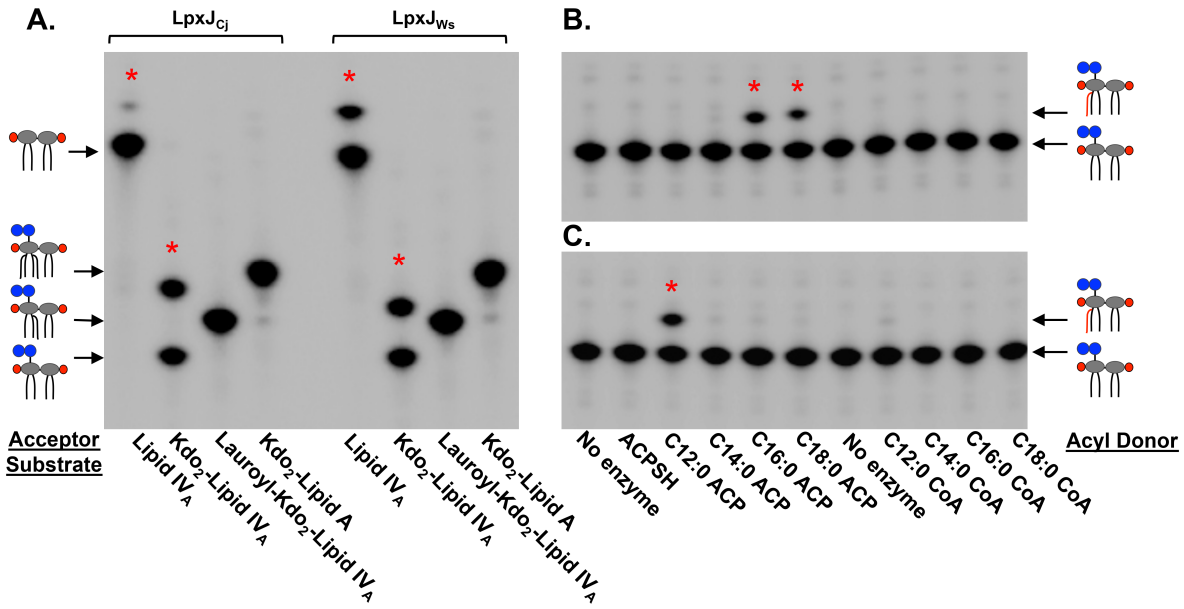

Figure 2.7 Enzymatic characteristics of $LpxJ_{Cj}$ and $LpxJ_{Ws}$

(A) Membranes from strain BN2 containing pWSK29*cjj81176_0482* (*$lpxJ_{Cj}$*) or pWSK29*ws1775* (*$lpxJ_{Ws}$*) were assayed with various [4′-^{32}P]-labeled lipid substrates and 5μM C12:0 acyl-ACP. $LpxJ_{Cj}$ and $LpxJ_{Ws}$ acylate [4′-^{32}P] lipid IV_A and Kdo_2-[4′-^{32}P] lipid IV_A substrates. Acylated reaction products are indicated with red asterisks (*). Empty vector control is the same as shown in Figure 4A. $LpxJ_{Cj}$ membranes **(B)** and $LpxJ_{Ws}$ membranes (C) were assayed with Kdo_2-[4′-^{32}P] lipid IV_A and 5μM acyl-ACPs/ acyl-CoAs as labeled. $LpxJ_{Cj}$ uses C16:0 and C18:0 acyl-ACPs as donor molecules, and $LpxJ_{Ws}$ uses C12:0 acyl-ACP. Acylated reaction products are indicated with red asterisks (*).

(*m/z* 738.4, cleavage 12), which demonstrates that acyl chain addition by each enzyme occurs at the distal glucosamine (Fig 2.8A,C,D).

In agreement with $LpxJ_{Hp}$, both $LpxJ_{Cj}$ and $LpxJ_{Ws}$ use acyl-ACP as a donor molecule, but not acyl-CoA, where $LpxJ_{Cj}$ can use C16:0 and C18:0 acyl-ACPs and $LpxJ_{Ws}$ prefers C12:0 acyl-ACP (Fig 2.7B, C). Although the *Campylobacter* enzyme can transfer C18:0, this is not likely to represent what occurs *in vivo*, as C. *jejuni* does not typically incorporate C18:0 into its lipid A structure. This activity may reflect relaxed substrate specificity or result from the available acyl-ACP substrate pool within the bacterial cell (82).

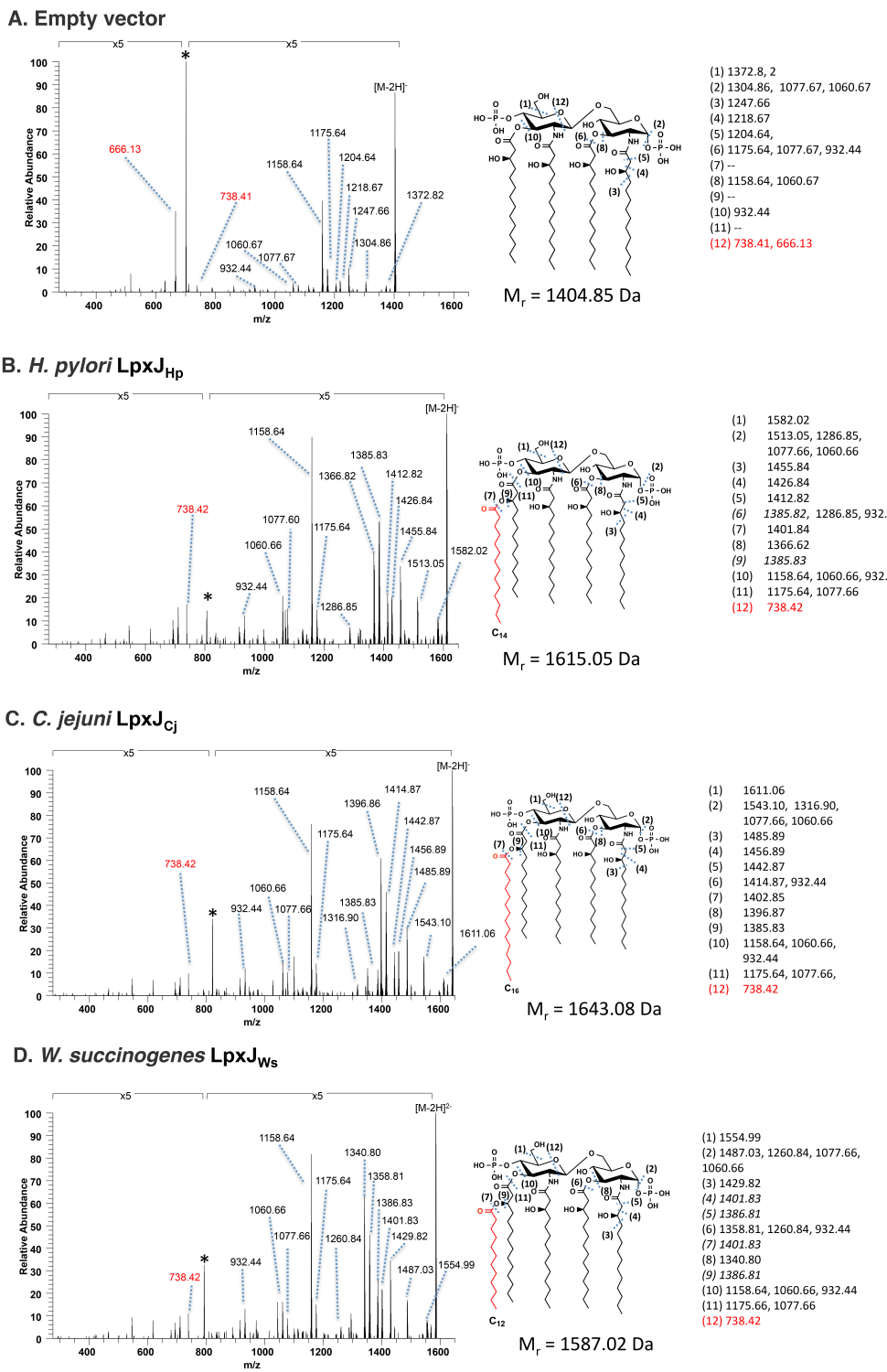

Figure 2.8 UVPD mass spectra of doubly deprotonated lipid A species and corresponding fragmentation maps

(A) Empty vector (M_r = 1404.85 Da), **(B)** *H. pylori* LpxJ (M_r = 1615.05 Da), **(C)** *C. jejuni* LpxJ (M_r = 1643.08 Da), and **(D)** *W. succinogenes* LpxJ (M_r = 1587.02 Da). Precursor fragment ions are labeled with an asterisk. Key fragment ions that allow the location of the extra acyl chain to be determined are labeled in red font. Cleavage sites that lead to isobaric fragment ions are italicized.

2.2.7 LpxJ activity can precede LpxL activity

In vitro assay results for the three LpxJ enzymes demonstrate their ability, or necessity, to perform acyltransfer to the 3′-primary chain before their respective LpxL enzymes transfer to the 2′-primary chain. This altered acylation order is unprecedented and in stark contrast to the strict LpxL-then-LpxM order established in *E. coli.* Evidence for reversed secondary acylation order can also be found in the radiolabeled lipid A isolated from strain BN2 expressing $LpxJ_{Hp}$ and $LpxJ_{Cj}$. The asterisks (*) in Fig 2.3, lanes 3 and 4, mark penta-acylated lipid A species that likely have the fifth chain attached as a secondary acyl chain to the 3′- as opposed to the 2′-primary chain. For example, $LpxJ_{Cj}$ transfers a C16:0 chain to the 3′-primary acyl chain, which generates a more hydrophobic product (*, lane 4) than penta-acylated BN2 lipid A, which has a secondary C12:0 chain at the 2′-primary chain (lower spot). The same is true for $LpxJ_{Hp}$, which transfers a C14:0 chain yielding a product (*, lane 3) that is slightly more hydrophobic than penta-acylated BN2 lipid A. Importantly, $LpxJ_{Hp}$ is more efficient in this *in vivo* system than the other two enzymes, probably due to its more flexible substrate specificity specificity. Both the alternative penta-acylated species produced by $LpxJ_{Hp}$ and $LpxJ_{Cj}$ are visible in their

MALDI-TOF spectra, annotated with an asterisk (*) in Fig 2.4B and C, respectively. Because $LpxJ_{Ws}$ transfers a C12:0 chain, its unique 3′-penta-acylated structure cannot be discerned from the *E. coli* structure (Fig 2.3, lane 5; Fig 2.4D).

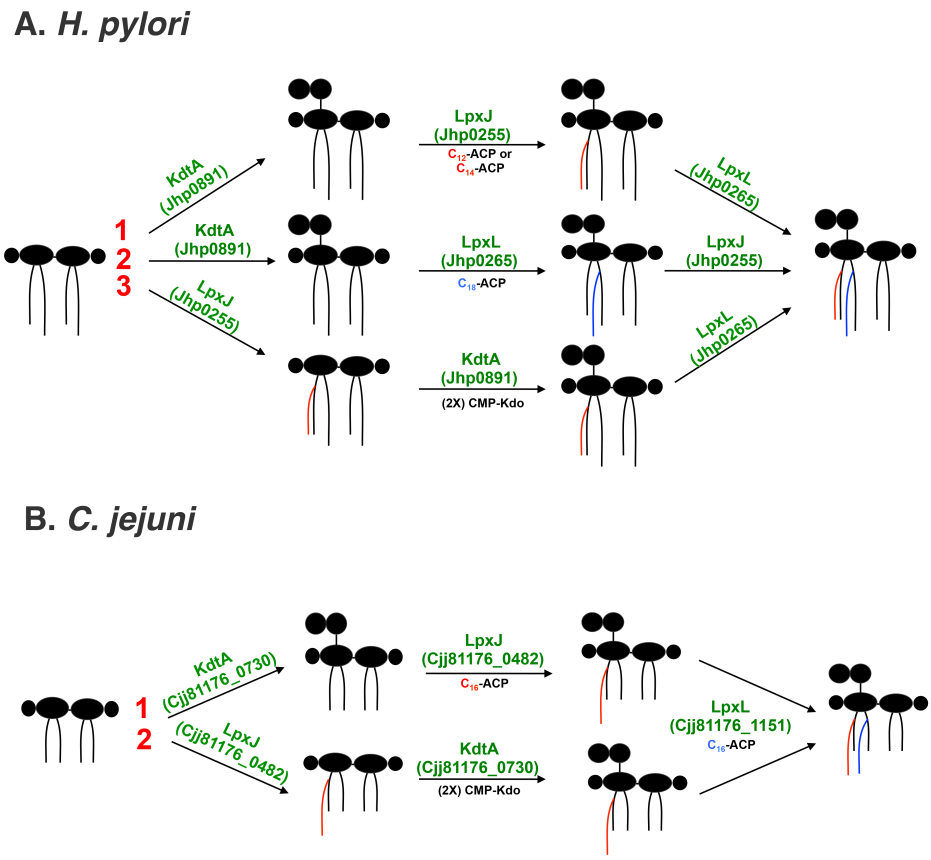

Figure 2.9 Multiple routes are possible at the end of the Raetz pathway in *H. pylori* and *C. jejuni*

(A) Due to the relaxed substrate specificity of $LpxJ_{Hp}$, *H. pylori* lipid A biosynthesis could follow three routes to the hexa-acylated end-product. **(B)** $LpxJ_{Cj}$ is specific for a tetra-acylated substrate regardless of Kdo sugars. Therefore, it could follow two routes to the hexa-acylated lipid A biosynthesis end-product. The same is true in *W. succinogenes* lipid A biosynthesis. This model does not consider the substrate specificities of KdtA and LpxL in these organisms, which are not fully characterized and will likely also determine the precise pathway taken.

2.3 DISCUSSION

Most gram-negative organisms produce lipid A, a complex bioactive molecule that anchors lipopolysaccharide to the outer bacterial membrane and is required for bacterial viability (76). Although the lipid A biosynthesis pathway is generally well-conserved across gram-negative bacteria, there remain exceptions. Here, we identify and characterize a previously unknown lipid A acyltransferase in *H. pylori* and two homologs in closely related Epsilonproteobacteria. These enzymes are distant by sequence from *E. coli* LpxM but perform a similar function, transferring a secondary acyl chain to the existing 3′ hydroxyacyl chain of lipid A (Fig 2.1, 2.9).

Although LpxJ and *E. coli* LpxM both transfer an acyl chain to the same position during lipid A biosynthesis in their respective organisms, they are unexpectedly different at the primary sequence level (Table 2.1) and possess distinct enzymatic characteristics. The only feature that LpxJ shares with LpxM is the presence of a putative acyl-acceptor binding pocket requisite for acyltransferase activity. Even within this binding pocket, however, there are divergences between LpxJ and LpxM. Specifically, LpxM contains the conserved $H(X)_4D/E$ active site motif, which was first identified in the glycerol-3-phosphate acyltransferase protein and is found in glycerophospholipid acyltransferases across bacterial, plant, and animal kingdoms (83–86). Within this active site motif the histidine and aspartic acid, or glutamic acid, residues act as an invariant catalytic dyad that activates the acceptor hydroxyl on the 3′-primary acyl chain of lipid A for nucleophilic attack of the acyl-ACP thioester bond (86). LpxJ and homologs in the DUF374 family lack the proximal coordinating aspartic or glutamic acid residue, which

suggests that the active site in DUF374-containing proteins has a different structural organization or acts through a different coordinating residue (83). Ultimately, this altered active site organization could change enzymatic substrate specificity, as the $H(X)_4D/E$ motif found in LpxL and LpxM is known to contact and coordinate the substrate during catalysis.

E. coli LpxM strongly prefers penta-acylated lipid A substrates and only shows activity on a tetra-acylated substrate when artificially over-expressed (19). This preference determines its activity as the last enzyme of the *E. coli* Raetz pathway, generating the LpxL-then-LpxM acylation order. Conversely, a novel feature of $LpxJ_{Hp}$ is its ability to act on both penta- and tetra-acylated substrates (Fig 2.6A). This suggests that it is capable of adding a secondary chain to the 3′-primary acyl chain before $LpxL_{Hp}$ adds a secondary chain to the 2′-primary acyl chain. Therefore, this enzyme does not require presence of a secondary acyl chain at the 2′-primary chain for enzymatic activity. Interestingly, $LpxJ_{Cj}$ and $LpxJ_{Ws}$ add only to a tetra-acylated lipid A, implying that these proteins strictly act in the reverse order of the canonical *E. coli* pathway, specifically requiring the absence of a secondary acyl chain on the 2′-primary chain for activity (Fig 2.7A, 2.9). In the case of $LpxJ_{Hp}$, the observed enzymatic flexibility could be the result of altered substrate specificity relative to the *C. jejuni, W. succinogenes*, and *E. coli* proteins, each of which utilizes a very specific (albeit different) lipid substrate. Further, $LpxJ_{Hp}$, $LpxJ_{Cj}$, and $LpxJ_{Ws}$ are able to perform acyltransfer regardless of the presence of Kdo sugars (Fig 2.6A, 2.7A); this introduces another deviation from the *E. coli* pathway,

which requires Kdosylated lipid A before LpxL and LpxM can add the secondary acyl chains (18, 19). With this, the enzymatic characteristics of LpxJ introduce the possibility of several routes in the final steps of the Raetz pathway, specifically, altered acylation and Kdosylation order (Fig 2.9). Some uncertainties remain as to how the observed *in vitro* enzymatic characteristics of these acyltransferases compare to precise activities *in vivo*. For example, $LpxL_{Hp}$ has not yet been shown to use $LpxJ_{Hp}$-acylated Kdo_2-lipid IV_A (that is, Kdo_2-lipid IV_A with a secondary acyl chain on the 3′-primary acyl chain) as substrate, only Kdo_2-lipid IV_A. This is in part due to the biochemical difficulty associated with generating the 3′-penta-acylated *in vitro* substrate. Without this result, it is difficult to definitively conclude that $LpxL_{Hp}$ participates in reversed acylation order during *in vivo* lipid A biosynthesis. Interestingly, the *C. jejuni* LpxJ protein can work in concert with *E. coli* LpxL to produce hexa-acylated lipid A, despite the fact that both enzymes prefer a tetra-acylated susbtrate (Fig 2.3, lane 4). This result suggests a possible trade-off in substrate specificity *in vivo*, allowing both $LpxJ_{Cj}$ and LpxL to sometimes use a less preferred penta-acylated substrate in order to complete lipid A biosynthesis in the *in vivo* *E. coli* system. However, this described activity for $LpxJ_{Cj}$ would be best understood in the organism of origin, *C. jejuni*.

The evolutionary pressure selecting for various orders of secondary acylation is unclear, but may be determined by the specificity of lipid transport protein, MsbA. This flippase translocates lipid A across the inner membrane from the cytoplasmic to periplasmic lipid leaflet after completion of the Raetz pathway; translocation by MsbA is

required for ultimate presentation of lipid A molecules on the bacterial surface (73). We hypothesize that the essential nature of LpxJ could be tied to MsbA, which might only recognize hexa-acylated lipid A or penta-acylated lipid A with a secondary acyl chain present at the 3′- primary acyl chain. If this were true, MsbA would not be able to flip the lipid A to the periplasmic leaflet in an LpxJ mutant, thus halting transport of the molecule to the bacterial cell surface leading to cell death. This theory is corroborated by the fact that mutants in $LpxL_{Hp}$ are viable (22), suggesting that the precise location of the secondary acyl chain at the 3′- and not the 2′-primary chain is critical for recognition of the lipid substrate by MsbA in *H. pylori*. The reversal in late acylation order could be a response to this potential narrow substrate range of MsbA as an effort to ensure that the 3′-primary chain gets acylated first since survival depends on it. In *C. jejuni* and *W. succinogenes*, there may be stronger pressure to maintain the reversed late acylation order, as their respective LpxJ enzymes can act only before LpxL, while LpxJ activity in *H. pylori* can precede or follow LpxL. It is currently unclear why these organisms function only in the reverse order while the *H. pylori* enzyme is more flexible.

The three enzymes characterized in this paper are all found in Epsilonproteobacterial species. However, the DUF374 protein class by which they are functionally classified represents an expansive array of other organisms including classes of bacteria such as Alpha, Delta, and Zetaproteobacteria; and even other phyla such as Fusobacteria, Chlamydiae, Acidobacteria, and Spirochaetes. The presence of DUF374 proteins in LpxM-deficient bacteria combined with the biochemical data presented here

strongly suggest that LpxJ represents a hitherto uncharacterized group of lipid A secondary acyltransferases.

The three DUF374 enzymes studied in this work possess novel characteristics relative to *E. coli* LpxM in terms of substrate specificity and order of acylation, suggesting that differences at the primary sequence level can explain differences in function. Additional work is required to determine a molecular explanation for the divergence in biochemical activity based on differences in residues within the predicted acyltransfer active site and is ongoing in our laboratory. Study of these enzymes is particularly important because modification and ultimate surface presentation of *H. pylori* lipid A is dependent on formation of a Raetz pathway end-product that can be recognized by the MsbA transport machinery. The unusual order of *H. pylori* lipid A biosynthesis demonstrates that one enzyme and its biochemical characteristics can alter the trajectory of a well-conserved biochemical pathway that is essential for bacterial survival.

Chapter 3: PmrD is required for modifications to *Escherichia coli* endotoxin that promote antimicrobial resistance[2]

3.1 INTRODUCTION

Bacteria often encounter adverse conditions that threaten survival in an unpredictable environment. The first line of defense for most gram-negative bacteria is the outer membrane, which contains lipopolysaccharide (LPS) in the outer leaflet that interfaces with the surroundings (1). LPS is a multi-component macromolecule anchored to the bacterial membrane via its lipid A domain, a potent activator of the host innate immune response (2, 48). In the presence of environmental stressors, numerous gram-negatives have evolved machinery to modify the lipid A moiety with chemical groups that promote bacterial survival by creating a fortified, more resistant outer membrane (73).

Lipid A modifications are often regulated by complex two-component system (TCS) protein networks that coordinate detection of various signals with targeted transcriptional regulation. A typical TCS consists of a sensor histidine kinase that detects specific environmental signals and a cognate response regulator, which carries out changes in expression of a subset of genes known as its regulon. Upon recognition of a given signal, the sensor first autophosphorylates and then phosphorylates the response regulator, causing it to activate or repress gene expression within the regulon. When the

[2] Large portions of this chapter have been previously published. Rubin EJ, Herrera CM, Crofts AA, Trent MS. 2015. PmrD Is Required for Modifications to Escherichia coli Endotoxin That Promote Antimicrobial Resistance. Antimicrob Agents Chemother 59:2051–2061. (E.J.R. designed and performed experiments and wrote the manuscript under the supervision of M.S.T.; C.M.H. performed quantitative PCR experiments; A.A.C. analyzed RNA sequencing data).

signal is no longer present or detectable, the sensor deactivates the response regulator by dephosphorylation, thereby terminating transcriptional control of affected genes (46–48). The research herein involves two such systems: PhoP-PhoQ (PhoPQ) and PmrA-PmrB (PmrAB), where the former protein in each pair is the response regulator and the latter is the sensor histidine kinase. PhoQ responds to queues including depletion of Mg^{2+} and the presence of cationic antimicrobial peptides (CAMPs) (40, 55, 87). Although its *in vivo* relevance is still to be fully elucidated, micromolar Mg^{2+} is a strong activating signal for PhoQ commonly used in the laboratory. PmrB senses CAMPs, mildly acidic pH, and high Fe^{3+} concentrations (54, 88, 89). These two major TCSs are widely distributed across gram-negative bacteria, particularly in enteric genera including *Salmonella, Escherichia, Klebsiella, Shigella,* and *Citrobacter*. Activation of PhoPQ and/or PmrAB affects numerous cellular processes, among them, in certain organisms, the induction of various lipid A modifications (Fig 3.1A).

For instance, the PmrAB regulon includes two genes involved in lipid A modification: *eptA,* coding for a phosphoethanolamine (pEtN) transferase, and *arnT,* coding for a 4-amino-4-deoxy-L-arabinose (L-Ara4N) transferase (62–65). Enzymes EptA and ArnT function at the inner membrane, transferring their respective amine-containing residues to the lipid A phosphate groups before transport across the periplasm (Fig 3.1B)(63, 65). Decoration of lipid A with pEtN or L-Ara4N groups masks the charge of one or both of its anionic phosphates. This reduces the net-negative charge of the

molecule, and the outer membrane as a whole, which helps protect the bacterium from positively-charged CAMPs (Fig 3.1B)(63, 64).

In *S. enterica,* PmrAB-dependent genes can also be activated indirectly in a process that requires cross talk through PhoPQ (66). The vehicle for interaction between these two-component systems is PmrD, a small PhoP-activated protein that binds to and mechanically blocks dephosphorylation of activated phospho-PmrA by its cognate sensor, PmrB (67–69)(Fig 3.1B). In effect, PmrD helps maintain PmrA in its active state, allowing it to continue influencing transcription of genes in its regulon. Consequently, *eptA* and *arnT* are also transcribed when environmental conditions exclusively activate PhoPQ, such as in low Mg^{2+}. In this way, disparate environmental signals that activate PhoPQ or PmrAB ultimately lead to the same phenotypic outcome in *S. enterica*: lipid A modifications that protect against CAMPs (66).

Conversely, cross talk between PhoPQ and PmrAB is thought not to occur in *E. coli*. Winfield and Groisman previously demonstrated that when wild-type K-12 strain MG1655 is grown in low Mg^{2+}, PmrA-dependent genes are not activated and bacterial survival is extremely impaired upon exposure to CAMP polymyxin B (90). These cellular responses instead require direct activation of PmrAB, suggesting that in *E. coli*, this system is not connected with PhoPQ. This phenotypic difference was first attributed to functional divergence between the *Salmonella* and *E. coli* PmrD proteins, suggesting that PmrD is an inactive connector of PhoPQ and PmrAB in the latter organism (90). However, it was later found that *E. coli* PmrD promotes connection of PhoPQ and

PmrAB when expressed heterologously in *S. enterica* (91). Ultimately, *E. coli* PmrB was demonstrated to possess vigorous phosphatase activity that exceeds that of its *S. enterica* homolog. Together, these findings suggested that in *E. coli,* PhoPQ and PmrAB are disconnected not because PmrD is inactive but because PmrB dephosphorylates PmrA faster than PmrD can protect it (91).

Former studies have analyzed gene expression and CAMP survival data to define a role for PmrD in *E. coli*, but have not involved phenotypic analysis of the lipid A. The lipid A profile can reveal the presence or absence of common structural modifications, including pEtN and L-Ara4N, and is therefore a direct read-out for activation of modification machinery and CAMP resistance. The structure of this molecule determines the biochemical status of the outer membrane and should agree with gene expression and survival data. Here, we isolate lipid A from wild-type and *pmrD* mutant *E. coli* to discover unexpectedly that, 1) pEtN/L-Ara4N modifications are present on lipid A isolated from wild-type *E. coli* grown in micromolar Mg^{2+}, and 2) under the same low Mg^{2+} conditions, *pmrD* is required for and actively promotes these PmrA-dependent modifications. In line with this, we proceed to confirm that *pmrD* is important for bacterial survival upon exposure to polymyxin B and influences expression of PmrA-dependent genes as shown by RNAseq analysis. Intriguingly, our findings also uncover the existence of a second PhoPQ-independent system that activates PmrD and therefore addition of PmrA-dependent pEtN and L-Ara4N groups to the lipid A in low Mg^{2+} growth conditions. In all, this research establishes that communication does occur

between PhoPQ and PmrAB in *E. coli* through PmrD, but in a more complex manner than expected.

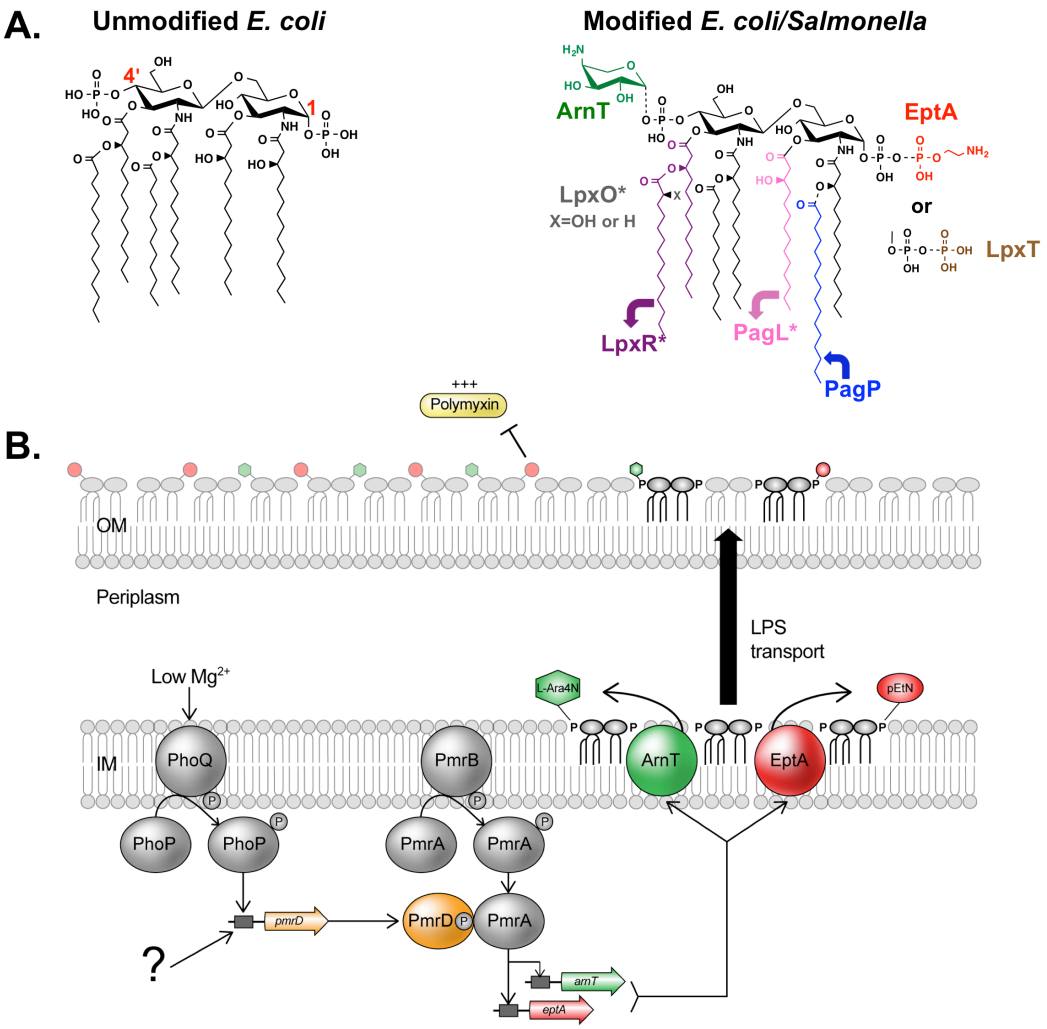

Figure 3.1 *E. coli* and *S. enterica* modify lipid A in response to environmental signals, altering the integrity of the outer membrane

(A) (Left) Typically, *E. coli* produces a lipid A structure comprised of a *β*-(1',6)-linked disaccharide of glucosamine that is *bis*-phosphorylated and hexa-acylated (2). Select glucosamine carbons are numbered in red. (Right) Lipid A can be modified by numerous enzymes and under various conditions. Modifications include addition of L-Ara4N by ArnT (green) and pEtN by EptA (red), addition of a phosphate group at the 1-phosphate by LpxT (brown), removal of the 3'-linked acyl chains by LpxR (purple), hydroxylation of the 3'-secondary acyl chain by LpxO (gray), removal of the 3-linked acyl chain by PagL (pink), and addition of a secondary palmitate chain at the 2-linked primary acyl chain by PagP (blue). Asterisks designate enzymes found in *S. enterica,* but not *E. coli* K-12. pEtN and L-Ara4N positions may be reversed and/or double addition of residues may occur (57, 92). **(B)** Model for PmrD-mediated crosstalk between PhoPQ and PmrAB.

Inner membrane sensor PhoQ is activated by low Mg^{2+} or CAMPs in the periplasm (40). It autophosphorylates then activates the cytosolic response regulator, PhoP, which increases transcription of the *pmrD* gene. The PmrD protein binds to phospho-PmrA, a response regulator associated with sensor PmrB. PmrD mechanically inhibits desphosphorylation of PmrA by PmrB, allowing continued transcription of PmrA-dependent genes including *eptA* and *arnT*. Ultimately, PmrD promotes addition of pEtN and L-Ara4N to the lipid A in PhoPQ-activating conditions, leading to polymyxin resistance. Our results implicate a second system (question mark) that is able to activate PmrD in an *E. coli phoPQ* double mutant.

3.2 RESULTS

3.2.1 pEtN and L-Ara4N lipid A modifications are induced in wild-type *E. coli* grown in low Mg^{2+} and are *pmrD*-dependent

Our laboratory has routinely demonstrated that *E. coli* grown in either rich media (such as luria broth) or minimal media containing high concentrations of Mg^{2+} (1-10 mM) produces 1-diphosphate lipid A. The 1-diphosphate structural variant arises when the inner membrane kinase LpxT (Fig 3.1A) transfers a phosphate group from undecaprenyl pyrophosphate to the 1-phosphate group of lipid A (89, 93). Conversely, when *E. coli* is cultured in low concentrations of Mg^{2+} (10-100 μM), we see lipid A containing PmrA-dependent lipid A modifications (pEtN and L-Ara4N) present in the radiolabeled profile (89). Here, we sought to repeat this result, and build on it to investigate a potential role for *pmrD* in the modification of *E. coli* lipid A. To this end, ^{32}P-radiolabeled lipid A was isolated from wild-type, *pmrD*$^-$, and complemented *pmrD*$^-$ *E. coli* strains in the W3110 K-12 background grown in both high (10 mM) and low (10 μM) Mg^{2+} N-minimal medium (Fig 3.2A). As previously observed, wild-type *E. coli* grown in low Mg^{2+} integrated both pEtN and L-Ara4N modifications in single and various double combinations (Fig 3.2A, lane 4), when compared with WD101, a strain constitutively

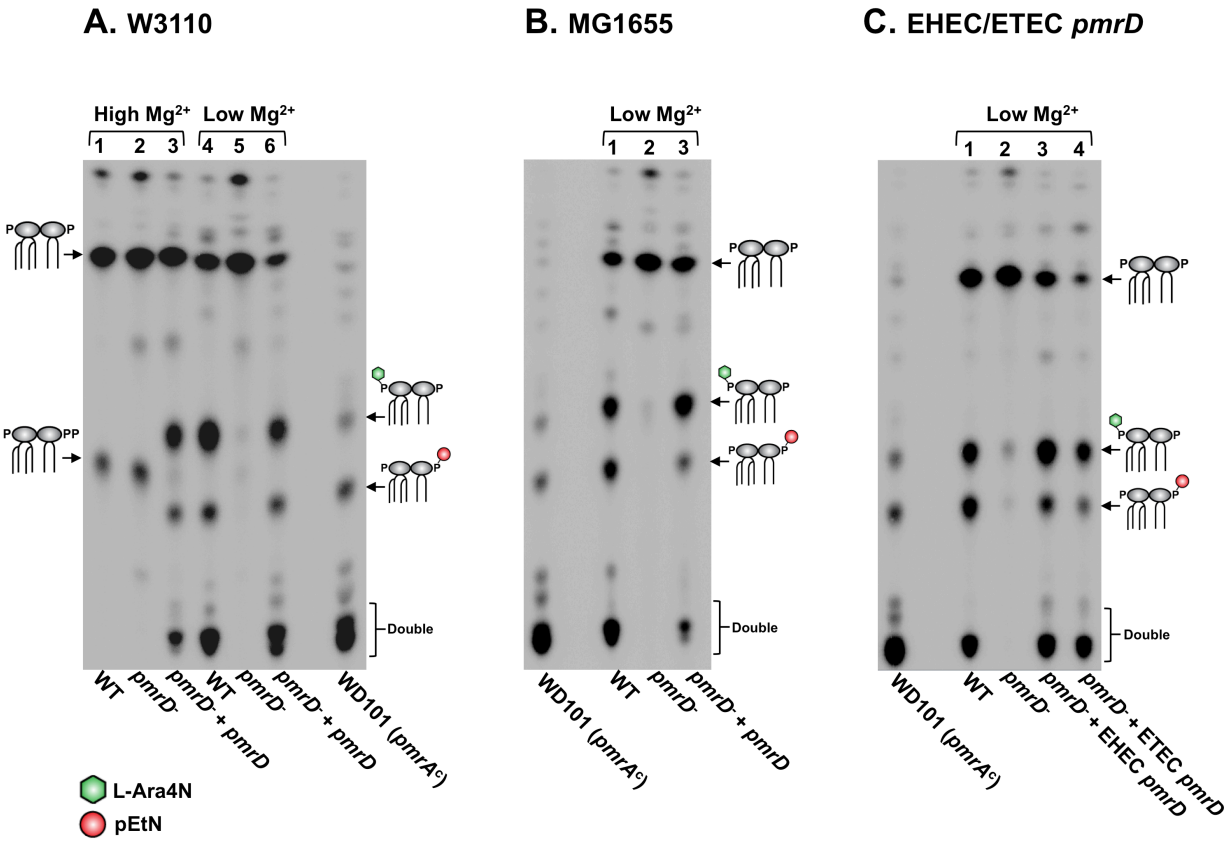

Figure 3.2 *pmrD* is required for addition of pEtN and L-Ara4N to lipid A in low Mg^{2+} conditions

Lipid A species observed in the profiles are depicted as cartoons; L-Ara4N, green hexagon and pEtN, red circle. Positive control strain WD101 produces lipid A constitutively modified with pEtN and L-Ara4N. **(A)** *E. coli* W3110 strains were grown in N-minimal medium with either 10 mM Mg^{2+} (high, lanes 1-3) or 10 µM Mg^{2+} (low, lanes 4-6). W3110 *pmrD* was expressed from low-copy plasmid pWSK29 in the W3110 *pmrD* mutant. **(B)** *E. coli* MG1655 strains were grown in N-minimal medium with 10 µM Mg^{2+}. MG1655 *pmrD* was expressed from low-copy plasmid pWSK29 in the MG1655 *pmrD* mutant. **(C)** W3110 *pmrD* from EHEC or ETEC was expressed from low-copy plasmid pWSK29 in the W3110 *pmrD* mutant in N-minimal medium with 10 µM Mg^{2+}.

expressing *pmrA* (63). Lipid A species modified at both phosphates may have either double pEtN, double L-Ara4N, or one of each group (57, 63, 65). In notable opposition to the wild-type lipid A profile, these modifications were completely absent in the *pmrD* mutant grown in the same conditions (Fig 3.2A, lane 5), while complementation of the *pmrD* mutant restored the presence of pEtN/L-Ara4N modifications (Fig 3.2A, lane 6). Conversely, lipid A profiles of both wild-type and *pmrD*$^-$ strains grown in high Mg^{2+} revealed a 1-diphosphate phenotype (Fig 3.2A, lanes 1, 2). pEtN/L-Ara4N modifications are absent in this growth condition presumably because high Mg^{2+} suppresses PhoPQ and thus *pmrD* transcription (40). However, when *pmrD* is expressed *in trans* in a *pmrD* mutant strain grown in high Mg^{2+}, pEtN/L-Ara4N modified lipid A is observed instead of the 1-diphosphate variant (Fig 3.2A, lane 3). This demonstrates that exogenous expression of *pmrD* from a low-copy plasmid is sufficient to induce PmrA-dependent lipid A modifications in a growth condition where they are otherwise not observed.

We also investigated the lipid A profile of closely related K-12 *E. coli* strain MG1655 to determine if our observations were strain specific. MG1655 was chosen based on its use in previous studies that questioned functionality of PmrD and the link between PhoPQ and PmrAB in *E. coli* (90). Our results establish that pEtN and L-Ara4N groups are also added to the lipid A when this K-12 strain is grown in low Mg^{2+} and that *pmrD* is required for their presence (Fig 3.2B). Further, expression of *pmrD* from both enterohemorrhagic *E. coli* (EHEC) and enterotoxigenic *E. coli* (ETEC) in the W3110

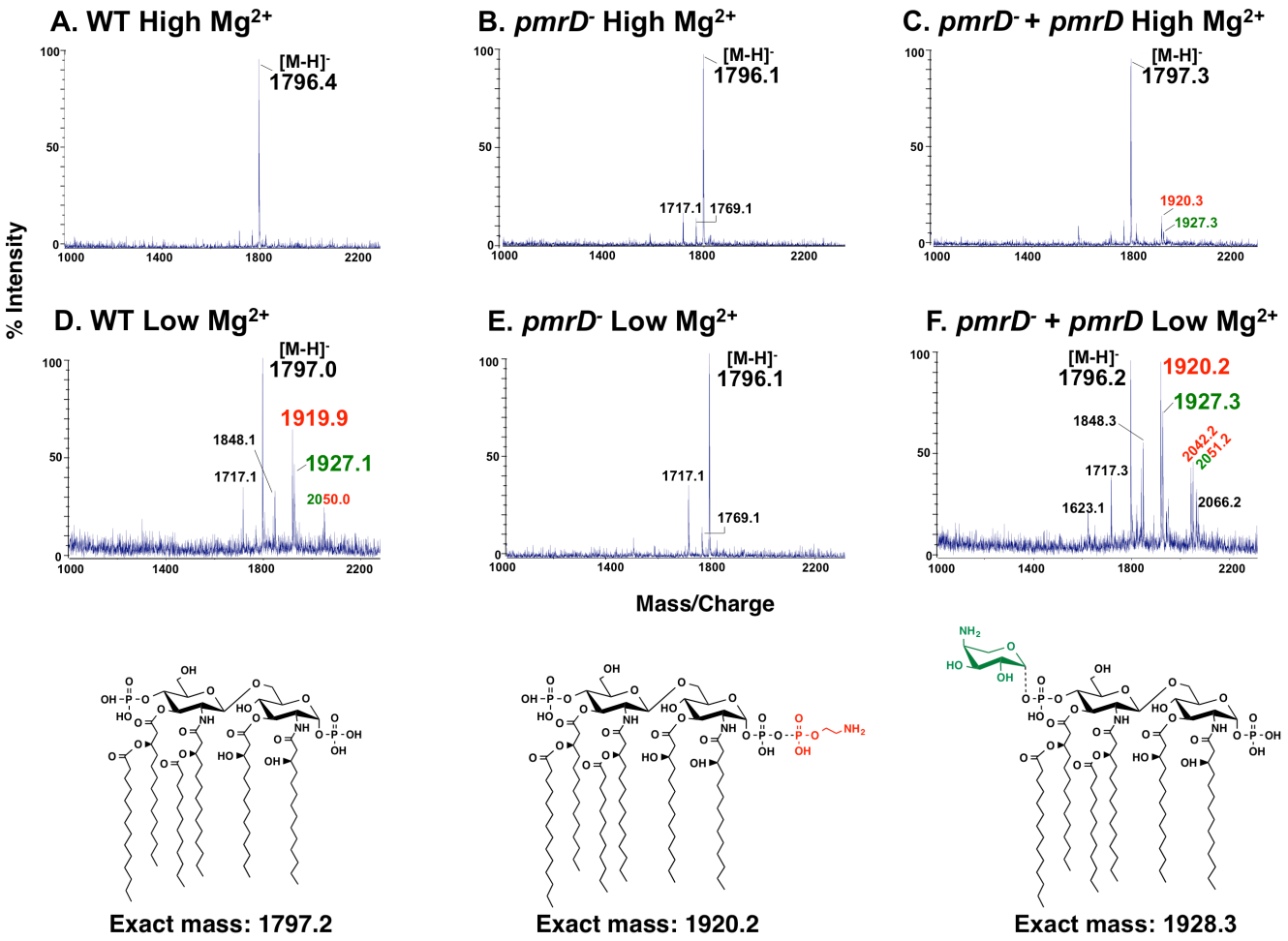

Figure 3.3 MALDI-TOF mass spectrometry of lipid A from *E. coli* W3110 wild-type, *pmrD-*, and complemented *pmrD* mutant in high and low Mg^{2+}

Structures and corresponding exact masses are provided for reference. **(A-C)** Lipid A from W3110 wild-type, *pmrD*-, and complemented *pmrD*- strains grown in 10 mM Mg^{2+} (high) generate major molecular ion peaks at *m/z* 1796.4, 1796.1, and 1797.3, respectively. These peaks correspond to hexa-acylated, *bis*-phosphorylated lipid A. The complemented *pmrD* mutant also produces minor peaks corresponding to single addition of pEtN (*m/z* 1920.3) and L-Ara4N (*m/z* 1927.3). **(D)** Lipid A from W3110 wild-type grown in 10 µM Mg^{2+} (low) produces a molecular ion at *m/z* 1797.0, representing a hexa-acylated, *bis*-phosphorylated species. It also generates major peaks corresponding to lipid A singly modified with pEtN (*m/z* 1919.9) and L-Ara4N (*m/z* 1927.1), as well as double modification with one of each residue at each phosphate (*m/z* 2050.0). The peak at *m/z*

1848.1 corresponds to 1-dephosphorylated hexa-acylated lipid A with one L-Ara4N. **(E)** *pmrD* mutant lipid A generates a major molecular ion at *m/z* 1796.1 when this strain is grown in low Mg^{2+}, indicating presence of hexa-acylated, *bis*-phosphorylated lipid A. **(F)** When grown in low Mg^{2+}, the complemented *pmrD* mutant produces major ions corresponding to single (*m/z* 1920.2) and double (*m/z* 2042.2) addition of pEtN, single (*m/z* 1927.3) addition of L-Ara4N, and addition of one pEtN and one L-Ara4N (*m/z* 2051.2). Minor peaks at *m/z* 1717 and 1769 correspond to lipid A species lacking a phosphate group or bearing a shorter acyl chain, respectively. Red labels indicate species with a pEtN group and green labels indicate species with a L-Ara4N residue.

pmrD mutant complemented lipid A modification to the same extent as the endogenous W3110 gene (Fig 3.2C, lanes 3, 4). This suggests that pathogenic *E. coli* also encode functional PmrD proteins that connect with the PmrAB system.

All results shown in Figure 3.2A were confirmed by MALDI-TOF mass spectrometry (Fig 3.3). Strains grown in high Mg^{2+} produced major molecular ions at approximately *m/z* 1797, indicating presence of hexa-acylated, *bis*-phosphorylated lipid A (Fig 3.3A, B, C), the predominant species observed in the radiolabeled profiles (Fig 3.2A, lanes 1, 2). Wild-type *E. coli* grown in low Mg^{2+} produced several major peaks corresponding to three main lipid A species; hexa-acylated, *bis*-phosphorylated (*m/z* 1797.0), pEtN-lipid A (*m/z* 1919.9), and L-Ara4N-lipid A (*m/z* 1927.1)(Fig 3.3D). Modified species were absent from lipid A of the *pmrD*$^{-}$ strain grown in low Mg^{2+}, which only generated a major molecular ion at *m/z* 1796.1, corresponding to hexa-acylated lipid A (Fig 3.3E). This spectrum was identical to that of a *pmrA* mutant in low Mg^{2+} (Fig 3.4). Complementation of the *pmrD* mutant in low Mg^{2+} led to restoration of the singly modified lipid A species observed in the wild-type strain, as well as doubly modified species ($pEtN_2$-lipid A at *m/z* 2042.2; pEtN/L-Ara4N-lipidA at *m/z* 2051.2)(Fig 3.3F).

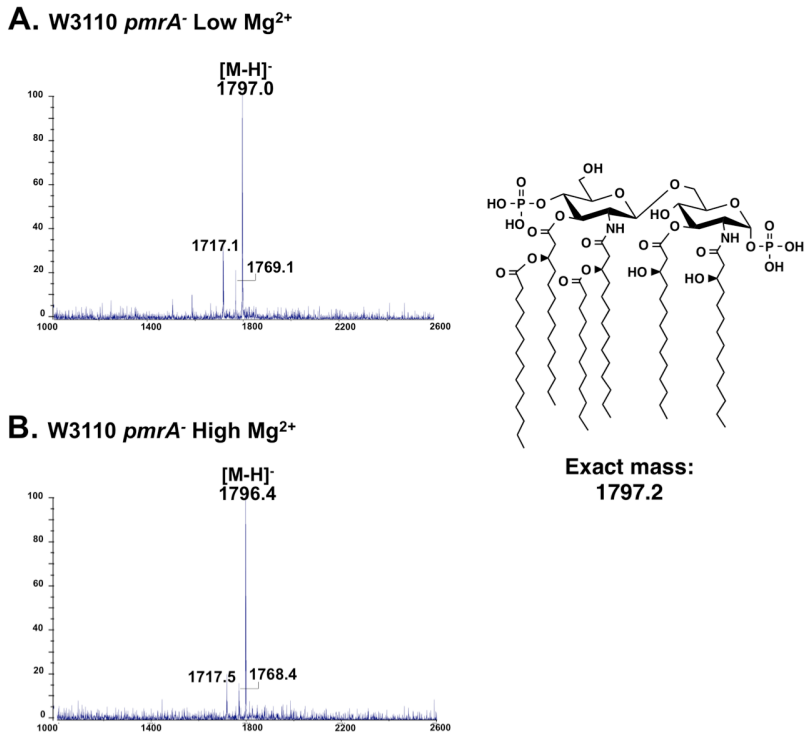

Figure 3.4 MALDI-TOF mass spectrometry of negative control strain W3110 *pmrA*$^{-}$

This strain serves as a negative control for the W3110 *pmrD*$^{-}$ strain. **(A,B)** W3110 *pmrA*$^{-}$ produces hexa-acylated lipid A in both 10 μM (low) and 10 mM (high) Mg^{2+} growth conditions, generating major peaks at *m/z* 1797.0 and *m/z* 1796.4, respectively. Minor peaks at *m/z* 1717.1 (low)/1717.5 (high) and *m/z* 1769.1 (low)/1768.4 (high) correspond to lipid A species lacking a phosphate group or bearing a shorter acyl chain, respectively.

This further demonstrates the role of *pmrD* in inducing PmrAB-dependent lipid A modification with pEtN and L-Ara4N when *E. coli* is grown in low Mg^{2+}. Taken together, this data shows that *pmrD* promotes pEtN and L-Ara4N lipid A modification under low Mg^{2+} growth conditions across different *E. coli* strains.

3.2.2 pEtN/L-Ara4N lipid A modifications are PmrA-dependent, but only partially PhoPQ-dependent

Previous research has defined the epistatic relationships among PmrD, PhoPQ, and PmrAB in *S. enterica* (67, 68). We initially analyzed the ^{32}P-labeled lipid A profiles of *phoPQ*$^-$ and *pmrA*$^-$ strains to explore whether similar relationships exist between these proteins in *E. coli* (Fig 3.5). It has been shown that in *E. coli, pmrD* expression and protein production are induced in low Mg^{2+} in a *phoP*-dependent manner (90). Given this, we expected that deletion of *phoPQ* from the genome would result in loss of pEtN and L-Ara4N lipid A modifications, since *pmrD* is required for addition of these groups, and *pmrD* expression is dependent on this two-component system.

Surprisingly, when we isolated lipid A from a *phoPQ* double mutant grown in low Mg^{2+} medium, it displayed a partially modified profile, containing mostly single and minimal double pEtN and L-Ara4N additions (Fig 3.5, lane 2). Densitometry analysis of the chromatographically separated radiolabeled lipid A in Figure 3.5 showed that approximately 40% of *phoPQ*$^-$ lipid A was modified versus 89% in the wild-type strain (Table 3.1). To confirm mutation of *phoP* and *phoQ* in the mutant, we performed semi-quantitative RT-PCR to demonstrate that neither gene was expressed when the strain was grown in low Mg^{2+} N-minimal medium (data not shown). As a follow-up, we generated a *phoPQpmrD* triple mutant to determine if the modifications we observed in the lipid A profile of the *phoPQ* mutant were *pmrD*-dependent. Indeed, we did not observe modifications in the *phoPQpmrD*$^-$ triple mutant but could restore them upon *in trans* expression of *pmrD* in this triple mutant (Fig 3.5, lanes 3, 4). These results imply that an

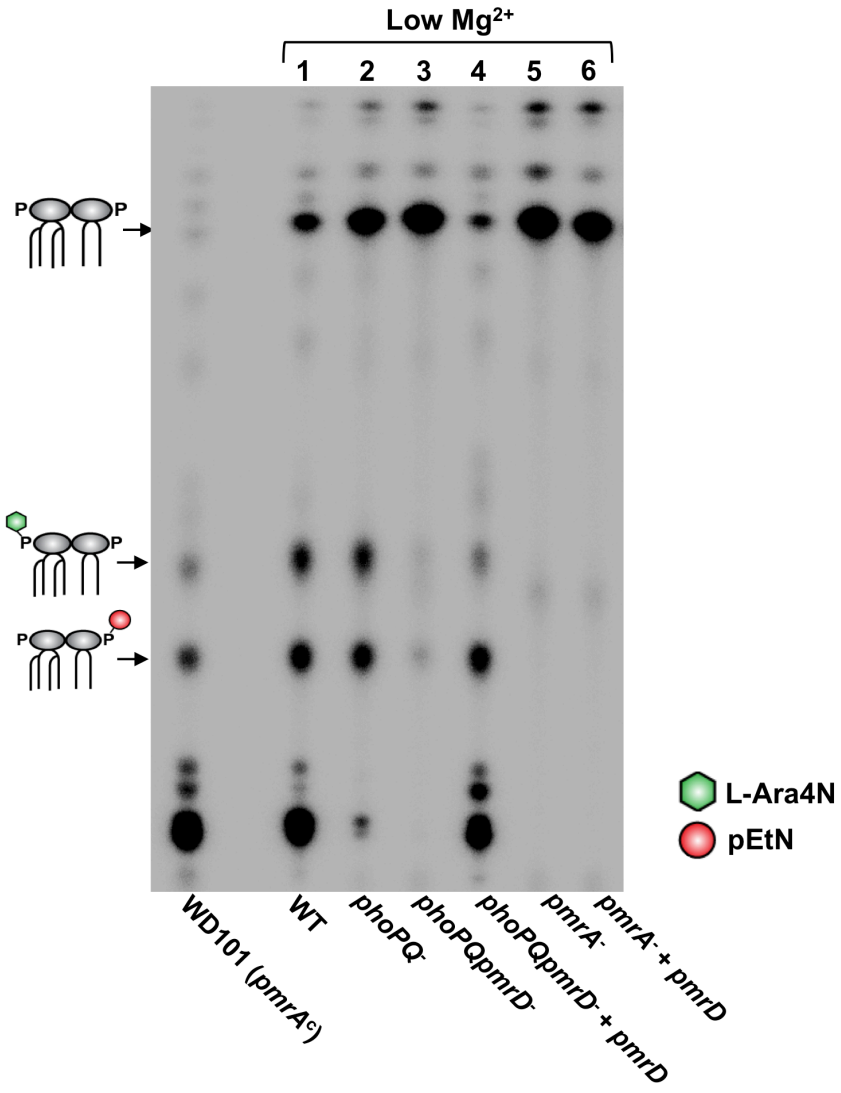

Figure 3.5 pEtN/L-Ara4N lipid A modifications are PmrA-dependent, but only partially PhoPQ-dependent

Lipid A species observed in the profiles are depicted as cartoons; L-Ara4N, green hexagon and pEtN, red circle. Positive control strain WD101 produces lipid A constitutively modified with pEtN and L-Ara4N. *E. coli* W3110 strains were grown in 10 μM Mg^{2+} (low) N-minimal media and radiolabeled lipid A was isolated and separated by TLC.

unknown factor or system can also activate *pmrD* expression, leading to completion of the *pmrA*-dependent lipid A modification pathway in the absence of *phoPQ*. As expected, a *pmrA* mutant was unable to modify its lipid A with pEtN and L-Ara4N and expression of *pmrD in trans* could not bypass this phenotype (Fig 3.5, lanes 5, 6). These results confirm that PmrD activity occurs upstream of PmrA, but challenge previous findings by showing that *pmrD* expression is not strictly PhoPQ-dependent.

Table 3.1: Densitometry analysis values for Figure 3.5

	% Modified[a]	**% Unmodified[b]**
WD101	98.52	1.48
WT	89.42	10.58
phoPQ$^-$	40.06	59.94
phoPQD$^-$	5.49	94.51
phoPQpmrD$^-$ + pmrD	90.56	9.44
pmrA$^-$	1.28	98.72
pmrA$^-$ + pmrD	1.08	98.92

.

3.2.3 *pmrD* is transcriptionally active in a *phoPQ* mutant and its expression is not influenced by PmrAB

Given the unexpected presence of pEtN/L-Ara4N modifications in the *phoPQ*$^-$ lipid A profile, we reasoned that a PhoPQ-independent factor or system must be activating *pmrD* transcription in this double mutant. We suspected that PmrA or PmrB could be candidates for transcriptional control of *pmrD* as a means to ensure expression of *eptA* and *arnT* in the absence of *phoPQ.* Additionally, *S. enterica* PmrA negatively regulates *pmrD* transcription, so such an interaction would not be unprecedented (94).

To address this possibility, we isolated RNA from wild-type, *phoPQ*$^-$, and *phoPQpmrA* and *phoPQpmrB* triple mutant strains grown in low Mg^{2+}. We then determined expression levels of several key genes by quantitative PCR analysis (Fig 3.6). Ribosomal RNA *rrsG* showed comparable expression levels across all strains relative to wild-type. Expression of PhoPQ-dependent response regulator *rstA* was drastically reduced (20-fold) in the three mutant strains. Contrarily, *pmrD* expression was reduced by approximately 1.7 fold relative to wild-type, but showed 12-fold higher expression than *rstA* in the *phoPQ* mutant. Since *rstA* expression is entirely dependent on PhoPQ, this data demonstrates that *pmrD* only depends partially on PhoPQ for transcriptional activation in agreement with the radiolabeled lipid A profiles shown in Figure 3.5. *pmrD* expression was not significantly different among *phoPQ*$^-$, *phoPQpmrA*$^-$, and *phoPQpmrB*$^-$. Next, we measured *pmrA* mRNA levels in the *phoPQ*$^-$ strain, which approximately matched the level observed in wild-type. Finally, PmrA-activated *arnT* showed roughly the same expression level as *pmrD* in *phoPQ*$^-$ relative to wild-type, and

was expectedly almost undetectable in the triple mutant strains. These results confirm that *pmrD* is expressed in a *phoPQ* mutant, but also suggest that PmrA and PmrB do not exert transcriptional control over *pmrD* in the absence of *phoPQ*.

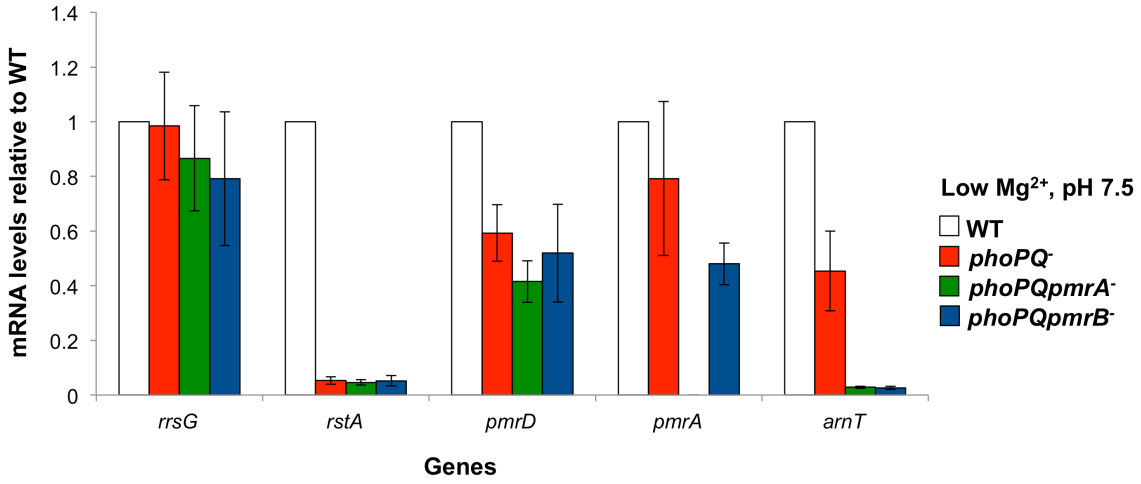

Figure 3.6 *pmrD* expression in a *phoPQ* mutant is not influenced by PmrAB

E. coli W3110 wild-type, *phoPQ*$^-$, *phoPQpmrA*$^-$, and *phoPQpmrB*$^-$ were grown in N-minimal medium with 10 µM Mg^{2+} (low) and RNA was isolated. Relative expression levels of each gene were determined by quantitative PCR. Results are representative of three biological replicates.

3.2.4 PmrD plays a role in expression of *pmrA*, thereby indirectly affecting expression of downstream *pmrA*-dependent genes

To confirm that presence of *pmrD* affects PmrA-dependent gene expression as it does lipid A profiles, we performed RNAseq analysis on W3110 wild-type and the *pmrD* mutant strain grown in low Mg^{2+} compared with high Mg^{2+}. Transcript levels for *eptA, arnT,* and *pmrA* all showed statistically significant upregulation in low versus high Mg^{2+} in the wild-type strain, compared with static, statistically insignificant changes in expression between the two Mg^{2+} conditions for the *pmrD* mutant (Table 3.2). This pattern also held for PmrA-dependent genes involved in synthesis of L-Ara4N (*ugd, arnABCD*). Conversely, in both strains, a PmrA-independent but PhoP-dependent gene, *rstA* (95) was expressed at similar levels in both low and high Mg^{2+}. This analysis was generated from the sequenced library of one biological replicate of each strain; a second biological replicate yielded similar results. RNAseq data for both biological replicates can be found online (http://aac.asm.org/content/59/4/2051/suppl/DCSupplemental).

RNAseq data were confirmed by quantitative PCR (Fig 3.7). For example, relative expression levels of *pmrA* and its downstream targets, *arnT* and *eptA,* decreased significantly in the *pmrD*$^{-}$ strain versus wild-type: 10-fold decline between strains for *pmrA*, 23-fold for *arnT*, and 72-fold for *eptA*. In contrast, *rstA* expression showed no significant change in expression between strains. These results demonstrate that PmrA-dependent gene expression is robust in low Mg^{2+} and PmrD plays a role in expression of the PmrA-regulon.

Table 3.2: Select RNAseq data comparing gene expression in wild-type and *pmrD*$^{-}$ *E. coli* strains grown in low versus high magnesium minimal medium

Gene	Product	Notes	Fold change in WT	WT P value	Fold change in *pmrD*$^{-}$	*pmrD*$^{-}$ P value
arnT	4-amino-4-deoxy-L-arabinose transferase	*pmrA/pmrD*-dependent	6.69	$<10^{-9}$	1.13	0.88
eptA	Phosphoethanolamine transferase	*pmrA/pmrD*-dependent	32.05	$<10^{-9}$	1.54	0.6
pmrA	DNA-binding response regulator in two-component regulatory system with pmrB	*pmrA/pmrD*-dependent	7.58	$<10^{-9}$	-1.25	0.45
ugd	UDP glucose 6-dehydrogenase	*pmrA/pmrD*-dependent	20.22	$<10^{-9}$	1.47	0.24
arnA (yfbG)	fused UDP-L-Ara4N formyltransferase/ UDP-glucouronic acid C-4'-decarboxylase	*pmrA/pmrD*-dependent	10.2	$<10^{-9}$	-1.32	0.31
arnB (yfbE)	UDP-4-amino-4-deoxy-L-arabinose oxoglutarate aminotransferase	*pmrA/pmrD*-dependent	69.60	$<10^{-9}$	-1.89	0.11
arnC (yfbF)	undecaprenyl phosphate 4-deoxy-4-formamido-L-arabinose transferase	*pmrA/pmrD*-dependent	110	$<10^{-9}$	-2.24	0.02
arnD (yfbH)	4-deoxy-4-formamido-L-arabinose-phosphoundecaprenol deformylase	*pmrA/pmrD*-dependent	18.4	$<10^{-9}$	-1.41	0.49
rstA	DNA-binding response regulator in two-component regulatory system with RstB	*phoP*-dependent *pmrA/pmrD*-independent	52	$<10^{-9}$	64.19	$<10^{-9}$
gyrA	gyrase subunit A	Housekeeping gene *pmrA/pmrD*-independent	-1.8	$<10^{-9}$	-1.53	$<10^{-9}$
rpsD	ribosomal protein	Housekeeping gene *pmrA/pmrD*-independent	-1.3	$<10^{-9}$	-1.62	$<10^{-9}$

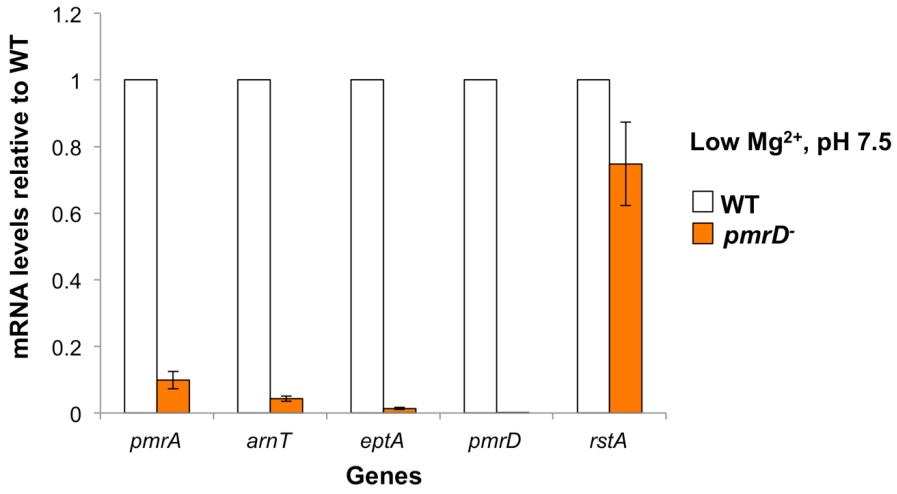

Figure 3.7 *pmrD* impacts transcription of *pmrA* and its downstream genes

Relative gene expression of *pmrA*, *arnT*, *eptA*, *pmrD* and *rstA* when *E. coli* W3110 wild-type and *pmrD* mutant were grown in N-minimal medium with 10 μM Mg^{2+} (low). Results are representative of 3 technical replicates.

3.2.5 Polymyxin B resistance in *E. coli* is *pmrD*-dependent in low Mg^{2+} but not in mildly acidic pH

pEtN and L-Ara4N lipid A modifications are especially important for bacterial survival in an environment where host-produced CAMPs are present. These chemical groups mask the negative charge of the lipid A molecule imparted by the phosphates that flank the glucosamine disaccharide. Thus, the overall charge of the bacterial cell surface becomes more neutral and better repels positively charged antimicrobial peptides than an unmodified outer membrane (54, 96)(Fig 3.1B). We reasoned that an *E. coli pmrD*

mutant would survive poorly with respect to wild-type when exposed to the CAMP polymyxin B due to the inability of the *pmrD* mutant to incorporate protective lipid A modifications (Fig. 3.2A).

Accordingly, we determined the ability of wild-type, *pmrD-,* and complemented *pmrD-* strains to survive in various concentrations of polymyxin B. To start, we grew these strains in low Mg^{2+} N-minimal medium (Fig 3.8A), the same condition known to induce pEtN/L-Ara4N modifications in wild-type. Under these parameters, we noticed a statistically significant (41.4%) decline in survival between wild-type and the *pmrD* mutant after a 1-hour exposure to 2.5 μg/ml polymyxin B. This difference was no longer observed upon expression of *pmrD* in the mutant strain. Repetition of the same assay conditions with 5 μg/ml polymyxin B increased the disparity between wild-type and the *pmrD* mutant even further, with a statically significant 68% decline in survival between the two strains that could also be reversed by overexpression of *pmrD* (Fig 3.8A).

We next determined survival at mildly acidic pH 5.8, a signal that induces pEtN and L-Ara4N lipid A modifications regardless of Mg^{2+} concentration and independently of the PhoPQ system (88, 89). While both PmrB and PhoQ can be activated at pH 5.8, the PmrA-dependent lipid A modifications seen in this condition are likely due predominantly to activation of PmrB since they are observed even when PhoQ is repressed (40, 53, 67, 88). Therefore, since this condition autonomously activates PmrAB and thus downstream lipid A modifications, it follows that presence of *pmrD* should be irrelevant to bacterial survival since its function is bypassed. Wild-type and the *pmrD*

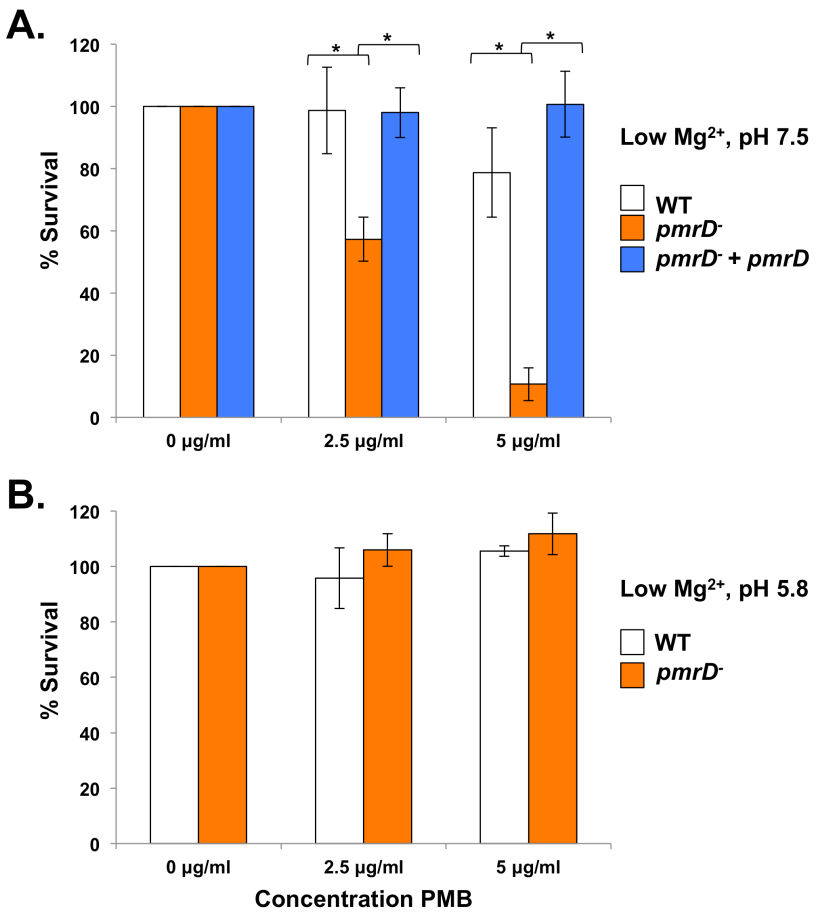

Figure 3.8 *pmrD* plays a role in polymyxin B resistance

(A) *E. coli* W3110 wild-type, *pmrD*-, and the complemented *pmrD* mutant were grown in N-minimal medium with 10 µM Mg^{2+} (low) at pH 7.5. Strains were challenged with 0, 2.5, or 5 µg/ml polymyxin B or phosphate buffered saline for 1 hour, serially diluted, and plated for survival. The wild-type strain survived at 98.7% and 78.75% in 2.5 and 5 µg/ml polymyxin B, respectively. The *pmrD* mutant survived at 57.3% and 10.68% when exposed to 2.5 and 5 µg/ml polymyxin B, respectively. **(B)** The same experiment described in panel A was performed at pH 5.8. Wild-type survived at 95.8% and 105.6% in 2.5 and 5 µg/ml polymyxin B, respectively. The *pmrD* mutant survived at levels that were not statistically significantly different from wild-type: 106% and 111.8% in 2.5 and 5 µg/ml polymyxin B, respectively. Results are representative of 3 biological replicates. (* = $p < 0.05$)

mutant did not show a statistically significant difference in survival when grown at pH 5.8 in low Mg^{2+} at either 2.5 or 5 μg/ml polymyxin B (Fig 3.8B). The survival data presented here clearly illustrate the necessity of *pmrD* for polymyxin B resistance when Mg^{2+} is limiting, and underscore that its activity occurs upstream of PmrAB.

3.3 DISCUSSION

A rapid response is crucial for bacterial survival when environmental conditions change. For gram-negative organisms, biochemical modification of outer membrane components can result in altered membrane characteristics tailored to defend against specific external insults. The lipid A portion of LPS is a common target for modification, as modulation of its charge and subtleties of its structure can drastically impact membrane integrity (2, 39, 48, 73).

When abundant in the environment, divalent cations such as Mg^{2+} and Ca^{2+} bind to LPS, creating ionic bridges between neighboring negative lipid A molecules; this contributes considerable stability to the outer membrane (39). Conversely, when divalent cations are limited, absence of this crucial reinforcement results in a vulnerable membrane and initiation of a bacterial response to address its weakened defenses (40). In *Salmonella,* this signal is sensed by PhoQ, and subsequently propagated to the PmrAB system via PmrD; this cascade ultimately leads to activation of enzymes EptA and ArnT that add polar residues to the lipid A (63, 65). While limiting Mg^{2+} is an important signal that negatively affects the gram-negative bacterial cell, it is unclear if *Salmonella* and *E. coli* encounter environments specifically depleted of Mg^{2+}, particularly in the course of

infection (55, 97–99). Although decoration of lipid A with pEtN and L-Ara4N results in a stronger membrane barrier that can be advantageous in low Mg^{2+}, the primary benefit of these positively-charged modifications is more likely linked with protection against CAMPs (60, 64). It is thought that low Mg^{2+} promotes activation of PhoQ in a manner that mimics activation of this sensor kinase by CAMPs. CAMPs compete with and displace divalent cations from PhoQ, allowing it to assume an active conformation; low Mg^{2+} concentrations may similarly promote this active conformation by allowing PhoQ to remain free from the membrane (55). In any case, the results presented here clearly demonstrate that this lipid A modification machinery is robustly activated by low Mg^{2+} growth conditions, which suggests there may exist an evolutionary pressure to modify the membrane under this condition.

Based on our research, this circuitry in *E. coli* is more complicated than previously thought. There has been a long-held belief in the field that cross talk does not occur between PhoPQ and PmrAB in this organism, based on one group's finding that PmrA-dependent genes are not transcribed when the organism is grown in PhoPQ-activating low Mg^{2+} (90). Previous findings from our laboratory, however, detected the presence of pEtN and L-Ara4N additions on lipid A isolated from wild-type *E. coli* grown in 10μM magnesium (89). Further, Hagiwara et al. suggested that PhoPQ and PmrD are necessary for full transcriptional induction of PmrA-dependent genes (100). These data are confirmed in the current work, which also highlight the necessity of *E. coli pmrD* for these PmrAB-dependent lipid A modifications, expression of PmrA-

dependent genes, and polymyxin B resistance in low Mg^{2+} conditions. Therefore, while previous research has largely labeled *E. coli* PmrD as an inactive two-component system connector protein, our findings demonstrate that it is active and necessary for lipid A modification.

Importantly, we uncovered a second, as yet unidentified system or factor that activates *pmrD* under low Mg^{2+} conditions in the absence of *phoPQ*. pEtN and L-Ara4N were clearly integrated into lipid A of the *phoPQ* double mutant (Fig 3.5), which was surprising given that *pmrD* expression had previously been shown to be strictly PhoP-dependent in *E. coli* (90). This phenotype could result either from activation of *pmrD* in a PhoPQ-independent manner, or a second connector protein having redundant activity with PmrD. Given that subsequent deletion of *pmrD* from the *phoPQ* mutant removes these modified species from the profile and evidence that *pmrD* is transcriptionally active in the *phoPQ* mutant (Fig 3.6), we conclude that the former possibility is more likely. It is difficult to predict whether this second system contributes to lipid A modification in the wild-type strain, or if it functions predominantly when PhoPQ is absent. Progress is ongoing in our laboratory to define the molecular machinery behind these findings. In all, these results suggest that *E. coli* has wired a second route to activate *pmrD* in the absence of its primary transcriptional activator PhoP. This underlines the importance of pEtN/L-Ara4N modifications in low Mg^{2+} and maintains the necessity of PmrD in their addition to lipid A.

Our findings introduce a new layer of complexity into the PhoPQ-PmrD-PmrAB story. This cascade has been characterized extensively in *S. enterica,* but the current work focuses on the dynamics of this system in *E. coli.* Our results strongly support that: 1) PmrD maintains the PhoPQ-PmrAB connection in this organism, and 2) a second system can respond to low Mg^{2+} in the absence of *phoPQ* to ensure activation of PmrD and fulfillment of the lipid A modification pathway. In all, these findings expand the repertoire of signals integrated and machinery employed by *E. coli* to respond to and defend against CAMPs.

Chapter 4: Conclusion

4.1 Future Directions and Concluding Themes

Decades of elegant research have described the structure of endotoxin, its biosynthesis pathway, and its role in activation of the innate immune response. Within each of these topics, a considerable amount of diversity has been discovered across this broad group of bacterial organisms: the precise chemical composition of lipid A produced, alternative mechanisms or properties of biosynthetic enzymes, and differential activation of TLR4/MD2 by lipid A structural variants, to name a few. The findings explained in these chapters build on this diversity with two new pieces of knowledge: introduction of a unique Raetz pathway acyltransferase in Epsilonproteobacteria including *H. pylori*, and reinterpretation of conditional post-translational control of lipid A modifications in *E. coli*.

The story of LpxJ is compelling because it uncovers a large and previously unknown family of acyltransferases, many of which may act in place of LpxM during lipid A biosynthesis in their respective organisms. This is certainly the case in three Epsilonproteobacteria, whose LpxJ enzymes can accept substrates of various acylation and Kdo-sylation states (25). In the absence of a crystal structure for both LpxJ and LpxM, it is difficult to provide a structural or mechanistic rationale for this flexibility. Future work should explore the role of inner membrane lipid A flippase, MsbA, in governing LpxJ substrate specificity since it is next in line to receive lipid A on its way to the cell surface. Given that LpxJ shares almost no homology with LpxM and resides in an

entirely different enzymatic family, it would be extremely interesting to determine an evolutionary explanation for this branching event.

Our findings for *E. coli* PmrD disprove a long-held belief in the field: that PmrD in this organism does not allow connection between the PhoPQ and PmrAB TCSs. A simple analysis of the lipid A profiles of wild-type, a *pmrD* mutant, and complemented *pmrD* mutant was employed to conclude definitively that PmrD does promote this connection in *E. coli*. Beyond this, existence of a previously unknown factor that activates *pmrD* expression in the absence of PhoPQ was serendipitously discovered (70). The primary focus of future work on this topic should be to find the genetic identity of this factor and characterize its relationship with *pmrD*, which may be achieved by a combination of RNAseq, Tn-seq, and lipid A profile analysis.

Regulation of lipid A modifications by small proteins like PmrD at the post-translational level turns out to be a fairly common theme in *E. coli* and other gram-negatives. Perhaps knowledge of these systems can be informative in finding and understanding the mystery activator of *pmrD*. For example, LpxT is the enzyme responsible for generating the 1-diphosphate species commonly found in the *E. coli* K-12 outer membrane; it does this by transferring a phosphate group to the 1-phosphate of lipid A from carrier lipid undecaprenyl pyrophosphate (89, 101, 102). LpxT activity can be repressed by small peptide, PmrR, which is activated by PmrAB in high Fe^{3+} conditions (103). Regulation of this lipid A modifying enzyme can be important in high Fe^{3+}: when a negatively-charged phosphate group is not added at the 1-phosphate, EptA is free to

transfer a positively charged pEtN to this site (89). As a result of this enzymatic trade-off, the net negative charge of the outer membrane decreases, which limits its association with Fe^{3+}, and thereby reduces PmrAB activation in a negative feedback loop (89, 103).

Inner membrane sensor histidine kinase, PhoQ is also subject to post-translational modification by several small proteins in *E. coli.* For instance, TCS EvgAS activates a 65 amino acid inner membrane protein, SafA (formerly known as B1500), which then complexes with and activates PhoQ (104). This connection is thought to diversify survival strategies in an acidic environment, as EvgAS is likely involved in the acid resistance response. MgrB is another small hydrophobic protein present in *E. coli, S. typhimurium,* and *Y. pestis.* Activated by PhoPQ, its function is to repress PhoQ activity at the inner membrane, thus providing negative feedback and fine tuning the response of this TCS (105).

More recently, PmrB of the PmrAB TCS has been demonstrated to be a phospho-donor for quorum sensing response regulator QseB in the absence of its cognate sensor, QseC (106). PmrB can phosphorylate QseB, but is inefficient at dephosphorylating it. Therefore, in absence of QseC, QseB is overactive, leading to aberrant transcription cascades and loss of virulence. These studies underscore that small proteins are a common mechanism promoting communication between TCSs, which often occurs in multi-layered networks.

4.2 THE NEXT STEPS FOR LIPID A: ANTIBIOTICS AND THERAPEUTICS

A number of fundamental open questions remain in the lipid A field, which are becoming increasingly important as the world recognizes the serious threat of antibiotic resistant gram-negative infections. At the top of the list, the reason for the essential nature of lipid A still remains elusive in the field, while a growing number of gram-negatives appear to be viable when lipid A biosynthesis is interrupted under specific growth conditions.

For instance, both *Neisseria meningitidis* and *Moraxella catarrhalis* are able to survive in the laboratory with a lipooligosaccharide (LOS)-deficient outer membrane. Instead of producing LPS, some gram-negatives make LOS, an outer membrane glycolipid that does not contain O-antigen and therefore only has core sugars attached to the lipid A anchor (107). Laboratory strains of *N. meningitidis* and *M. catarrhalis* without detectable LOS were found to have mutations in *lpxA,* which encodes the first enzyme of lipid A biosynthesis (Fig 1.2) and is almost always lethal when mutated in gram-negatives (10, 108, 109). Recently, an LOS-deficient clinical isolate of *N. meningitidis* was identified with a causative missense mutation in the gene encoding the fourth Raetz pathway enzyme, LpxH (110). Further, multi-drug resistant nosocomial pathogen *Acinetobacter baumannii* can spontaneously lose its LOS in the presence of high concentrations of the CAMP colistin by inactivation of *lpxA, lpxC,* or *lpxD* (Fig 4.1A)(111, 112). Loss of LOS has also been shown to accompany colistin-resistance of multiple *A. baumannii* clinical isolates due to nonsense mutation of *lpxA* or insertion mutation of *lpxD* (Fig 4.1B)(112). Although loss of LOS/LPS is regarded as an extreme

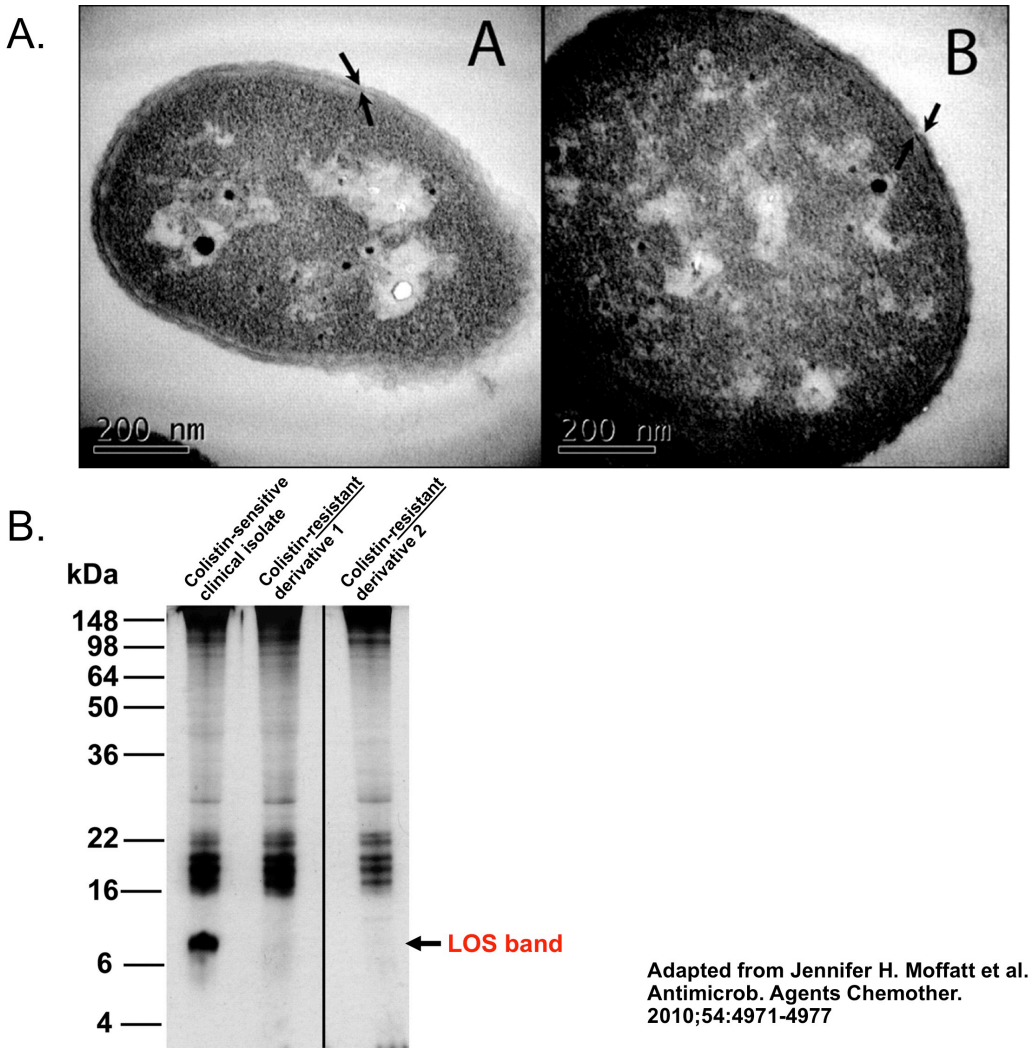

Figure 4.1: *Acinetobacter baumannii* can survive without LOS in the laboratory and the clinic

This figure has been adapted from Jennifer H. Moffatt et al. 2010. Antimicrob. Agents Chemother. 54:4971–4977.

(A) Transmission electron micrographs of colistin-susceptible *A. baumannii* strain ATCC 19606 (left) and colistin-resistant *lpxA* mutant 19606R (right). Arrows indicate the presence of intact inner and outer membranes in both strains, suggesting that 19606R constructs an outer membrane despite loss of LOS. **(B)** Carbohydrate-specific silver stain of proteinase-K treated whole cell lysates. The profile of a colistin-sensitive clinical isolate from a human bronchoalveolar lavage fluid sample contains a band representing LOS that migrates at approximately 8kDa. This band is missing from two genetic derivatives of this clinical strain characterized by colistin resistance.

measure to achieve antibiotic resistance, it can clearly occur in select organisms via multiple mutations in the lipid A biosynthesis pathway that are typically lethal. These results forecast a coming shift for the clinical community that will require creative drug combinations to overcome this new resistance mechanism.

Acquisition of antibiotic resistance is a widespread and startlingly rapid process that is quickly becoming the next global public health emergency. Development of effective lipid A biosynthesis inhibitors is now a top priority for the research and clinical communities; with the exception of the few organisms that do not require LPS, most gram-negatives would be extremely sensitive to such an antibiotic. Further, given that each enzyme in the pathway is essential, a bacterium would need to make drastic unprecedented biochemical changes to achieve resistance to such a toxic compound.

One promising target is LpxC, which catalyzes deacetylation of UDP-3-*O*-(acyl)-*N*-acetylglucosamine in the second step of the Raetz pathway (11). Although second sequentially, LpxC performs the first committed step of lipid A biosynthesis, as the first step catalyzed by UDP *N*-acetylglucosamine acyltransferase LpxA is energetically unfavorable (113). Further, LpxC is well-conserved across gram-negatives and does not share homology with any mammalian proteins, properties that make it an ideal target for a highly-specific antibiotic with few off-target effects (114). Resolution of the LpxC crystal structure has allowed elucidation of its catalytic mechanism and substrate binding chemistry (114, 115). In the years since, several potent inhibitors have been identified that act by competing with the substrate, UDP-3-*O*-(*R*-3-hydroxymyristoyl)-GlcNAc to

block catalysis (Fig 4.2A). Though none of these are currently ready for clinical use, progress is ongoing to optimize potency, minimize unintended targets, and increase the range of organisms against which these compounds are effective. Similar approaches in drug development could also be taken with essential enzymes further down the pathway, including late acyltransferase LpxJ in *H. pylori.* While an exact or comparable crystal structure is missing for this particular enzyme, a high-throughput small molecule screen could be used to discover inhibitors. Such a drug could be extremely valuable in fighting *H. pylori* infection, as it would prevent completion of lipid A biosynthesis, leaving the bacterium to die due to lack of a viable outer membrane.

While it is crucial to discover lipid A biosynthesis inhibitors in the fight against antiobiotic resistance, lipid A can also be exploited to help in prevention of other diseases in the form of a vaccine adjuvant. Monophosphorylated lipid A (MPL) is an FDA-approved adjuvant and structural variant of lipid A that stimulates a safe and effective inflammatory cytokine profile for boosting the immunogenicity of vaccines (Fig 4.2B)(116). Building on this, a library of *E. coli* strains producing one of two "template" lipid A structures (Fig 4.2C) and expressing combinations of various lipid A modification enzymes was recently engineered for intended use in both therapeutic and pharmaceutical applications (8). The strains in this library produce a range of lipid A structures that elicit a corresponding diversity in cytokine response. This tool demonstrates that even the subtlest structural alterations can dramatically change the physiological response to lipid

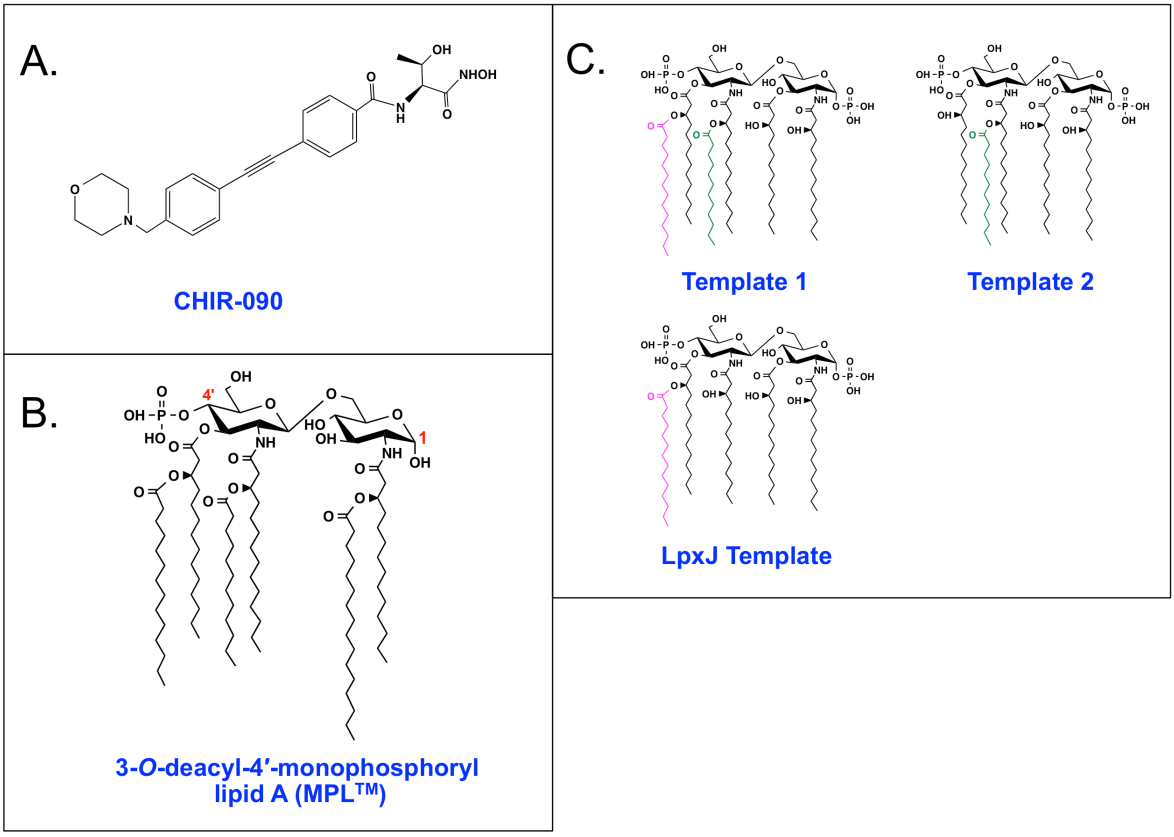

Figure 4.2: Molecular engineering applications in lipid A studies

(A) Structure of LpxC inhibitor CHIR-090 (117). This hydroxamate compound follows a two-step slow, tight-binding inhibition of LpxC and is bactericidal for a wide range of gram-negative pathogens. **(B)** Chemical structure of 3-*O*-deacyl-4′-monophosphoryl lipid A, the primary lipid A species present in the FDA-approved vaccine adjuvant, MPL™. **(C)** Lipid A structural templates 1 and 2 were used as frameworks for modification enzymes to build a combinatorially engineered lipid A library for therapeutic use (8). Expression of LpxJ in place of LpxM would create a third template to add diversity to this library.

A in a manner useful for clinical and industry applications. Following this idea, LpxJ could conceivably be used to make a unique lipid A template to introduce diversity into this library. If expressed in place of *E. coli* LpxM, LpxJ would allow for synthesis of penta-acylated lipid A with a 3′- (instead of 2′-) secondary acyl chain (Fig 4.2C). Given the wide range of immunogenicity elicited by the current library, it is likely that adding a third template could refine and resolve the spectrum even further.

Another intriguing avenue for the future of lipid A related studies is exploring the concept of host-specific TLR4 polymorphisms that affect an individual's immune reaction to lipid A and its structural variants. For example, a common polymorphism causes a change in identity for two residues within the TLR4 protein: amino acid 299 from aspartate to glycine, and residue 399 from threonine to isoleucine (118). These amino acid changes are thought to affect TLR4 dimerization and are associated with overall TLR4 hyporesponsiveness and increased susceptibility to infection with gram-negative bacteria and septic shock (118–120). The decreased reactivity displayed by this TLR4 variant is even more pronounced upon stimulation with MPL versus *bis*-phosphorylated lipid A, suggesting it is sensitive to differences in precise lipid A structure (120). It would be extremely interesting to determine the impact of other modifications such as variation in acyl chain length and number, and presence of groups like pEtN and L-Ara4N.

The findings presented here help stretch the arms of endotoxin into many exciting and potentially game-changing arenas for the future of medicine. In a few years, lipid A

may even be able to put its stamp on the world's first HIV and cancer vaccines. For all these reasons, it seems inevitable that this bioactive molecule will remain in the international research spotlight for many years to come.

Chapter 5: Experimental Procedures

5.1 Materials and Methods

5.1.1 Bacterial strains and growth conditions

The bacterial strains, plasmids, and oligonucleotides used in this study are listed in Section 5.2. Primary plate cultures of *E. coli* were grown from glycerol stock on LB agar or broth medium or N-minimal media (0.1M Bis-Tris pH 7.5 or 5.8, 5 mM KCl, 7.5 mM $(NH_4)_2SO_4$, 0.5 mM K_2SO_4, 1 mM KH_2PO_4, 0.10% casamino acids, 0.20% glucose, 0.0002% thiamine, 15 μM $FeSO_4$, 10 μM or 10 mM $MgSO_4$) at 37°C with appropriate antibiotics; ampicillin (100 μg/ml), kanamycin (30 μg/ml), or chloramphenicol (30 μg/ml). Primary plate cultures of *H. pylori* were grown from glycerol stock on blood agar medium containing vancomycin (10 μg ml^{-1}) at 37 °C for 36 to 60 h in a microaerobic atmosphere (5% O_2, 10% CO_2, 85% N_2).

5.1.2 Isolation and analysis of lipid A species from $^{32}P_i$-labeled cells

Various strains were grown either in LB or N-minimal medium at 37 °C with 2.5 μCi/ml $^{32}P_i$ (Perkin Elmer). Bacteria were harvested at OD_{600} ~0.8 and washed with 5 ml phosphate-buffered saline. ^{32}P-labeled lipid A was isolated as described previously and spotted onto a Silica Gel TLC plate (~10,000 cpm per lane)(27). Lipids were separated using a chloroform, pyridine, 88% formic acid, and water solvent system (50:50:16:5, vol/vol). TLC plates were exposed to a PhosphorImager screen (Kodak) and analyzed using a Bio-Rad Molecular Imager in conjunction with Quantity One software.

5.1.3 Mass spectrometry of lipid A species

Matrix assisted laser desorption-ionization time-of-flight (MALDI TOF) mass spectrometry was performed using a MALDI-TOF/TOF mass spectrometer (ABI 4700 Proteomics Analyser) as previously described (22). Ultraviolet photodissociation (UVPD) mass spectrometry was performed in the negative mode on a Thermo Scientific Orbitrap Elite mass spectrometer (Bremen, Germany) equipped with a 193 nm ArF excimer laser from Coherent (ExiStar XS, Santa Clara, CA) using a recently described setup (121). Lipid A samples were prepared for UVPD-MS by diluting samples to approximately 1 μM with 50:50 methanol:chloroform (Sigma Aldrich, St. Louis, MO). Lipid A solutions were directly infused via electrospray ionization using a potential of 4 kV and a sheath gas flow rate of 10 arbitrary units. All UVPD mass spectra were acquired in the Orbitrap mass analyzer using a resolution of 15,000 and a total of ten 6 mJ pulses per scan.

5.1.4 Construction of genetic mutant and chromosomal complementation of *H. pylori* J99 jhp0255 ($lpxJ_{Hp}$).

Vectors and oligonucleotides used in Chapter 2 are listed in Section 5.2, Tables 5.1 and 5.2, respectively. The *jhp0255* coding sequence, including 1,369 bp upstream and 1,000 bp downstream was amplified by PCR (primers 1 and 2, Table 5.2) from *H. pylori* J99 genomic DNA using *Pfu* Turbo (Stratagene) according to the manufacturer's instructions. The resultant DNA fragment was digested with NheI and XhoI, gel purified, and cloned behind the T7*lac* promoter in vector pET21a. Next, a kanamycin resistance cassette was obtained by PCR (primers 5 and 6, Table 5.2) from the *E. coli-H. pylori* shuttle vector,

pHel3, and inserted into pET21a containing *jhp0255*. This was accomplished by encoding BamHI and NotI restriction sites on the pET21a:*jhp0255* vector via inverse PCR (primers 3 and 4, Table 5.2), then digesting the kanamycin fragment and pET21a:*jhp0255* vector with BamHI and NotI. This allowed excision of the *jhp0255* coding sequence and subsequent replacement/ligation with the kanamycin cassette. The resulting plasmid (*jhp0255*KO+/-) containing an interrupted *jhp0255*-coding gene, was transformed into *H. pylori* J99 by natural transformation (122). Due to the essential nature of the gene, knock-out attempts were unsuccessful (see Results).

Chromosomal complementation was achieved by cloning *jhp0255* into vector pET0634comp. This plasmid allows for insertion of a chosen coding sequence into the *rdxA* locus on the genome, inactivating the *rdxA* gene. RdxA is a nitroreductase that converts metronidazole from an inactive pro-drug to its active form, so inactivation of the gene renders the bacterium resistant to metronidazole (22, 123). The *jhp0255* coding sequence was amplified by PCR (primers 13 and 14, Table 5.2) from *H. pylori* J99 genomic DNA using *Pfu* Turbo (Stratagene) according to the manufacturer's instructions. The resultant DNA fragment was digested with BamHI and EcoRI, gel purified, and ligated to BamHI/EcoRI, alkaline phosphatase-treated pET0634comp vector. The completed plasmid (pET0634comp*jhp0255*) was transformed into wild type *H. pylori* J99 by natural transformation and resistant colonies were selected on blood agar plates containing 10 μg ml^{-1} metronidazole. Resistant colonies were restreaked on fresh metronidazole plates and successful insertion of the complementation cassette at the *rdxA*

locus was confirmed by PCR of genomic DNA (primers 15 and 16, Table 5.2). With a second copy of *jhp0255* now present at the *rdxA* locus, we proceeded to prove that we could then knock out *jhp0255* at its normal locus. To achieve this, we transformed plasmid *jhp0255*KO+/- into the *rdxA::jhp0255* strain by natural transformation. Resistant colonies were obtained when bacteria were plated on blood agar containing 30 μg ml^{-1} kanamycin. Colonies were restreaked on fresh kanamycin plates and successful insertion of the kanamycin cassette at the *jhp0255* locus was confirmed by PCR of genomic DNA (primers 17 and 18, Table 5.2).

5.1.5 Generation of low-copy plasmids for expression of late acyl transferases from Epsilonproteobacteria and the *E. coli pmrD* gene

Vectors and oligonucleotides used in Chapter 2 are listed in Section 5.2, Tables 5.1 and 5.2, respectively. The acyltransferases of *H. pylori* J99 (*jhp0255*, primers 7 and 8, Table 5.2), *C. jejuni* 81-176 (*cjj81176_0482*, primers 9 and 10, Table 5.2), and *W. succinogenes* (*ws1775*, primers 11 and 12, Table 5.2) were cloned into vector pET21a (Novagen) behind the T7*lac* promoter. The PCR product from *jhp0255*, amplification was digested with NdeI and BamHI, and *cjj81176_0482* and *ws1775* were digested with NdeI and SalI. Digested PCR products were ligated individually overnight into pET21a at 16 °C using T4 DNA ligase (New England BioLabs) to generate pET21a*jhp0255*, pET21a*cjj81176_0482*, pET21a*ws1775*. Next, each plasmid was cut with XbaI and XhoI, excising the respective gene coding regions along with a ribosomal binding site. The resultant fragments were ligated individually into pWSK29 to give pWSK29*jhp0255*, pWSK29*cjj81176_0482*, and pWSK29*ws1775* for expression of the acyltransferases in *E.*

coli. The three vectors were transformed into XL-1 Blue (Stratagene) for propagation, then BN2 and MKV15b for radiolabeling and mass spectrometry experiments, respectively.

Vectors and oligonucleotides used in Chapter 3 are listed in Section 5.2, Tables 5.3 and 5.4, respectively. W3110 *pmrD* was cloned out of *E. coli* genomic DNA (primers 1 and 2, Table 5.4). The resultant fragment was digested with NdeI and BamHI and ligated overnight into pET21a at 16 °C using T4 DNA ligase to generate pET21a*pmrD*. Next, the plasmid was cut with XbaI and XhoI, excising the *pmrD* coding region along with a ribosomal binding site, which were ligated into pWSK29 to give pWSK29*pmrD*. The vector was transformed into XL-1 Blue (Stratagene) for propagation and various K-12 strains for expression of *pmrD.* Based on consistency in sequence between strains, primers 1 and 2 (Table 5.4) were used to clone *pmrD* from strain W3110, MG1655, EHEC, and ETEC. All cloned vectors were sequenced prior to use.

5.1.6 Preparation of radiolabeled lipid substrates for *in vitro* enzymatic assays

The substrate [4′-^{32}P] lipid IV_A was prepared from 125 μCi of [γ-^{32}P]ATP and the tetra-acyl-disaccharide 1-phosphate lipid acceptor, using the overexpressed 4′ kinase in the membranes of *E. coli* strain BLR(DE3)/pLysS/pJK2 as previously described (58). Kdo_2-[4′-^{32}P] lipid IV_A was generated by adding purified *E. coli* Kdo transferase (KdtA) immediately following the 4′ kinase, as previously described (124). Following the Kdo transfer reaction, membranes from *E. coli* strain BLR(DE3)HtrB and *E. coli* strain BLR(DE3)/MsbB as well as C12:0-acyl carrier protein (ACP) were added to generate

Kdo_2-[4′-^{32}P] lipid A, as previously described (58). Kdo_2-lauroyl-[4′-^{32}P] lipid IV_A was generated as Kdo_2-[4′-^{32}P] lipid A, with the omission of BLR(DE3)/MsbB membranes and addition of C12:0-ACP at a 1:1 molar ratio.

5.1.7 *In vitro* assay of $LpxJ_{Hp}$, $LpxJ_{Cj}$, and $LpxJ_{Ws}$ activities.

All enzymes were assayed under optimized conditions in a 10 µl reaction mixture containing 50 mM HEPES, pH 7.5, 0.2% Triton X-100, 2.5 µM lipid A substrate ([4′-^{32}P] lipid IV_A, Kdo_2-[4′-^{32}P] lipid IV_A, Kdo_2-lauroyl-[4′-^{32}P] lipid IV_A, or Kdo_2-[4′-^{32}P] lipid A at ~5,000 cpm nmol^{-1}) with either 5 µM ACPSH, C12:0-ACP/CoA, C14:0-ACP/CoA, C16:0-ACP/CoA, C18:0-ACP/CoA. Washed BN2 membranes expressing each late acyltransferase were used in the following concentrations as enzyme source: $LpxJ_{Hp}$ 0.01 mg ml^{-1}, $LpxJ_{Cj}$ 0.01 mg ml^{-1}, $LpxJ_{Ws}$ 0.005 mg ml^{-1}. Reactions were incubated at 30 °C for 30 minutes, terminated by spotting 4.5 µl onto Silica Gel thin-layer chromatography (TLC) plates, and dried under cool air for 20 min. Reaction products were separated using a chloroform, pyridine, 88% formic acid, and water solvent system (30:70:16:10, vol/vol). TLC plates were exposed to a PhosphorImager screen and analyzed using a Bio-Rad Molecular Imager in conjunction with Quantity One software.

5.1.8 Preparation of cell-free extracts, double-spun cytosol, and washed membranes

200 mL of *E. coli* cultures were grown to an A_{600} of ~1.0 at 37 °C and harvested by centrifugation at 10,000 x g for 10 min at 4 °C. Cell free extracts, membrane-free cytosol, and washed membranes from all samples were prepared at 4 °C as previously described

and stored in aliquots at -20 °C (58). Protein concentration was determined by the bicinchoninic acid assay method using bovine serum albumin as the standard (125).

5.1.9 Generation of *E. coli* mutants

Strains and oligonucleotides used in Chapter 3 are listed in Section 5.2, Tables 5.3 and 5.4, respectively. All mutant strains with the exception of W3110 *phoPQ*$^-$ were generated by P1 *vir* phage transduction from individual Keio collection mutants for *pmrD, pmrA,* or *pmrB* as previously described (126, 127). These strains include: W3110 *pmrD*$^-$*, pmrA*$^-$*, phoPQpmrD*$^-$*, phoPQpmrA*$^-$*,* and *phoPQpmrB*$^-$, and MG1655 *pmrD*$^-$. Candidate colonies were evaluated using a primer within the kanamycin cassette of each mutation (primer 6, Table 5.4) and an outside primer specific to an up- or downstream neighboring gene (primer 3 for *pmrD,* primer 4 for *pmrA,* and primer 5 for *pmrB,* Table 5.4). W3110 *phoPQ*$^-$ was generated in the DY330 strain based on the λ Red recombination system (128) using primers 18 and 19 (Table 5.4) as previously described (89).

5.1.10 Total RNA Isolation and Quantitative RT-PCR

E. coli strains were grown overnight in LB liquid culture. The following day, bacteria were spun down, washed with N-minimal media without Mg^{2+} or iron, and inoculated at OD_{600} 0.1 into N-minimal media pH 7.5 containing 10 μM $MgSO_4$. Cultures were grown to approximately OD_{600} 0.6, then cells were harvested and total RNA extracted with the Qiagen RNeasy Mini kit followed by treatment with RNase free DNase (Qiagen). cDNA synthesis was performed with the High Capacity cDNA Reverse Transcription Kit (AB Applied Biosystems). The quantification of target genes by qPCR was performed using

2X SYBR® Green PCR master mix (AB Applied Biosystems) and specific primers for each transcript (Section 5.2, Table 5.4). Data analysis was performed using ABI 7900HT Fast Real Time PCR System and the Software Sequence Detection Systems (SDS) version 2.4 (AB Applied Biosystems). The relative expression ratio of the target transcript was calculated in comparison to the *gyrB* transcript as the reference gene following the Pfaffl method (129).

5.1.11 Construction of Illumina libraries, RNA sequencing, and data analysis

Total RNA was depleted of rRNA using the Ribo-Zero™ rRNA Removal Kit for gram-negative bacteria (Epicentre). Illumina libraries were built from rRNA-depleted total RNA using the NEBNext® Ultra™ Directional RNA Library Prep Kit for Illumina®. RNA sequencing data were mapped to the *E. coli* W3110 reference genome in CLC Bio Genomics Workbench software and expression values were determined using RPKM. Baggerly's test on proportion of counts between samples determined a p-value and weighted proportions fold change per gene (130). A weighted proportion absolute change of 4-fold and an FDR corrected p-value of ≤ 0.01 were used as cutoffs as previously described (131). Reads mapping to the last 21 bp of the *pmrD* gene in the W3110 *pmrD* mutant were discarded based on use of the Keio *pmrD* mutant as the source of the W3110 mutant strain.

5.1.12 Polymyxin B survival assays

E. coli strains were grown overnight in LB liquid culture. The following day, bacteria were spun down, washed with N-minimal media without Mg^{2+} or iron, and inoculated at

OD 0.1 into N-minimal media of one of the following conditions: 1) pH 7.5, 10 μM $MgSO_4$ or 2) pH 5.8, 10 μM $MgSO_4$. Cultures were grown to OD_{600} 0.6 and split in half; one half of the culture was treated with either 2.5 or 5 μg/ml polymyxin B, and the other half was treated with an equivalent volume of PBS. Cultures were incubated at 37 °C for 1 hour then serially diluted and plated on LB agar. Survival values were calculated by dividing the number of bacteria after treatment with polymyxin B relative to those incubated in the presence of PBS and then multiplied by 100.

5.2 BACTERIAL STRAINS AND OLIGONUCLEOTIDES

Table 5.1: Bacterial strains and plasmids used in Chapter 2

Strains	Genotype or Description	Source or Reference
H. pylori		
J99	Wild type	ATCC 700824
J99/*rdxA::jhp0255*	J99 complemented with *jhp0255 ($lpxJ_{Hp}$)* at *rdxA* locus	This work
J99/*rdxA::jhp0255, jhp0255::kanR*	J99 complemented with *jhp0255 ($lpxJ_{Hp}$)* at *rdxA* locus, kanamycin resistance cassette in *jhp0255 ($lpxJ_{Hp}$)*	This work
C. jejuni		
81-176	Serotype HS: 23, 26	(132)
W. succinogenes		
DSM1740	Wild type	ATCC 29543
E. coli		
XL1-Blue	*recA1 endA1 gyrA96 thi-1 hsdR17 supE44 relA1 lac* [F' *proAB lacIqZΔM15*::Tn10 (Tetr)]	Stratagene
BN1	Δ*eptA* Δ*lpxT* Δ*pagP*	(8)
BN2	Δ*eptA* Δ*lpxT* Δ*pagP* Δ*lpxM*	(8)
MKV15b	Δ*lpxL* Δ*lpxM* Δ*lpxP*	(133)
Plasmids		
pET21a	Vector containing a T7 promoter; ampicillin resistance	Novagen
*jhp0255*KO+/-	pET21a containing *jhp0255* plus 1000bp upstream and 1000bp downstream, with *jhp0255* coding sequence replaced with kanamycin resistance cassette	This work

Table 5.1 (continued)

pWSK29	Low copy vector containing T7 and T3 RNA polymerase promoters; ampicillin resistance	(133)
pWSK29*jhp0255*	pWSK29 containing *jhp0255* coding sequence plus ribosome binding site for expression in *E. coli*	This work
pWSK29*cjj81176_0482*	pWSK29 containing *cjj81176_0482* coding sequence plus ribosome binding site for expression in *E. coli*	This work
pWSK29*ws1775*	pWSK29 containing *ws1775* coding sequence plus ribosome binding site for expression in *E. coli*	This work
pET0634comp	pET21a containing *hp0954* (*rdxA* locus) with flanking regions; *hp0954* coding sequence is replaced by *jhp0634*; used as template plasmid for complementation at *rdxA* locus	(22)
pET0634comp*jhp0255*	pET0634comp containing *jhp0255* instead of *jhp0634* interrupting *rdxA* locus	This work

Table 5.2: Oligonucleotides used in Chapter 2

Primer Name	Sequence (restriction site)	Restriction Site
1 Fjhp0255+upNheI	GCGCGCGCTAGCGCACATTA TTTAAAGGCTTGTATT	NheI
2 Rjhp0255+downXhoI	GCGCGCCTCGAGTATTTAGCT CTTGGCTCAATGTAA	XhoI
3 RipKOjhp0255BamHI	GCGCGCGGATCCTTAGTTGCC TTTAGTGGTTGCCAT	BamHI
4 FipKOjhp0255NotI	GCGCGCGCGGCCGCGGGTTT GAAGAATCTCAAAGGGGT	NotI
5 FKanRBamHI	GCGCGCGGATCCAAGGTTTT AGAATGCAAGGAACAGTG	BamHI
6 RKanRNotI	GCGCGCGCGGCCGCGGTACT AAAACAATTCATCCAGTA	NotI
7 Fjhp0255 NdeI	GCGCGCCATATGAGCTTAAA ATTTTTCAGG	NdeI
8 Rjhp0255 BamHI	GCGCGCGGATCCTTAAGCAC CCAAACCCCTTTG	BamHI
9 F0482+NdeI	GCGCGCCATATGCAAAGCGT ATGGTTTTATAT	NdeI
10 R0482+SalI	GCGCGCGTCGACTCATTCCTT AAATTGATCAGCTA	SalI
11 ws1775F	GCGCGCCATATGTTGGCGCTG GCTATCTTGC	NdeI
12 ws1775R	GCGCGCGTCGACTCACTCTAT CTCCTCGGTCATC	SalI
13 Fjhp0255BamHI_634comp	GCGCGCGGATCCACACCCCA TAAAGAGCAGGTTTAA	BamHI

Table 5.2 (continued)

14 Rjhp0255EcoRI_634comp	GCGCGCGAATCCTTAAGCACCCAAACCCCTTTGAGA	EcoRI
15 RdxA Forward	CGCTTCGTATCTTTATAGCCG	-
16 RdxA Reverse	CTAGCTTGATTTTCACCACAGCCAC	-
17 up_0255kanRKO_F	AAAAAGGCCATACAGCTTATTTAG	-
18 down_0255kanRKO_R	TAGCACAAAAGATAAAAAAATGT	-

Table 5.3: Bacterial strains and plasmids used in Chapter 3

Strains	Genotype or Description	Source or Reference
W3110	Wild type, F^- I^- rph-1 INV(*rrnD, rrnE*) 1 *rph*-1	*E. coli* genetic stock center (Yale)
W3110 *pmrD::kan*	W3110 containing kanamycin cassette at *pmrD*	This work
W3110 *pmrD::kan + pmrD*	W3110 *pmrD*- complemented with pWSK29*pmrD*	This work
W3110 *phoPQ::cam*	W3110 containing chloramphenicol cassette at *phoPQ*	This work
W3110 *phoPQ::cam, pmrD::kan*	W3110 *phoPQ*- containing kanamycin cassette at *pmrD*	This work
W3110 *phoPQ::cam, pmrD::kan + pmrD*	W3110 *phoPQpmrD*- expressing pWSK29*pmrD*	This work
W3110 *ΔpmrA*	W3110 with *pmrA* deleted, no marker	This work
W3110 *ΔpmrA + pmrD*	W3110 *pmrA*- expressing pWSK29*pmrD*	This work
MG1655	F^-, $lambda^-$, *rph*-1	Gift from S. Payne
MG1655 *pmrD::kan*	MG1655 containing kanamycin cassette at *pmrD*	This work
MG1655 *pmrD::kan + pmrD*	MG1655 *pmrD*- complemented with pWSK29*pmrD*	This work
WD101	W3110 constitutive *pmrA* mutant, polymyxin B resistant	(63)
EHEC EDL 933	Serotype O157:H7	ATCC
ETEC H10407	Serotype O78:H11	ATCC
XL1-Blue	*recA1 endA1 gyrA96 thi-1 hsdR17 supE44 relA1 lac* [F' *proAB lacIqZΔM15*::Tn10 (Tetr)]	Stratagene
Plasmids		
pET21a	Vector containing a T7 promoter; Amp resistance	Novagen
pET21a*pmrD*	pET21a containing W3110 *pmrD* coding sequence	This work
pWSK29	Low copy vector containing T7 and T3 RNA polymerase promoters; Amp resistance	(134)

Table 5.3 (continued)

pWSK29*pmrD*	pWSK29 containing W3110 *pmrD* coding sequence plus ribosome binding site	This work
pWSK29EHEC*pmrD*	pWSK29 containing EHEC *pmrD* coding sequence plus ribosome binding site	This work
pWSK29ETEC*pmrD*	pWSK29 containing ETEC *pmrD* coding sequence plus ribosome binding site	This work

Table 5.4: Oligonucleotides used in Chapter 3

Primer	Sequence (restriction site)	Restriction Site
1 ECpmrDF_NdeI	GCGCGCCATATGGAATGGCTGGTCAAAAAA	NdeI
2 ECpmrDR_BamHI	GCGCGCGGATCCTTACTGAGTTTTCCCTGC	BamHI
3 pmrDkeiocheck_R	GAGTGGGTGCAACGTCAGCAA	-
4 pmrAkeiocheck_R	GCTGCGGATGATATTCTGCAA	-
5 pmrBkeiocheck_R	TTTGGCTATATGCTGGTCGCG	-
6 k1 (128)	CAGTCATAGCCGAATAGCCT	-
7 GyrBF	ACGCTGCTGTTGACCTTCTT	-
8 GyrBR	TCCTGCTTGCCTTTCTTCAC	-
9 PmrDF	ATGGAATGGCTGGTCAAAAA	-
10 PmrDR	CATTCTGCAAAGGCGAGAGT	-
11 EptAF	CAGCGACTGGCAAATCT	-
12 EptAR	TAGTTTCACGCGGGTAGC	-
13 PmrAF	GGGCGGTGAAGAGTTGATT	-
14 PmrAR	TTGGTCGAGGGTTCATTGTC	-
15 ArnTF	TCAGCCAAGCCGCTATATTC	-
16 ArnTR	ATCACCGCTGACAAATCTCC	-
17 RstAF	GTGGAAGATGATGCGGAAGT	-
18 RstAR	CCTGGTAGCATGATGTCGAGT	-
19 PhoP1	ATAATCGCGTTACACTATTTTAATAATTAAGACAGGGAGAAATAAAAATGTGTAGGCTGGAGCTGCTTCG	-

Table 5.4 (continued)

20 PhoQP2	TTAACGTAATGCGTGAAGTATGGGCA TATTTATTCATCTTTCGGCGCAGAATG GGAATTAGCCATGGTCC	-

References

1. **Funahara Y, Nikaido H**. 1980. Asymmetric localization of lipopolysaccharides on the outer membrane of Salmonella typhimurium. J Bacteriol **141**:1463–1465.

2. **Whitfield C, Trent MS**. 2014. Biosynthesis and Export of Bacterial Lipopolysaccharides. Annu Rev Biochem **83**:99–128.

3. **Poltorak A, He X, Smirnova I, Liu MY, Van Huffel C, Du X, Birdwell D, Alejos E, Silva M, Galanos C, Freudenberg M, Ricciardi-Castagnoli P, Layton B, Beutler B**. 1998. Defective LPS signaling in C3H/HeJ and C57BL/10ScCr mice: mutations in Tlr4 gene. Science **282**:2085–2088.

4. **Hoshino K, Takeuchi O, Kawai T, Sanjo H, Ogawa T, Takeda Y, Takeda K, Akira S**. 1999. Cutting edge: Toll-like receptor 4 (TLR4)-deficient mice are hyporesponsive to lipopolysaccharide: evidence for TLR4 as the Lps gene product. J Immunol Baltim Md 1950 **162**:3749–3752.

5. **Tobias PS, Soldau K, Gegner JA, Mintz D, Ulevitch RJ**. 1995. Lipopolysaccharide binding protein-mediated complexation of lipopolysaccharide with soluble CD14. J Biol Chem **270**:10482–10488.

6. **Miyake K**. 2006. Roles for accessory molecules in microbial recognition by Toll-like receptors. J Endotoxin Res **12**:195–204.

7. **Park BS, Song DH, Kim HM, Choi B-S, Lee H, Lee J-O**. 2009. The structural basis of lipopolysaccharide recognition by the TLR4-MD-2 complex. Nature **458**:1191–1195.

8. **Needham BD, Carroll SM, Giles DK, Georgiou G, Whiteley M, Trent MS**. 2013. Modulating the innate immune response by combinatorial engineering of endotoxin. Proc Natl Acad Sci U S A **110**:1464–1469.

9. **Cohen J**. 2002. The immunopathogenesis of sepsis. Nature **420**:885–891.

10. **Anderson MS, Raetz CR**. 1987. Biosynthesis of lipid A precursors in Escherichia coli. A cytoplasmic acyltransferase that converts UDP-N-acetylglucosamine to UDP-3-O-(R-3-hydroxymyristoyl)-N-acetylglucosamine. J Biol Chem **262**:5159–5169.

11. **Young K, Silver LL, Bramhill D, Cameron P, Eveland SS, Raetz CR, Hyland SA, Anderson MS**. 1995. The envA permeability/cell division gene of Escherichia coli encodes the second enzyme of lipid A biosynthesis. UDP-3-O-(R-3-

hydroxymyristoyl)-N-acetylglucosamine deacetylase. J Biol Chem **270**:30384–30391.

12. **Babinski KJ, Ribeiro AA, Raetz CRH**. 2002. The Escherichia coli gene encoding the UDP-2,3-diacylglucosamine pyrophosphatase of lipid A biosynthesis. J Biol Chem **277**:25937–25946.

13. **Metzger LE, Raetz CRH**. 2010. An alternative route for UDP-diacylglucosamine hydrolysis in bacterial lipid A biosynthesis. Biochemistry (Mosc) **49**:6715–6726.

14. **Kelly TM, Stachula SA, Raetz CR, Anderson MS**. 1993. The firA gene of Escherichia coli encodes UDP-3-O-(R-3-hydroxymyristoyl)-glucosamine N-acyltransferase. The third step of endotoxin biosynthesis. J Biol Chem **268**:19866–19874.

15. **Garrett TA, Kadrmas JL, Raetz CR**. 1997. Identification of the gene encoding the Escherichia coli lipid A 4'-kinase. Facile phosphorylation of endotoxin analogs with recombinant LpxK. J Biol Chem **272**:21855–21864.

16. **Crowell DN, Anderson MS, Raetz CR**. 1986. Molecular cloning of the genes for lipid A disaccharide synthase and UDP-N-acetylglucosamine acyltransferase in Escherichia coli. J Bacteriol **168**:152–159.

17. **Clementz T, Raetz CR**. 1991. A gene coding for 3-deoxy-D-manno-octulosonic-acid transferase in Escherichia coli. Identification, mapping, cloning, and sequencing. J Biol Chem **266**:9687–9696.

18. **Clementz T, Bednarski JJ, Raetz CR**. 1996. Function of the htrB high temperature requirement gene of Escherchia coli in the acylation of lipid A: HtrB catalyzed incorporation of laurate. J Biol Chem **271**:12095–12102.

19. **Clementz T, Zhou Z, Raetz CR**. 1997. Function of the Escherichia coli msbB gene, a multicopy suppressor of htrB knockouts, in the acylation of lipid A. Acylation by MsbB follows laurate incorporation by HtrB. J Biol Chem **272**:10353–10360.

20. **Wyckoff TJ, Lin S, Cotter RJ, Dotson GD, Raetz CR**. 1998. Hydrocarbon rulers in UDP-N-acetylglucosamine acyltransferases. J Biol Chem **273**:32369–32372.

21. **Dotson GD, Kaltashov IA, Cotter RJ, Raetz CR**. 1998. Expression cloning of a Pseudomonas gene encoding a hydroxydecanoyl-acyl carrier protein-dependent UDP-GlcNAc acyltransferase. J Bacteriol **180**:330–337.

22. **Stead CM, Beasley A, Cotter RJ, Trent MS**. 2008. Deciphering the unusual acylation pattern of Helicobacter pylori lipid A. J Bacteriol **190**:7012–7021.

23. **Carty SM, Sreekumar KR, Raetz CR**. 1999. Effect of cold shock on lipid A biosynthesis in Escherichia coli. Induction At 12 degrees C of an acyltransferase specific for palmitoleoyl-acyl carrier protein. J Biol Chem **274**:9677–9685.

24. **Vorachek-Warren MK, Carty SM, Lin S, Cotter RJ, Raetz CRH**. 2002. An Escherichia coli mutant lacking the cold shock-induced palmitoleoyltransferase of lipid A biosynthesis: absence of unsaturated acyl chains and antibiotic hypersensitivity at 12 degrees C. J Biol Chem **277**:14186–14193.

25. **Rubin EJ, O'Brien JP, Ivanov PL, Brodbelt JS, Trent MS**. 2014. Identification of a broad family of lipid A late acyltransferases with non-canonical substrate specificity. Mol Microbiol **91**:887–899.

26. **Blaser MJ**. 1998. Helicobacter pylori and gastric diseases. BMJ **316**:1507–1510.

27. **Tran AX, Karbarz MJ, Wang X, Raetz CRH, McGrath SC, Cotter RJ, Trent MS**. 2004. Periplasmic cleavage and modification of the 1-phosphate group of Helicobacter pylori lipid A. J Biol Chem **279**:55780–55791.

28. **Stead CM, Zhao J, Raetz CRH, Trent MS**. 2010. Removal of the outer Kdo from Helicobacter pylori lipopolysaccharide and its impact on the bacterial surface. Mol Microbiol **78**:837–852.

29. **Cullen TW, Giles DK, Wolf LN, Ecobichon C, Boneca IG, Trent MS**. 2011. Helicobacter pylori versus the host: remodeling of the bacterial outer membrane is required for survival in the gastric mucosa. PLoS Pathog **7**:e1002454.

30. **Tran AX, Whittimore JD, Wyrick PB, McGrath SC, Cotter RJ, Trent MS**. 2006. The lipid A 1-phosphatase of Helicobacter pylori is required for resistance to the antimicrobial peptide polymyxin. J Bacteriol **188**:4531–4541.

31. **Teghanemt A, Zhang D, Levis EN, Weiss JP, Gioannini TL**. 2005. Molecular basis of reduced potency of underacylated endotoxins. J Immunol Baltim Md 1950 **175**:4669–4676.

32. **Rietschel ET, Kirikae T, Schade FU, Ulmer AJ, Holst O, Brade H, Schmidt G, Mamat U, Grimmecke HD, Kusumoto S**. 1993. The chemical structure of bacterial endotoxin in relation to bioactivity. Immunobiology **187**:169–190.

33. **Muotiala A, Helander IM, Pyhälä L, Kosunen TU, Moran AP**. 1992. Low biological activity of Helicobacter pylori lipopolysaccharide. Infect Immun **60**:1714–1716.

34. **Ogawa T, Asai Y, Sakai Y, Oikawa M, Fukase K, Suda Y, Kusumoto S, Tamura T**. 2003. Endotoxic and immunobiological activities of a chemically synthesized lipid A of Helicobacter pylori strain 206-1. FEMS Immunol Med Microbiol **36**:1–7.

35. **Ogawa T, Suda Y, Kashihara W, Hayashi T, Shimoyama T, Kusumoto S, Tamura T**. 1997. Immunobiological activities of chemically defined lipid A from Helicobacter pylori LPS in comparison with Porphyromonas gingivalis lipid A and Escherichia coli-type synthetic lipid A (compound 506). Vaccine **15**:1598–1605.

36. **Nguyen LT, Haney EF, Vogel HJ**. 2011. The expanding scope of antimicrobial peptide structures and their modes of action. Trends Biotechnol **29**:464–472.

37. **Peschel A, Sahl H-G**. 2006. The co-evolution of host cationic antimicrobial peptides and microbial resistance. Nat Rev Microbiol **4**:529–536.

38. **Peschel A**. 2002. How do bacteria resist human antimicrobial peptides? Trends Microbiol **10**:179–186.

39. **Nikaido H**. 2003. Molecular basis of bacterial outer membrane permeability revisited. Microbiol Mol Biol Rev MMBR **67**:593–656.

40. **García Véscovi E, Soncini FC, Groisman EA**. 1996. Mg2+ as an extracellular signal: environmental regulation of Salmonella virulence. Cell **84**:165–174.

41. **Raoult D, Aboudharam G, Crubézy E, Larrouy G, Ludes B, Drancourt M**. 2000. Molecular identification by "suicide PCR" of Yersinia pestis as the agent of medieval black death. Proc Natl Acad Sci U S A **97**:12800–12803.

42. **Chouikha I, Hinnebusch BJ**. 2012. Yersinia--flea interactions and the evolution of the arthropod-borne transmission route of plague. Curr Opin Microbiol **15**:239–246.

43. **Matsuura M, Takahashi H, Watanabe H, Saito S, Kawahara K**. 2010. Immunomodulatory effects of Yersinia pestis lipopolysaccharides on human macrophages. Clin Vaccine Immunol CVI **17**:49–55.

44. **Montminy SW, Khan N, McGrath S, Walkowicz MJ, Sharp F, Conlon JE, Fukase K, Kusumoto S, Sweet C, Miyake K, Akira S, Cotter RJ, Goguen JD, Lien E**. 2006. Virulence factors of Yersinia pestis are overcome by a strong lipopolysaccharide response. Nat Immunol **7**:1066–1073.

45. **Telepnev MV, Klimpel GR, Haithcoat J, Knirel YA, Anisimov AP, Motin VL**. 2009. Tetraacylated lipopolysaccharide of Yersinia pestis can inhibit multiple Toll-like receptor-mediated signaling pathways in human dendritic cells. J Infect Dis **200**:1694–1702.

46. **Stock AM, Robinson VL, Goudreau PN**. 2000. Two-Component Signal Transduction. Annu Rev Biochem **69**:183–215.

47. **Laub MT**. 2011. The Role of Two-Component Signal Transduction Systems in Bacterial Stress Responses, p. 45–58. *In* Hengge, R, Storz, G (eds.), Bacterial Stress Responses, Second Edition. American Society of Microbiology.

48. **Needham BD, Trent MS**. 2013. Fortifying the barrier: the impact of lipid A remodelling on bacterial pathogenesis. Nat Rev Microbiol **11**:467–481.

49. **Harris JB, LaRocque RC, Qadri F, Ryan ET, Calderwood SB**. 2012. Cholera. Lancet **379**:2466–2476.

50. **Hankins JV, Madsen JA, Giles DK, Brodbelt JS, Trent MS**. 2012. Amino acid addition to Vibrio cholerae LPS establishes a link between surface remodeling in gram-positive and gram-negative bacteria. Proc Natl Acad Sci U S A **109**:8722–8727.

51. **Henderson JC, Fage CD, Cannon JR, Brodbelt JS, Keatinge-Clay AT, Trent MS**. 2014. Antimicrobial peptide resistance of Vibrio cholerae results from an LPS modification pathway related to nonribosomal peptide synthetases. ACS Chem Biol **9**:2382–2392.

52. **Herrera CM, Crofts AA, Henderson JC, Pingali SC, Davies BW, Trent MS**. 2014. The Vibrio cholerae VprA-VprB two-component system controls virulence through endotoxin modification. mBio **5**.

53. **Prost LR, Daley ME, Le Sage V, Bader MW, Le Moual H, Klevit RE, Miller SI**. 2007. Activation of the bacterial sensor kinase PhoQ by acidic pH. Mol Cell **26**:165–174.

54. **Wösten MM, Kox LF, Chamnongpol S, Soncini FC, Groisman EA**. 2000. A signal transduction system that responds to extracellular iron. Cell **103**:113–125.

55. **Bader MW, Sanowar S, Daley ME, Schneider AR, Cho U, Xu W, Klevit RE, Le Moual H, Miller SI**. 2005. Recognition of antimicrobial peptides by a bacterial sensor kinase. Cell **122**:461–472.

56. **Ruby T, McLaughlin L, Gopinath S, Monack D**. 2012. Salmonella's long-term relationship with its host. FEMS Microbiol Rev **36**:600–615.

57. **Gibbons HS, Kalb SR, Cotter RJ, Raetz CRH**. 2005. Role of Mg2+ and pH in the modification of Salmonella lipid A after endocytosis by macrophage tumour cells. Mol Microbiol **55**:425–440.

58. **Trent MS, Pabich W, Raetz CR, Miller SI**. 2001. A PhoP/PhoQ-induced Lipase (PagL) that catalyzes 3-O-deacylation of lipid A precursors in membranes of Salmonella typhimurium. J Biol Chem **276**:9083–9092.

59. **Bishop RE, Gibbons HS, Guina T, Trent MS, Miller SI, Raetz CR**. 2000. Transfer of palmitate from phospholipids to lipid A in outer membranes of gram-negative bacteria. EMBO J **19**:5071–5080.

60. **Murata T, Tseng W, Guina T, Miller SI, Nikaido H**. 2007. PhoPQ-mediated regulation produces a more robust permeability barrier in the outer membrane of Salmonella enterica serovar typhimurium. J Bacteriol **189**:7213–7222.

61. **Kawasaki K, Ernst RK, Miller SI**. 2004. 3-O-deacylation of lipid A by PagL, a PhoP/PhoQ-regulated deacylase of Salmonella typhimurium, modulates signaling through Toll-like receptor 4. J Biol Chem **279**:20044–20048.

62. **Gunn JS, Lim KB, Krueger J, Kim K, Guo L, Hackett M, Miller SI**. 1998. PmrA-PmrB-regulated genes necessary for 4-aminoarabinose lipid A modification and polymyxin resistance. Mol Microbiol **27**:1171–1182.

63. **Trent MS, Ribeiro AA, Lin S, Cotter RJ, Raetz CR**. 2001. An inner membrane enzyme in Salmonella and Escherichia coli that transfers 4-amino-4-deoxy-L-arabinose to lipid A: induction on polymyxin-resistant mutants and role of a novel lipid-linked donor. J Biol Chem **276**:43122–43131.

64. **Zhou Z, Ribeiro AA, Lin S, Cotter RJ, Miller SI, Raetz CR**. 2001. Lipid A modifications in polymyxin-resistant Salmonella typhimurium: PMRA-dependent 4-amino-4-deoxy-L-arabinose, and phosphoethanolamine incorporation. J Biol Chem **276**:43111–43121.

65. **Lee H, Hsu F-F, Turk J, Groisman EA**. 2004. The PmrA-regulated pmrC gene mediates phosphoethanolamine modification of lipid A and polymyxin resistance in Salmonella enterica. J Bacteriol **186**:4124–4133.

66. **Gunn JS, Miller SI**. 1996. PhoP-PhoQ activates transcription of pmrAB, encoding a two-component regulatory system involved in Salmonella typhimurium antimicrobial peptide resistance. J Bacteriol **178**:6857–6864.

67. **Kox LF, Wösten MM, Groisman EA**. 2000. A small protein that mediates the activation of a two-component system by another two-component system. EMBO J **19**:1861–1872.

68. **Kato A, Groisman EA**. 2004. Connecting two-component regulatory systems by a protein that protects a response regulator from dephosphorylation by its cognate sensor. Genes Dev **18**:2302–2313.

69. **Luo S-C, Lou Y-C, Rajasekaran M, Chang Y-W, Hsiao C-D, Chen C**. 2013. Structural basis of a physical blockage mechanism for the interaction of response regulator PmrA with connector protein PmrD from Klebsiella pneumoniae. J Biol Chem **288**:25551–25561.

70. **Rubin EJ, Herrera CM, Crofts AA, Trent MS**. 2015. PmrD Is Required for Modifications to Escherichia coli Endotoxin That Promote Antimicrobial Resistance. Antimicrob Agents Chemother **59**:2051–2061.

71. **Raetz CRH, Whitfield C**. 2002. Lipopolysaccharide endotoxins. Annu Rev Biochem **71**:635–700.

72. **Stead C, Tran A, Ferguson D, McGrath S, Cotter R, Trent S**. 2005. A Novel 3-Deoxy-D-manno-Octulosonic Acid (Kdo) Hydrolase That Removes the Outer Kdo Sugar of Helicobacter pylori Lipopolysaccharide. J Bacteriol **187**:3374–3383.

73. **Raetz CRH, Reynolds CM, Trent MS, Bishop RE**. 2007. Lipid A modification systems in gram-negative bacteria. Annu Rev Biochem **76**:295–329.

74. **Lepper PM, Triantafilou M, Schumann C, Schneider EM, Triantafilou K**. 2005. Lipopolysaccharides from Helicobacter pylori can act as antagonists for Toll-like receptor 4. Cell Microbiol **7**:519–528.

75. **Moran AP**. 2007. Lipopolysaccharide in bacterial chronic infection: insights from Helicobacter pylori lipopolysaccharide and lipid A. Int J Med Microbiol IJMM **297**:307–319.

76. **Raetz CR**. 1990. Biochemistry of endotoxins. Annu Rev Biochem **59**:129–170.

77. **Rubin EJ, Trent MS**. 2013. Colonize, evade, flourish: How glyco-conjugates promote virulence of Helicobacter pylori. Gut Microbes **4**.

78. **Belunis CJ, Clementz T, Carty SM, Raetz CR**. 1995. Inhibition of lipopolysaccharide biosynthesis and cell growth following inactivation of the kdtA gene in Escherichia coli. J Biol Chem **270**:27646–27652.

79. **Moran AP, Lindner B, Walsh EJ**. 1997. Structural characterization of the lipid A component of Helicobacter pylori rough- and smooth-form lipopolysaccharides. J Bacteriol **179**:6453–6463.

80. **Punta M, Coggill PC, Eberhardt RY, Mistry J, Tate J, Boursnell C, Pang N, Forslund K, Ceric G, Clements J, Heger A, Holm L, Sonnhammer ELL, Eddy SR, Bateman A, Finn RD**. 2011. The Pfam protein families database. Nucleic Acids Res **40**:D290–D301.

81. **Alm RA, Ling LS, Moir DT, King BL, Brown ED, Doig PC, Smith DR, Noonan B, Guild BC, deJonge BL, Carmel G, Tummino PJ, Caruso A, Uria-Nickelsen M, Mills DM, Ives C, Gibson R, Merberg D, Mills SD, Jiang Q, Taylor DE, Vovis GF, Trust TJ**. 1999. Genomic-sequence comparison of two unrelated isolates of the human gastric pathogen Helicobacter pylori. Nature **397**:176–180.

82. **Cullen TW, O'Brien JP, Hendrixson DR, Giles DK, Hobb RI, Thompson SA, Brodbelt JS, Trent MS**. 2013. EptC of Campylobacter jejuni mediates phenotypes involved in host interactions and virulence. Infect Immun **81**:430–440.

83. **Heath RJ, Rock CO**. 1998. A conserved histidine is essential for glycerolipid acyltransferase catalysis. J Bacteriol **180**:1425–1430.

84. **Turnbull AP, Rafferty JB, Sedelnikova SE, Slabas AR, Schierer TP, Kroon JT, Simon JW, Fawcett T, Nishida I, Murata N, Rice DW**. 2001. Analysis of the structure, substrate specificity, and mechanism of squash glycerol-3-phosphate (1)-acyltransferase. Struct Lond Engl 1993 **9**:347–353.

85. **Tamada T, Feese MD, Ferri SR, Kato Y, Yajima R, Toguri T, Kuroki R**. 2004. Substrate recognition and selectivity of plant glycerol-3-phosphate acyltransferases (GPATs) from Cucurbita moscata and Spinacea oleracea. Acta Crystallogr D Biol Crystallogr **60**:13–21.

86. **Six DA, Lambert B, Raetz CRH, Doerrler WT**. 2012. Density gradient enrichment of Escherichia coli lpxL mutants. Biochim Biophys Acta **1821**:989–993.

87. **Gunn JS, Richards SM**. 2007. Recognition and Integration of Multiple Environmental Signals by the Bacterial Sensor Kinase PhoQ. Cell Host Microbe **1**:163–165.

88. **Perez JC, Groisman EA**. 2007. Acid pH activation of the PmrA/PmrB two-component regulatory system of Salmonella enterica. Mol Microbiol **63**:283–293.

89. **Herrera CM, Hankins JV, Trent MS**. 2010. Activation of PmrA inhibits LpxT-dependent phosphorylation of lipid A promoting resistance to antimicrobial peptides. Mol Microbiol **76**:1444–1460.

90. **Winfield MD, Groisman EA**. 2004. Phenotypic differences between Salmonella and Escherichia coli resulting from the disparate regulation of homologous genes. Proc Natl Acad Sci U S A **101**:17162–17167.

91. **Chen HD, Jewett MW, Groisman EA**. 2011. Ancestral genes can control the ability of horizontally acquired loci to confer new traits. PLoS Genet **7**:e1002184.

92. **Zhou Z, Ribeiro AA, Raetz CRH**. 2000. High-resolution NMR Spectroscopy of Lipid A Molecules Containing 4-Amino-4-deoxy-l-arabinose and Phosphoethanolamine Substituents DIFFERENT ATTACHMENT SITES ON LIPID A MOLECULES FROM NH4VO3-TREATED ESCHERICHIA COLI VERSUS kdsA MUTANTS OF SALMONELLA TYPHIMURIUM. J Biol Chem **275**:13542–13551.

93. **Touzé T, Tran AX, Hankins JV, Mengin-Lecreulx D, Trent MS**. 2007. Periplasmic phosphorylation of lipid A is linked to the synthesis of undecaprenyl phosphate: Periplasmic dephosphorylation of undecaprenyl-PP. Mol Microbiol **67**:264–277.

94. **Kato A, Latifi T, Groisman EA**. 2003. Closing the loop: the PmrA/PmrB two-component system negatively controls expression of its posttranscriptional activator PmrD. Proc Natl Acad Sci U S A **100**:4706–4711.

95. **Minagawa S, Ogasawara H, Kato A, Yamamoto K, Eguchi Y, Oshima T, Mori H, Ishihama A, Utsumi R**. 2003. Identification and molecular characterization of the Mg2+ stimulon of Escherichia coli. J Bacteriol **185**:3696–3702.

96. **Gunn JS, Ryan SS, Van Velkinburgh JC, Ernst RK, Miller SI**. 2000. Genetic and functional analysis of a PmrA-PmrB-regulated locus necessary for lipopolysaccharide modification, antimicrobial peptide resistance, and oral virulence of Salmonella enterica serovar typhimurium. Infect Immun **68**:6139–6146.

97. **Garcia-del Portillo F, Foster JW, Maguire ME, Finlay BB**. 1992. Characterization of the micro-environment of Salmonella typhimurium-containing vacuoles within MDCK epithelial cells. Mol Microbiol **6**:3289–3297.

98. **Miller SI, Kukral AM, Mekalanos JJ**. 1989. A two-component regulatory system (phoP phoQ) controls Salmonella typhimurium virulence. Proc Natl Acad Sci U S A **86**:5054–5058.

99. **Alpuche Aranda CM, Swanson JA, Loomis WP, Miller SI**. 1992. Salmonella typhimurium activates virulence gene transcription within acidified macrophage phagosomes. Proc Natl Acad Sci U S A **89**:10079–10083.

100. **Hagiwara D, Yamashino T, Mizuno T**. 2004. A Genome-wide view of the Escherichia coli BasS-BasR two-component system implicated in iron-responses. Biosci Biotechnol Biochem **68**:1758–1767.

101. **Touzé T, Tran AX, Hankins JV, Mengin-Lecreulx D, Trent MS**. 2008. Periplasmic phosphorylation of lipid A is linked to the synthesis of undecaprenyl phosphate. Mol Microbiol **67**:264–277.

102. **Zhou Z, Lin S, Cotter RJ, Raetz CRH**. 1999. Lipid A Modifications Characteristic of Salmonella typhimurium Are Induced by NH4VO3 inEscherichia coli K12 DETECTION OF 4-AMINO-4-DEOXY-l-ARABINOSE, PHOSPHOETHANOLAMINE AND PALMITATE. J Biol Chem **274**:18503–18514.

103. **Kato A, Chen HD, Latifi T, Groisman EA**. 2012. Reciprocal control between a bacterium's regulatory system and the modification status of its lipopolysaccharide. Mol Cell **47**:897–908.

104. **Eguchi Y, Itou J, Yamane M, Demizu R, Yamato F, Okada A, Mori H, Kato A, Utsumi R**. 2007. B1500, a small membrane protein, connects the two-component systems EvgS/EvgA and PhoQ/PhoP in Escherichia coli. Proc Natl Acad Sci U S A **104**:18712–18717.

105. **Lippa AM, Goulian M**. 2009. Feedback inhibition in the PhoQ/PhoP signaling system by a membrane peptide. PLoS Genet **5**:e1000788.

106. **Guckes KR, Kostakioti M, Breland EJ, Gu AP, Shaffer CL, Martinez CR 3rd, Hultgren SJ, Hadjifrangiskou M**. 2013. Strong cross-system interactions drive the activation of the QseB response regulator in the absence of its cognate sensor. Proc Natl Acad Sci U S A **110**:16592–16597.

107. **Kahler CM, Stephens DS**. 1998. Genetic basis for biosynthesis, structure, and function of meningococcal lipooligosaccharide (endotoxin). Crit Rev Microbiol **24**:281–334.

108. **Steeghs L, den Hartog R, den Boer A, Zomer B, Roholl P, van der Ley P**. 1998. Meningitis bacterium is viable without endotoxin. Nature **392**:449–450.

109. **Peng D, Hong W, Choudhury BP, Carlson RW, Gu X-X**. 2005. Moraxella catarrhalis bacterium without endotoxin, a potential vaccine candidate. Infect Immun **73**:7569–7577.

110. **Piet JR, Zariri A, Fransen F, Schipper K, van der Ley P, van de Beek D, van der Ende A**. 2014. Meningitis caused by a lipopolysaccharide deficient Neisseria meningitidis. J Infect **69**:352–357.

111. **Henry R, Vithanage N, Harrison P, Seemann T, Coutts S, Moffatt JH, Nation RL, Li J, Harper M, Adler B, Boyce JD**. 2012. Colistin-resistant, lipopolysaccharide-deficient Acinetobacter baumannii responds to lipopolysaccharide loss through increased expression of genes involved in the synthesis and transport of lipoproteins, phospholipids, and poly-β-1,6-N-acetylglucosamine. Antimicrob Agents Chemother **56**:59–69.

112. **Moffatt JH, Harper M, Harrison P, Hale JDF, Vinogradov E, Seemann T, Henry R, Crane B, St Michael F, Cox AD, Adler B, Nation RL, Li J, Boyce JD**. 2010. Colistin resistance in Acinetobacter baumannii is mediated by complete loss of lipopolysaccharide production. Antimicrob Agents Chemother **54**:4971–4977.

113. **Anderson MS, Bull HG, Galloway SM, Kelly TM, Mohan S, Radika K, Raetz CR**. 1993. UDP-N-acetylglucosamine acyltransferase of Escherichia coli. The first step of endotoxin biosynthesis is thermodynamically unfavorable. J Biol Chem **268**:19858–19865.

114. **Barb AW, Zhou P**. 2008. Mechanism and inhibition of LpxC: an essential zinc-dependent deacetylase of bacterial lipid A synthesis. Curr Pharm Biotechnol **9**:9–15.

115. **Gennadios HA, Whittington DA, Li X, Fierke CA, Christianson DW**. 2006. Mechanistic inferences from the binding of ligands to LpxC, a metal-dependent deacetylase. Biochemistry (Mosc) **45**:7940–7948.

116. **Casella CR, Mitchell TC**. 2008. Putting endotoxin to work for us: monophosphoryl lipid A as a safe and effective vaccine adjuvant. Cell Mol Life Sci CMLS **65**:3231–3240.

117. **McClerren AL, Endsley S, Bowman JL, Andersen NH, Guan Z, Rudolph J, Raetz CRH**. 2005. A slow, tight-binding inhibitor of the zinc-dependent deacetylase LpxC of lipid A biosynthesis with antibiotic activity comparable to ciprofloxacin. Biochemistry (Mosc) **44**:16574–16583.

118. **Arbour NC, Lorenz E, Schutte BC, Zabner J, Kline JN, Jones M, Frees K, Watt JL, Schwartz DA**. 2000. TLR4 mutations are associated with endotoxin hyporesponsiveness in humans. Nat Genet **25**:187–191.

119. **Lorenz E, Mira JP, Frees KL, Schwartz DA**. 2002. Relevance of mutations in the TLR4 receptor in patients with gram-negative septic shock. Arch Intern Med **162**:1028–1032.

120. **Yamakawa N, Ohto U, Akashi-Takamura S, Takahashi K, Saitoh S-I, Tanimura N, Suganami T, Ogawa Y, Shibata T, Shimizu T, Miyake K**. 2013. Human TLR4 polymorphism D299G/T399I alters TLR4/MD-2 conformation and response to a weak ligand monophosphoryl lipid A. Int Immunol **25**:45–52.

121. **Shaw JB, Li W, Holden DD, Zhang Y, Griep-Raming J, Fellers RT, Early BP, Thomas PM, Kelleher NL, Brodbelt JS**. 2013. Complete Protein Characterization Using Top-Down Mass Spectrometry and Ultraviolet Photodissociation. J Am Chem Soc.

122. **Haas R, Meyer TF, van Putten JP**. 1993. Aflagellated mutants of Helicobacter pylori generated by genetic transformation of naturally competent strains using transposon shuttle mutagenesis. Mol Microbiol **8**:753–760.

123. **Smeets LC, Bijlsma JJ, Boomkens SY, Vandenbroucke-Grauls CM, Kusters JG**. 2000. comH, a novel gene essential for natural transformation of Helicobacter pylori. J Bacteriol **182**:3948–3954.

124. **Belunis CJ, Raetz CR**. 1992. Biosynthesis of endotoxins. Purification and catalytic properties of 3-deoxy-D-manno-octulosonic acid transferase from Escherichia coli. J Biol Chem **267**:9988–9997.

125. **Smith PK, Krohn RI, Hermanson GT, Mallia AK, Gartner FH, Provenzano MD, Fujimoto EK, Goeke NM, Olson BJ, Klenk DC**. 1985. Measurement of protein using bicinchoninic acid. Anal Biochem **150**:76–85.

126. **Sambrook, J., and Russell, D.W.** 2001. Molecular Cloning: A Laboratory Manual. Cold Spring Laboratory Press, Cold Spring Harbor, NY.

127. **Baba T, Ara T, Hasegawa M, Takai Y, Okumura Y, Baba M, Datsenko KA, Tomita M, Wanner BL, Mori H**. 2006. Construction of Escherichia coli K-12 in-frame, single-gene knockout mutants: the Keio collection. Mol Syst Biol **2**:2006.0008.

128. **Datsenko KA, Wanner BL**. 2000. One-step inactivation of chromosomal genes in Escherichia coli K-12 using PCR products. Proc Natl Acad Sci U S A **97**:6640–6645.

129. **Pfaffl MW**. 2001. A new mathematical model for relative quantification in real-time RT-PCR. Nucleic Acids Res **29**:e45.

130. **Baggerly KA, Deng L, Morris JS, Aldaz CM**. 2003. Differential expression in SAGE: accounting for normal between-library variation. Bioinforma Oxf Engl **19**:1477–1483.

131. **Davies BW, Bogard RW, Young TS, Mekalanos JJ**. 2012. Coordinated Regulation of Accessory Genetic Elements Produces Cyclic Di-Nucleotides for V. cholerae Virulence. Cell **149**:358–370.

132. **Cullen TW, Trent MS**. 2010. A link between the assembly of flagella and lipooligosaccharide of the Gram-negative bacterium Campylobacter jejuni. Proc Natl Acad Sci U S A **107**:5160–5165.

133. **Vorachek-Warren MK, Ramirez S, Cotter RJ, Raetz CRH**. 2002. A triple mutant of Escherichia coli lacking secondary acyl chains on lipid A. J Biol Chem **277**:14194–14205.

134. **Wang RF, Kushner SR**. 1991. Construction of versatile low-copy-number vectors for cloning, sequencing and gene expression in Escherichia coli. Gene **100**:195–199.